Norges miljø- og biovitenskapelige universitet

Master's Thesis 2016 60 ECTS

Department of Chemistry, Biotechnology and Food Science (IKBM), at the Norwegian University of Life Sciences

Quorum sensing circuits in *Pseudomonas aeruginosa* regulate N_2O reduction

Kristine Lindtveit
Microbiology

Quorum sensing circuits in *Pseudomonas aeruginosa* regulate N_2O reduction

Master Thesis

Kristine Lindtveit

Institute of Chemistry, Biotechnology and Food Science

Norwegian university of Life Sciences

Ås 2016

Mater Thesis Supervisors

PhD Linda Liberg Bergaust (Main supervisor)
NMBU-N group, researcher
Norwegian University of Life Sciences
IKBM
NMBU
Dep. of Chemistry, Biotechnology and Food Science
Norwegian University of Life Sciences
P.O. Box 5003, N-1432 Aas, Norway
Phone: +47 67232449
linda.bergaust@nmbu.no

Daniel Aleksantri Milligan (co-supervisor)
NMBU-N group, PhD
IKBM
NMBU
Dep. of Chemistry, Biotechnology and Food Science
Norwegian University of Life Sciences
P.O. Box 5003, N-1432 Aas, Norway
Phone: +47 67232538
linda.bergaust@nmbu.no

Åsa Frostegard, Professor (co-supervisor)
Coordinator of NORA Marie Curie ITN, https://nora.nmbu.no/
NMBU Nitrogen Group http://www.nmbu.no/nitrogengroup/
Dep. of Chemistry, Biotechnology and Food Science
Norwegian University of Life Sciences
P.O. Box 5003, N-1432 Aas, Norway
Tel: +47-67232473
mob: +47-416 00 678
asa.frostegard@nmbu.no

Acknowledgements

The experiments were conducted at the Institute of Chemistry, Biotechnology and Food Science (IKBM) at the Norwegian University of Life Sciences, during spring and autumn 2016, in connection with completion of a Master degree in Microbiology.

One student, Kristine Lindtveit, performed the experiments at the institute´s laboratories following the experimental set-up, designed by Scientist Linda Liberg Bergaust.

During experimental preparations, experimental performance and collection of results, I was frequently and whole-heartedly thankful for the assistance of Ph.D student Daniel Aleksanteri Milligan; the clever advices from a skilful Technician Rannei Tjåland and her technician-colleague Inga Lena Angel. Also, I am thankful to Åsa Helena Frostegård for the possibility to make a Poster-presentation, for the 4th Norwegian Microbiology Meeting (NoMi-16), Sarpsborg. Most of all, I am grateful for the excellent supervision and refreshingly sharp work attitude given by my supervisor Linda L. Bergaust.

Table of Contents

Abstract

Many bacteria respire in the absence of oxygen through reduction of nitrogen oxides (NO_x) in the process called denitrification. Denitrification is the main greenhouse gas emitter by its release of N_2O when high amounts of N-fertilizers are applied globally. pH is known to be a regulatory factor for N_2O emission, but little is known about how quorum sensing regulates denitrification. When respiratory physiology of denitrifying organisms is studied under a defined set of conditions, their phenotypic traits are encompassed by the term denitrification regulatory phenotype (DRP). *Pseudomonas aeruginosa* is a model organism, well studied due to its widespread denitrifying and opportunistic pathogenic abilities. Detailed gas kinetics of this proteobacterium was studied to characterize its DRP.

DRP of strains from *P. aeruginosa* (a type strain and PAO1 wild type) were characterized with respect to their denitrification phenotype at different initial oxygen concentrations (0, and 7%). This was done by monitoring O_2, CO_2, NO_2^-, NO, N_2O and N_2 by gas chromatography (GC) and an NO-analyzer during their transition from aerobic respiration to denitrification. This study showed that the denser the culture, the higher the accumulation of N_2O during denitrification, and implied that quorum sensing (QS) is mediating the N_2O emission from denitrification. The question became whether this occurred due to the regulation by one or both of the AHL systems.

Further characterization on how QS regulates the denitrification phenotype was done by monitoring denitrification gases under treatment with AHLs on PAO1 *rhlI*$^-$*lasI*$^-$ mutant and a QS-inhibitor on its PAO1 parent strain (PAO1-UW). Their transcriptional activities of *narG, nirS, norB,* and *nosZ* during transition from aerobic respiration to denitrification were quantified by ddPCR. The gas measurements, as well as cell densities, cell numbers and initial biomass were measured to describe specific aerobic and anaerobic respiration rates (μ_{oxic} and μ_{anoxic} h^{-1}), cell yields per e-acceptor and mRNA per cell.

The results showed that the AHL systems´ regulatory effect on denitrification in PAO1 is inhibiting N_2OR activity, most likely on a post-transcriptional level. This was directly due to repression of N_2O reductase by the Las quorum sensing system.

Sammendrag

Mange bakterier respirerer ved fravær av oksygen gjennom reduksjon av nitrogenoksider (NO_x) i en prosess kalt denitrifikasjon. Denitrifikasjon er hoved-klimagass frigjøreren gjennom sitt utslipp av N_2O når store mengder N-kunstgjødsel anvendes globalt. pH er en kjent reguleringsfaktor for N_2O utslipp, mens quorum sensing (bakterielt kommunikasjonssystem) er en svært lite gjennomsøkt reguleringsmekanisme ved denitrifikasjon. Når respirasjonsfysiologien hos denitrifiserende organismer studeres under definerte forhold, blir de fenotypiske karakterene omfattet av terminen en "denitrifikasjonsregulatorisk fenotype" (DRP). *Pseudomonas aeruginosa* er en modellorganisme som er velstudert på grunn av dens utbredte denitrifiserende og opportunistiske patogene egenskaper. Detaljert gasskinetikk av denne proteobakterien ble studert for å karakterisere dens DRP.

DRP av stammer fra *P. aeruginosa* (en type stamme og PAO1 villtypen) ble karakterisert med hensyn til deres denitrifikasjonsfenotype under ulike initielle oksygen konsentrasjoner (0 og 7 %). Dette ble gjort ved overvåkning av O_2, CO_2, NO_2^-, NO, N_2O og N_2 gjennom gasskromatografi (GC) og nitrogen okside-analyse (NOA) under deres overgang fra aerob respirasjon til denitrifikasjon. Dette studiet viste at jo høyere celletettheten var, desto høyere ble N2O akkumuleringen under denitrifikasjon, og antydet at quorum sensing (QS) er medvirkende til N2O utslippet fra denitrifikasjon. Spørsmålet ble om dette skjedde på grunn av reguleringen fra en eller flere AHL systemer.

Videre karakterisering av hvordan quorum sensing regulerer denne denitrifikasjonsfenotypen ble gjort ved å overvåke denitrifikasjonsgassene under behandling med ulike AHL på en PAO1 *rhlI*$^-$*lasI*$^-$ mutant og en QS-hemmer på dens PAO1 forelderstamme. Deres transkripsjons aktivitet av narG, nirS, norB, og nosZ under overgangen fra aerob respirasjon til denitrifikasjon ble kvantifisert ved ddPCR. Gassmålingene, såvel som celletetthet, celletall og initiell biomasse ble målt for å beskrive spesifikk aerob og anaerob respirasjons rate (μ_{oxic} and μ_{anoxic} h-1), celleutbytte per e- akseptor og mRNA per celle.

Resultatene viste at AHL systemenes regulerende effekt på denitrifikasjon i PAO1 hemmer N_2OR aktivitet, mest sannsynlig på et post-transkripsjonelt nivå. Dette var direkte på grunn av N_2O reduktase-undertrykkelsen ved Las quorum sensing systemet.

INTRODUCTION

Many microorganisms, mainly bacteria, are able to maintain a respiratory metabolism in the absence of oxygen through reducing nitrogen oxides (NO_x) in the process called denitrification. Denitrification is the main soil contributor to the currently rising greenhouse gas, N_2O. Imperatively, to understand this process, denitrification must be studied at its biochemical and regulatory level. When respiratory physiology of denitrifying organisms is studied under a defined set of conditions, their phenotypic traits are encompassed by the term denitrification regulatory phenotype (DRP). *Pseudomonas aeruginosa* is a model organism, well studied due to its widespread denitrifying, as well as opportunistic pathogenic abilities. Detailed gas kinetics of this proteobacterium has revealed a new denitrification regulatory trait: the denser the culture, the higher the accumulation of N_2O during denitrification. In this study, I show that this was directly due to repression of N_2O reductase by the Las quorum sensing system. Apparently, this was not due to transcriptional regulation of the functional gene, *nosZ*, but rather a post-transcriptional and/or metabolic control of N_2OR activity.

Nitrogen (N), is the most abundant constituent of our atmosphere, and essential for life as it is a component of many macromolecules, like proteins and nucleic acids. The global nitrogen cycle includes N in all its oxidation states, from fully oxidized nitrate (NO_3^-) to fully reduced ammonium (NH_4^+) (fig.1). All are biologically available but only recycled by microbial activity (Bothe et al., 2006). The bacteria, archaea and some fungi recycle N by redox reactions, in which some of them utilize the electrons for their energy supply (van Spanning et la., 2007). In other words, some of these organisms, when driven by the cycling of nitrogen, exploit N directly as terminal electron acceptors to drive their electrochemical proton potential for ATP production (Zumft and Cardenas, 1979).

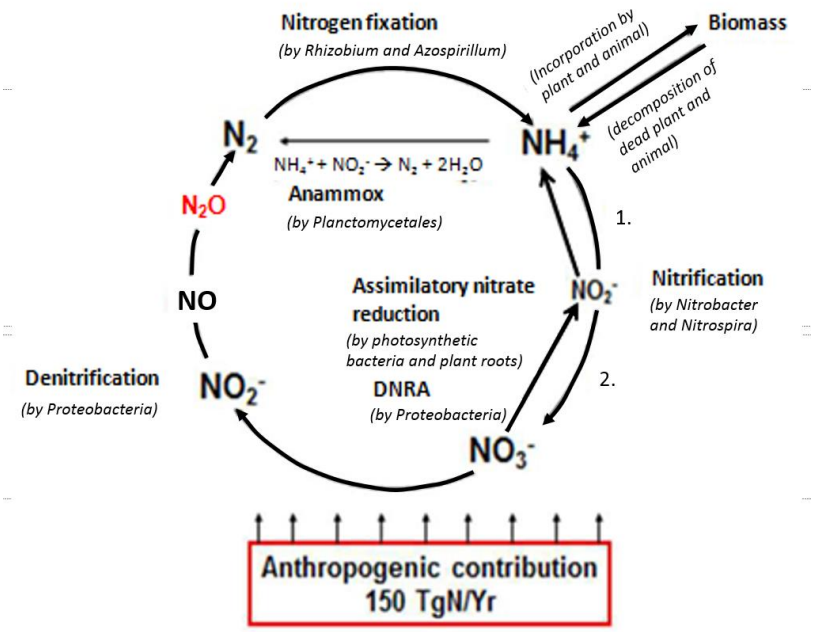

Figure 1. *The nitrogen cycle, encompassing nitrogen in all its oxidation states from fully oxidized nitrate (NO_3^-) to fully reduced ammonium (NH_4^+). Each completed arrow indicates the final product of a given mechanism: nitrogen fixation (production of NH_4^+); DNRA: dissimilatory nitrate reduction to ammonium (production of NH_4^+); Assimilatory nitrate reduction (production of NH_4^+ by plants); Ammonification/decomposition-mechanism (production of NH_4^+); Anammox (production of N_2); Nitrification (production of* ***1.*** *NO_2^-, and* ***2.*** *NO_3^-); and Denitrification (production of N_2O and N_2). (Source: Kraft et al., 2011; Richardson et al., 2009; van Elsas et al., 2006).*

Nitrogen fixation is the production of NH_4^+ by an energy expensive enzyme, nitrogenase. Both free-living microorganisms and bacteria in symbiosis utilize nitrogenases to incorporate N from atmospheric N_2 into their biomass (Bothe et al., 2006). DNRA, dissimilatory nitrate reduction to ammonium (NH_4^+) provides energy through respiration or fermentation with NH_4^+ released by different γ -, δ-, and ϵ-proteobacteria (van Elsas et al. 2006). Assimilatory nitrate reduction is the production of NH_4^+ in plants and microorganisms to cover N-requirements. This mechanism does not recycle N by releasing NH_4^+ back to environment, but incorporates (assimilate) N directly into the biomass-buildup (Bothe et al., 2006). Ammonification is the decomposition of dead biomass (debris) in a three-step process of cell-lysis, hydrolysis of proteins, and metabolism by heterotrophs that excrete NH_4^+. The anammox mechanism, discovered in the 90's, was found to contribute to 50 % of N turnover in marine environments

(Kuenen, 2008). This mechanism provides energy in anoxic environments, by oxidizing NH_4^+ with nitrite as a terminal electron acceptor to release N_2. Traditional nitrification is one step oxidation of reduced N to NO_2^- in some organisms, followed by a second step of NO_2^- oxidation to NO_3^- by completely separate microorganisms. These organisms live completely different lifestyles (autotrophic and heterotrophic), and both steps occur in oxic environments to conserve energy (Bothe et al., 2006). A more recent discovery is that of Comammox where both steps of nitrification (NH_4^+ oxidation to NO_3^-) is performed under oxic conditions by one organism: the complete ammonia oxidizers (Daims et al., 2015). Denitrification is the dissimilatory reduction of nitrate to N_2 via nitrite, NO and N_2O, chiefly taking place under anoxic conditions (van Spanning et al., 2007).

Whether nitrogen is retained or released back to the atmosphere in a given environment depends on the dominating N-transforming pathway (Kraft et al., 2011). One or more of these mechanisms may dominate, depending on the type of environment, and affects life in various ways (van Elsas et al., 2006). One such life affecting connection is during modern agricultural practices, which cause a shift in the global N cycle by leading a steady annual increase in net emission of the greenhouse gas N_2O (Smith and Conen, 2004).

Environmental aspects

In pre-industrial times, the global N had 12,000 years of balanced cycling, with biological N-fixation (BNF) and lightning providing the only natural creation of biologically available N (fig.2). However, in the current situation, half of the 6.25 % of N in any given biomass now derive from fertilizers or fossil fuels (Hanke and Strous, 2010).

The BNF process incorporates atmospheric N_2 into tissue of legumes through the symbiotic relationship with N-fixing bacteria (*Azospirillum* and *Rhizobium*). Nitrogen is the most growth-limiting variable of plant-life, which depends on a few N_2 transforming enzymes. These are in turn oxygen sensitive and highly energy demanding (Tortora et al. 2007). To enhance growth on agricultural land, we therefore apply synthetic nitrogen (N) fertilizers that contain bioavailable NH_4^+ and NO_3^-.

Synthetic N-fertilizers are both cheap and highly yield-effective, compared to BNF derived growth yield (Herridge et al., 2008). Previously, we enhanced plant growth by

spreading nitrate salts[1] (NO_3^-) that were extracted from large, natural deposits (Penrose, 1910; Urbansky et al., 2001). However, when the "Green revolution" (50`s) came, it was predicted that natural deposits of nitrate salts were not going to satisfy future demands. The development of an artificial nitrogen fixation process, from F. Haber and C. Bosch, gave us a cheaper way to continue with increased crop yield (Ussiri and Lal, 2013). Since then, humans have doubled the pre-industial nitrogen budget through development and commersialization of the Haber-Bosch process (Galloway et al., 2004).

A number of environmental challenges are linked to anthropogenic N input. NO_3^- is a water soluble N-form and moves in soil quite readily (relatively low retention time), while NH_4^+ binds to soil particles (relatively high retention time) (Stotzky, 1967). At the present, estimated annual global input of anthropogenic N is 150 Tg yr^{-1} (Schlesinger, 2009). Much of this is lost from agricultural fields annually when soils are saturated with water. For example during springtime, water percolates through soil towards groundwater, or leaches through soil as surface runoff towards lakes and rivers. 35 TgN yr^{-1} NO_3^- is water-transported (leached) as surface runoff into rivers and cause coastal eutrophic water (Galloway et al., 2004; Schlesinger, 2009). If prolonged, it results in algae blooms, followed by oxygen depletion, and subsequent environments that constitute strong group-organism domination and low trophic diversity (Gong and Xie, 2001). The total estimated nitrogen that contaminates groundwater by percolating through soil is 15 TgN yr^{-1} (of the total 150 TgN yr^{-1}) (Schlesinger, 2009). Although NO_3^- concentration in the groundwater fluxes with nitrogen load applied on soil, its long residence time means it provides a possible long-term sink for nitrogen. Thereby, it exposes humans to toxic drinking water. Areas where infants have fatal methemoglobinemia[2] are strongly correlating with drinking water that derives from high nitrate containing groundwater (higher concentrations than 1.9 mg/L NO_3^-N) (Almasri and Kaluarachchi, 2004; Knobeloch et al., 2000; Rupert, 2008).

The relative long retention time of NH_4^+ in soil, in addition to excessive

---

[1]Historically, the nitrate salts were utilized for production of, not only fertilizers, but also large amounts of gunpowder (Penrose, 1910).

[2] Methemoglobinemia is a form of tissue hypoxia, or low transport efficiency of oxygen to tissue due to high levels of ferric iron [fe3+] in the red blood cells rather than the normal ferrous iron [Fe2+], and is therefore deadly in many cases (ATSDR, 2015).

NH_4^+ based fertilization over prolonged time, accelerate soil nitrification processes (2 mol H^+ pr mol NH_4^+-N), which leads to excess H^+ release during NH_4^+ oxidation (Guo et al., 2010). Ultimately, indirect soil acidification (pH reduction) by synthetic N-fertilizers surrenders plant and microbial life to high organism domination and low, functional diversity: characteristics of unhealthy ecosystems (Chen et al., 2013; Tortora et al., 2007).

Even so, the losses of nitrogen from agricultural fields, have forced us to continue our increased application of N-fertilizers (Galloway et al., 2004). In pre-industrial times, humans added approximately zero industrial N-fertilizers. Atmospheric N_2O accumulations protrude from this twist in the cycle, and have steadily been on the rise since the 1950's (Galloway et al., 2004).

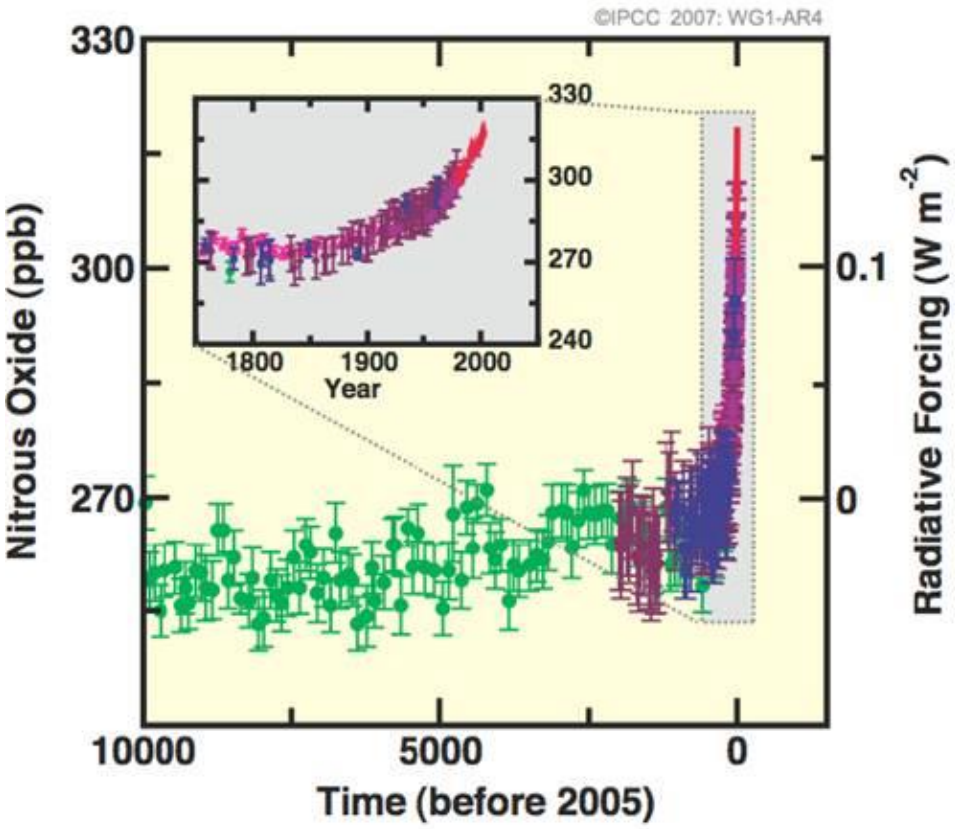

Figure 2. *Atmospheric nitrous oxide concentrations during the last 12,000 years (10,000 BC to 2005) and the effect on radiative force (W m^{-2}). N_2O concentrations the last 200 years are zoomed out* (IPCC, 2007).

N_2O; the forgotten climate gas

N_2O is a greenhouse gas approximately 300 times more potent than CO_2 (IPCC, 2014). Although the atmospheric concentration of N_2O (330 ppb, or 0.00003%) is one order of magnitude lower than CO_2 (430 ppm, or 0.039 %) its radiative forcing (W m^{-2}) contributes significantly to atmospheric warming, which has risen since pre-industrial times (1.5°C) (Ramaswamy et al., 2001). Additionally, its instability in the stratosphere, where it easily reacts with ozone (O_3), makes it an important factor for O_3 depletion and ozone holes (Cicerone, 1987; Ravishankara et al., 2009). The ozone layer protects the biosphere from DNA-damaging UV-radiation (Madsen, 2008).

Independent observations from ice core data and direct atmospheric measurements, compares the N_2O accumulation from pre-industrial times (1850) until today (2014) with the last 12,000 years (fig.2). N_2O has risen dramatically by atmospheric levels of 270 ppb (1850) to 330 ppb (2014). The annual increase in atmospheric N_2O was 1.3% (1970-2000), and today it is 2.2 % (2000-2010) (IPCC, 2014).

The largest N_2O emissions come from agricultural soils by a total of 17 Tg/y N_2O-N output. The majority of N-input (150 Tg/yr) also comes from agriculture, through BNF and artificial BNF (N-fertilizers) (Herridge et al., 2008). The N-fertilizers boosts microbial processes, mostly nitrification and denitrification, which are responsible for 65 % of total annual N_2O-N emission (Anderson and Levine, 1986; Smith and Conen, 2004). In addition, areas of waterlogged soils or coastal waters that receive NO_3^- rich surface runoff are most likely to contain high nitrifying and denitrifying communities (Schlesinger, 2009; Tortora *et al.* 2007). As an illustration, denitrifiers inside the gut of earthworms, which are essential to soils drainage and aeration, have been found to account for 50 % of the total N_2O emitted (0.3 Tg/yr) (Horn et al., 2005).

Nitrification has N_2O as a by-product, but denitrification is the only process with N_2O as an intermediate. While both processes are relevant sources of N_2O, denitrification is assumed the largest (Richardson et al., 2009).

Both high rate of denitrification and truncated denitrification has been provoked by the high N-fertilization since the 50´s (Zumft and Kroneck, 2007). In fact, the latest estimation implies that the all of the total 17 TgN/yr emissions comes from denitrification (Galloway et al., 2004; Schlesinger et al. 2009). Thus, denitrification is the most profound source of N_2O emission (Torres et al., 2014).

Denitrification

Microbial denitrification is the dissimilatory reduction of nitrate (NO_3^-) to nitrogen gas (N_2) via nitrite (NO_2^-), nitric oxide (NO), and nitrous oxide (N_2O) taking place under oxygen limited conditions (Zumft, 1997). Both of the prokaryotic and eukaryotic cell type may denitrify, but only prokaryotes carry out the final step: the reduction of N_2O to N_2 (Zumft and Kroneck, 2007). Many genes govern the synthesis and activities of the core metallo-enzymes that catalyze this sequential reduction of nitrate to N_2 (fig.3) (Tavares et al., 2006).

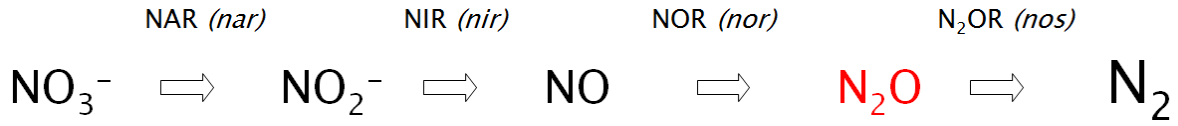

Figure 3. *Complete denitrification pathway containing four reaction steps: dissimilatory stepwise reduction of NO_3^- to NO_2^-, NO, N_2O and finally to N_2 via the metallo-enzymes NAR, NIR, NOR and N_2OR, encoded by nar, nir, nor and nos genes, respectively. These enzymes, through redox-chemistry of metals (Fe, Cu, and Mo), reduce all available nitrogen oxides (Zumft, 1997).*

Gram-negative bacteria[3] belonging to the Proteobacterial phylum are the most studied bacteria in terms of denitrification apparatus (Zumft, 1997). Bacterial nitrate reductase exists as three distinct enzymes that are all molybdenum-dependent and perform the reduction of NO_3^- to NO_2^- ($NO_3^- + 2H^+ -> NO_2^- + H_2O$). These are the assimilatory Nas in the cytoplasm, the periplasmic dissimilatory Nap and the membrane-bound respiratory Nar (encoded by *narK$_1$K$_2$GHJI*) (Moreno-Vivian et al., 1999). Only Nap and Nar are denitrification enzymes, and many denitrifiers have both (Bedzyk and Rick, 1999;

[3] **Gram`s method:** Often the first step in characterizing bacteria. The method is based on staining bacterial cells with crystal violet and a safranine counter stain in order to differentiate them into one of two large bacterial groups: G- and G+. G+ and G- bacteria differ with respect to their cell wall composition. A G+ cell has thick layer of peptidoglycan outside the cell membrane and retains crystal violet, whereas the G- has a thinner layer of peptidoglycan, and the crystal violet blue is easily washed out during a decolourization step. The safranine counter stain makes G- cells appear red or pink in the microscope (Reece et al., 2011).

Schreiber et al., 2007). While the dissimilatory Nap provides a reducing power for cell redox balance, only Nar is a respiratory enzyme, meaning that it contributes in the electrochemical gradient (Brondijk et al., 2004). (fig.4). Organisms carrying Nar must import nitrate to the cytoplasm, and the resulting nitrite must be transported back out to the periplasmic space where the other NO_x reductases, Nir, Nor and N_2OR reside fig.4). This is performed by the nitrate/proton symporter $NarK_1$ and nitrate/nitrite antiporter $NarK_2$, which are found required for anaerobic growth (Sharma et al., 2006). For example, species of *Paracoccus* and *Pseudomonas* provides nitrate/proton symporter $NarK_1$ transport mechanisms to get NO_3^- into cytoplasm, and a nitrate/nitrite antiporter $NarK_2$ that provides for NO_2^- transport back to periplasm (Härtig et al., 1999; Wood et al., 2002).

The two-electron transfer reduction of NO_2^- to NO ($NO_2^- + 2H^+ -> NO + H_2O$), taking place in the periplasm, is often termed the defining step of denitrification. This is because NO metabolism is closely linked with physiology and regulation of NO_2^- reduction (Kuroki et al., 2014). Nir was first discovered in *P. aeruginosa* (encoded *nirS*) and is dependent on soluble cytochrome cd1 (Silvestrini et al., 1989). The Nir encoded by *nirK*, is a copper nitrite reductase gene, widespread across phyla and often found in prokaryotes with a truncated denitrification apparatus (Jones et al., 2008; Murphy et al., 2002).

The activity of nitric oxide reductase (NOR) is to catalyze the reduction of two NO molecules into one N_2O molecule ($2NO + 2H^+ + 2e^- \rightarrow N_2O + H_2O$) in the periplasmic space (fig.4). The transmembrane NOR enzyme shows no proton translocation and varies between three types of complexes, which all carry two highly conserved Fe-centres (a high spin haem *b* and a non-heme iron, Fe_B). These catalyze the two-electron reduction of NO to N_2O (Hendriks et al., 1998). Usually found in full-fledged denitrifies, is the cNOR, and is named thus because it derives its electrons from the soluble electron donor cyt c (Hendriks et al., 2000). The cNor is a complex that consists of membrane-bound subunits NorC and NorB (Spiro, 2012). The best-characterized NorBC complex resides in *P. aeruginosa* (encoded *norB)*, where the NorC receive the electrons indirectly from the same transmembrane cytochrome bc1 as the Nir, via the soluble periplasmic cyt c (Chen and Strous, 2013). The third NOR is an unusual hybrid of complex called qcuANor (Kraft et al., 2011; Spiro, 2012). The qCu_ANor has been recognized as a single-subunit (NorB-unit) and membrane-bound enzyme that uses menaquinol as an electron donor. This is instead of the cyt c, and is more associated with dissimilatory processes of a non-respiratory type, such as scavenging of NO in gram-positives (Suharti et al., 2001)

Before completing the denitrification apparatus, the Nap and Nar that both perform nitrate reduction, are often the only NO_x reductases found in many organisms. This is because dissimilatory nitrate reduction is a more frequently distributed process (Kraft et al., 2011; Madsen, 2008; Strouse et al, 2006; Zumft, 1997). Such truncated denitrification is widespread. Organisms may carry only parts of the denitrification apparatus and have NO or N_2O as the final product of nitrate/nitrite reduction (Greenberg and Becker, 1977). A truncated denitrification apparatus, even if it only existed of Nar or N_2OR alone, still allows energy conservation through the generation of ATP, albeit with lower yields. Also, the NO_x reductases may not necessarily be expressed for respiration, but rather as a scavenging mechanism of NO or by dissipation of excess reduced compounds when maintaining a redox balance within the cell (Zumft, 2005).

The fourth enzyme is called dissimilatory nitrous oxide reductase (N_2OR), and is the only enzyme known that reduces N_2O as its primary function (Jones et al., 2008; Zumft and Kroneck, 2007). Two types of multicopper (Cu_A and Cu_Z) N_2OR types exist that perform the reduction ($N_2O + 2H^+ + 2e^- \rightarrow N_2 + H_2O$). The first is a z-type, which receives its electrons from the same cytochrome as the Nir and NOR (cyt c via the quinol pool).The second is called the c-type, which receives e- from [4Fe-S] clustered membrane bound proteins (Kern and Simon, 2009). The two Cu centres, Cu_A and Cu_Z, contain a novel discorvery: where the electron entry site occurs at the Cu_A species in the catalytic Cu-sulfur complex: the tetranuclear Cu_Z centre is the first found and is only known to exist in N_2OR enzymes (Zumft and Kroneck, 2007).

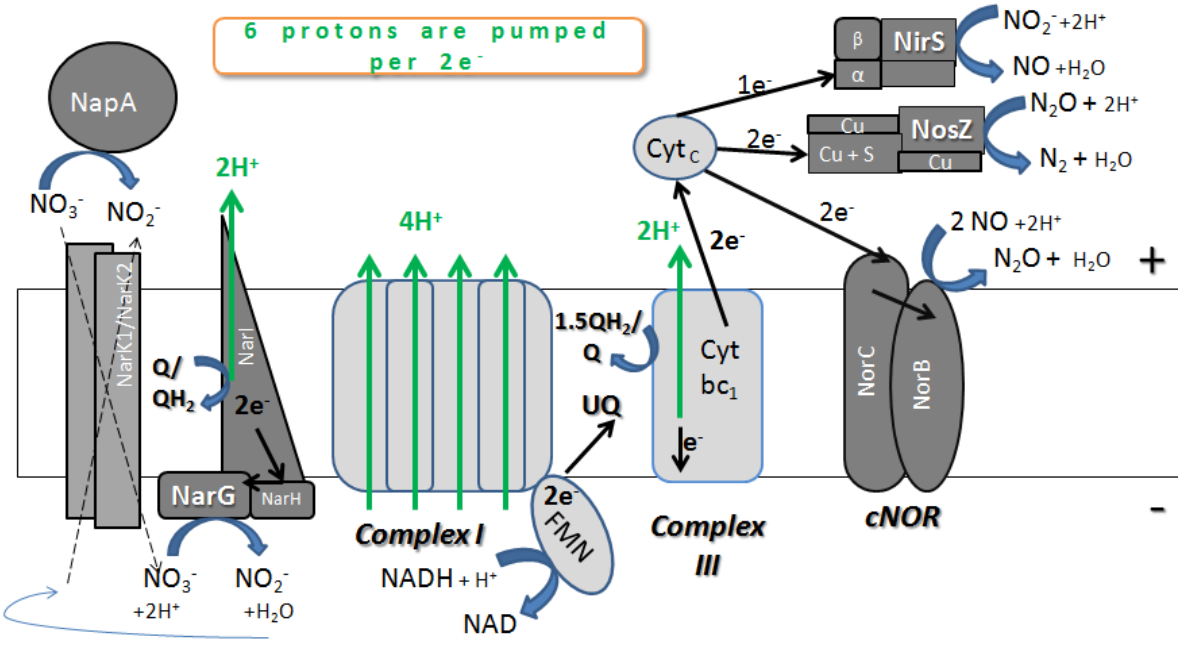

Figure 4. *Detailed schematic overview of the biochemistry of denitrification. The electron transport chain builds up an electrochemical proton potential across the cell membrane through the denitrification apparatus (+ periplasm and – cytoplasm). 6 protons are pumped per 2e-, compared to 10 protons pumped per 2e- during oxygen respiration (Chen and Strous, 2013). Thin or stippled Dark grey boxes depict denitrifying enzyme complexes (NapA, NarG, NirS, cNor and NosZ). Grey box transporting Light grey boxes are oxidases: Complex I; Complex III (cytochrome bc_1); cytochrome c. The Quinone/quinol pool is illustrated in between the two oxidase complexes (I and III). NB! Periplasmic nitrate reductase napA in PAO1 is localized in the Periplasm with the enzymatic reaction: NO_2^- + an oxidized electron acceptor ⇔ NO_3^- + a reduced electron acceptor, favoured in the opposite direction. (Illustration derrives from: Chen and Strous, 2013; Kraft et al., 2011; Spiro, 2012).*

Regulation of denitrification

The energy provided by denitrification is lower than oxygen respiration by four protons per every two e^- (fig.2). This occurs because all the NO_x species (NO_3^-, NO_2^-, NO and N_2O) have lower relative oxidation potentials than oxygen, meaning that the amount of ATP molecules generated will never be as high as for aerobic respiration (Tortora *et al*. 2007). Since this energy yield is not quite as high as for oxygen respiration, microbial growth is greatly affected. Thus, the transition from aerobic respiration to denitrification occurs by a regulatory tight and fine-tuned response system at transcriptional levels of the NO_x reductases (Chen and Strous, 2013).

The coordination occurs via two-component systems and proteins belonging to the FNR family of transcriptional regulators. These constitute a system that directs the overall cell respiratory process (Härtig et al., 1999). Generally, they directly control transcription initiations and frequencies in response to environmental factors (inducers). Firstly, oxygen exposure limits FNR-tendency to dimerize, which decreases its affinity for DNA (Spiro, 2012). The $[4Fe\text{-}4S]^{2+}$ cluster in FNR becomes free from oxygen under low oxygen conditions. At this point, these transcriptional regulators become active and bind to conserved FNR/ANR box (TTGATNNNNATCAA) within functional genes of the denitrification apparatus (Khoroshilova et al., 1997; Winteler and Haas, 1996). For example, the transcriptional regulatory response sensors, called ANR and DNR, activate promoter with binding motif: 5'end-TTGATTCCTATCAA-3'end at the *narK$_1$K$_2$GHJI* operon in low oxygen environments (Hasegawa et al., 1998; Schreiber et al., 2007). Essentially, this induces the cascade events of a fine-tuned regulation of denitrification regulatory phenotype in *P. aeruginosa*.

FNRs function both as sensors for oxygen tensions, and for NO_3^- and NO, as well as directly initiating transcription of the denitrification enzymes (Arai et al.1997; Härtig et al., 1999). An example is when FixK in Bradyrhizobium, NarXL in Pseudomonas, or NarR (FNR related nitrate sensor) detects NO_3^- presence in *Paracoccus denitrificans*. These fine-tune the expression of *nir* and *nor* and ultimately, enhances FNR activated gene expressions of all the *nar, nir, nor* and *nos* genes (Kraft et al., 2011; Spiro, 2012; Zumft, 1997). Simultaneous transcription of two core genes, *nir* and *nor*, is essential for preventing cytotoxic and genotoxic levels of NO. The NO molecule is a Reactive Nitrogen Species (RNS) that is highly reactive and toxic intermediate of the pathway (Spiro, 2012).

NO has high affinity for metal centres in proteins and can be a cause of nitrosative stress in microorganisms. As part of the eukaryotic innate immunity

response[4] called oxidative burst, NO is naturally produced as a general strategy to defend against pathogens (Tortora et al. 2007). Signals like NO and O_2 is therefore strong signal inducers to microorganisms for a tight control on gene transcription for metabolic purposes, virulence activation, and even biofilm production (Pessi and Haas, 2000; Spiro, 2012; Vasil and Clark, 2011).

In order to distinguish and characterize bacteria in their regulation of denitrification and accumulation of NO_x intermediates, a most useful term is Denitrification Regulatory Phenotype (DRP) (Bergaust et al., 2011). DRP is characterizing the amounts of accumulating intermediates and transcriptional activities in direct linkage with transitions between external available electron acceptors (Bergaust et al., 2008; Bergaust et al., 2010). In other words, how the organisms regulate their denitrification apparatus in response to conditional factors has a consequence for the NO_x accumulations. Soil microbial communities may transcribe only parts of the apparatus for denitrification (truncated denitrification), and a denitrifying population may emit different amounts of N_2O. Since DRP differ across species and has never been found to give any good linkage with16S taxonomy, it has never been any better way to describe DRP than by functional studies that analyse NO_x accumulations and gene transcripts responses during transitions from oxic to anoxic condition (Bakken et al., 2011).

One external master regulator of the denitrification process, in addition to oxygen levels, is pH (Liu et al., 2014). Numerous studies, in both soil, among extracted soil communities and in pure cultures, have shown that there is a strong positive correlation between soil acidity and $N_2O/(N_2O + N_2)$ product ratios (i.e. net N_2O emissions) (Bergaust et al., 2010; Čuhel et al., 2010; Liu et al., 2010; Samad et al., 2016; Simek and Cooper, 2002). Even though the *nirS, norB* and *nosZ* genes are transcribed, the N_2OR activity is low, or inhibited (Bergaust et la., 2010). Therefore, pH is the primary manipulator on N_2OR activity (Liu et al., 2014). Post-transcriptionally, acidity interferes with the periplasmic assembly of the N_2O reductase at the Cu_z centre in the N_2OR (Unpublished). The periplasm, not surprisingly, is more alike to surrounding pH compared to cytoplasmic pH (Wilks and Slonczewski, 2007). This has implications for N_2O emissions from large soil areas acidified by the prolonged increase in N-fertilization practice (Guo et al., 2010).

The characterization of DRP from many different organisms, in accordance with

[4] Innate immune system: Nonspecific defence of host (plant or animal) against microbial infection.

genetic potential and regulatory responses, reveals mechanisms behind the observed phenomenon of high N_2O emission from soil (Bergaust et al., 2011). Partly, the understanding of the mechanisms are due to the detailed knowledge obtained from observing model organisms, like *Paracoccus denitrificans* (Bergaust et al., 2010). I focus my study on pure cultures of another well-observed model organism: the complete denitrifier and opportunistic pathogen, *Pseudomonas aeruginosa*.

Pseudomonas aeruginosa

P. aeruginosa is a Gram-negative, motile rod belonging to the Ɣ-proteobacteria that thrives by oxygen respiration, yet dominates anoxic environments where it perform complete denitrification, or arginine and pyruvate fermentation (Vasil and Clark, 2011; Zumft, 1997; Jo et al., 2014). *P. aeruginosa* carries a massive respiratory apparatus, which includes five terminal oxidases and a full set of NO_x reductases (Vasil and Clark, 2011). This allows the organism to thrive under a range of conditions, and *P. aeruginosa* is an efficient denitrifier in the absence of oxygen. During denitrification, it uses nitrate all the way to N_2O, and finally to N_2, as alternative electron acceptors in the electron transport chain. That way, *P. aeruginosa* upholds respiratory growth under oxygen limitation.

It is frequently found in habitats of soils, water systems, as well as with a variety of plants and animals (Green et al., 1974). *P. aeruginosa* has a large genome that varies between 5.5 and 7 Mbp with a GC content of around 66.6% (Stover et al., 2000). The genome contains the largest regulatory gene apparatus sequenced in a bacterium (Klogether et al., 2010). Its size is not primarily a result of gene duplication, and the genetic complexity allows a high phenotypic plasticity. This large and diverse metabolic apparatus is consistent with its wide environmental adaptability (Mathee et al., 2008). This species carries genes that regulate antibiotic efflux, protein secretion, nutrient import and chemo-sensing (Stover et al., 2000; Westbrock-Wadman et al., 1999). Its physiological flexibility allows both free living states and symbiotic relationships, as well as living as an opportunistic pathogen in plant and animal hosts.

It is also a notorious opportunistic pathogen and is responsible for some community-acquired infections and 11-13.8 % of hospital acquired infections, primarily in immunocompromised individuals (for example, AIDS and cystic fibrosis (CF) patients) (Driscoll et al., 2007). Due to its adaptability, its wide distribution and pathogenicity *P. aeruginosa* has been one of a selected few paradigm model organisms for studying denitrification. It is also intensely studied with respect to its quorum sensing circuits,

which govern a massive regulon.

Transcriptional regulation of denitrification activity in *Pseudomonas* requires the activation of ANR and DNR global response regulators (fig.5). DNR controls denitrification directly, while ANR only performs an indirect control (Arai et al., 1995). Both are iron-dependent with oxygen sensitive Fe-S cluster when acting as sensory devices for denitrification activation: while ANR is inhibited the same way as FNR by the presence of oxygen, DNR never react with oxygen, but responds to presence of NO (Castiglione et al., 2009). When oxygen levels are low, ANR becomes active and induce transcription of *narXL*, *Nar*, and *dnr* (Vasil and Clark, 2011). DNR activates all denitrification gene expressions, and its activity is enhanced by NO_3^- presence through the two-component regulatory NarXL system (Härtig et al., 1999). NarX acts as nitrate sensor and the NarL is a transcriptional factor protein that positively regulates denitrification proteomes for *narG* operon, *nirQ*, and *dnr* (Schreiber et al., 2007). NarXL activates *nirQ*, which encodes a nitrite reductase regulator gene and result in the fine-tuned expressions of *nirS* and *norB* (Jüngst and Zumft, 1992).

Even though the signal cascades with fine-tuned responses from *P. aeruginosa* during denitrification are well known, there are still questions to be answered. Quorum sensing systems of *P. aeruginosa* are yet to be fully discovered when it comes to its effect on denitrification. Quorum sensing, as a major regulator on respiration, might unlock how bacteria regulate their energy metabolism during biofilm production (Toyofuku et al., 2007).

Quorum sensing (QS) circuits

Quorum sensing is the cell density dependent accumulation of small, diffusible signal molecules, generally called N-acyl-homoserine lactones (AHLs) (Waters and Bassler, 2005). These induce their own synthesis (autoinduction), as well as provide for cell-to-cell communication and gene transcription control in bacteria (Dekimpe and Dézekiel, 2009) QS circuits are the extensive global regulating system among bacteria that controls their growth dynamics (Ishida et al., 2007). When N-acyl-homoserine lactones (AHLs) (gram negatives), and oligopeptide inducers (gram positives) accumulate towards a critical concentration they typically enhance their own expression, thereby creating a positive feedback loop (Dekimpe and Dézekiel, 2009) (Waters and Bassler, 2005). This results in high concentration of autoinducers, which induce transcription of target genes in the entire population. For example, in the marine luminous bacterium *Vibrio fischerii*,

where quorum sensing was first discovered, these AHLs accumulate in the environment until a critical concentration is reached, whereupon induction of luminescence occurs that result in a 1000-fold increase in light production (Engebrecht et al., 1983). Quorum sensing induces the bacterial population to produce bioluminescence as their cell density increases inside a light-organ of the Hawaiian sepiolid squid *Euprymna scolopes*, and the fish *Monocentris japonica* of the Indo-West and Central Pacific Ocean (Engebrecht et al., 1983; Waters and Bassler, 2005). Upon this phenomenon, the most important induction mechanism is the AHL-autoinduction through the AHL receptors as the cell population density increases (Fuqua et al., 1994). This starts at the QS-circuit of AHL-synthesizer (LuxI) and AHL-receptors (LuxR), which both act as global direct transcriptional regulators.

There are different types of quorum sensing circuits with species-specific AHLs produced that depends on the bacterial group transcribing the LuxR-LuxI-protein family. LuxI are synthesizers and LuxR are response regulators. For example, quorum sensing in an actively growing population of *P. aeruginosa* consists of at least three systems: two N-Acyl-homoserine lactone (AHL) signals from the LasR-LasI and RhlR-RhlI, and the 2-heptyl-3-hydroxy-4-quinolone signal (PQS). LasR-LasI and RhlR-RhlI, both relate to the same protein family of LuxR-LuxI transcriptional regulators and has been the most studied of the three. In a hierarchical order, the LasR-LasI system activates the RhlR-RhlI in response to AHL signal induction (Schuster and Greenberg, 2006). The signal molecule called N-3-oxo-dodecanoyl-homoserine lactone (3O-C12-HSL) binds to LasR-receptor. The second system produces the N-butanoyl-L-homoserine lactone (C4-HSL) signal molecule at the expression of the RhlI signal synthase upon contact with its respective RhlR receptor (Smith and Iglewski, 2003). 3O-C12-HSL in *P. aeruginosa* is also called the PAI molecule in therapeutic studies for controlling *P. aeruginosa* infections (Pearson et al. 1994). During infection, QS activates several virulence gene expressions (Passador et al. 1993).

However, not only virulence genes are activated in response to QS. Denitrification is also strongly linked to these systems (Toyofuku et al. 2007). Based on transcription analysis and protein-based assays, a QS- mutant will have an elevated level of ANR-regulated processes. Denitrification (a highly relevant ANR-regulated process in *P. aeruginosa*) occurs in much higher levels in the QS-mutants, where denitrifying NO_x has been demonstrated at the levels of mRNA (Hammond et al., 2015). For a *P. aeruginosa* population this means that the NO_x reductases of denitrification are already known to be repressed by increased cell density (Toyofuku et al., 2007). However, any detailed knowledge of how this cell-to-cell communication ultimately affects anaerobic

respiration in growing cultures is limited.

Results from phenotypic studies of two strains of *P. aeruginosa* (the type strain and PAO1) are indicating that the last step of denitrification, the reduction of N_2O to N_2, is the step most strongly affected by cell density. The most pronounced phenotype was in PAO1, which seemed largely unable to reduce N_2O when denitrifying at intermediate cell density (Results, fig.21). I take these results to further investigate if, not only oxygen, but also quorum sensing is involved in down-regulation of denitrification. Particularly, the interesting regulatory spot is directly on the transcription of *nosZ*.

Investigation

All physiological investigations that seek to characterize DRP require that we empirically estimate critical biological parameters. These facilitated set-up and analysis during the first and two following investigations on DRP, and are: specific growth rate (μ h^{-1}) during aerobic and anaerobic growth, cell numbers and initial biomass. The first investigations were done on PAO1 and the type strain by measuring in detail their accumulated nitrite and gaseous intermediates (NO, N_2O and N_2) in continuously stirred batch cultures during their transition from aerobic respiration to denitrification. The two up-following physiological experiments were set-up accordingly: First, a denitrification phenotype test on a *rhlI-lasI-* mutant in presence with exogenous AHLs - and unsupplemented medium, and its parent strain with and without a QS-inhibitor ((N-decanoyl cyclopentylamine). Second, the *rhlI-lasI-* mutant and parent strain were compared with respect to their transcription of *narG, nirS, norB*, and *nosZ* during transition from aerobic respiration to denitrification.

The first characterization on DRP in *P. aeruginosa* revealed a peculiar response: when N_2O accumulated during denitrification it appeared to increase dramatically with cell density. The question became whether this occurred due to regulation by one or both of the AHL systems. The results showed that the AHL systems´ regulatory effect on denitrification in PAO1 is inhibiting N_2OR activity, most likely on a post-transcriptional level.

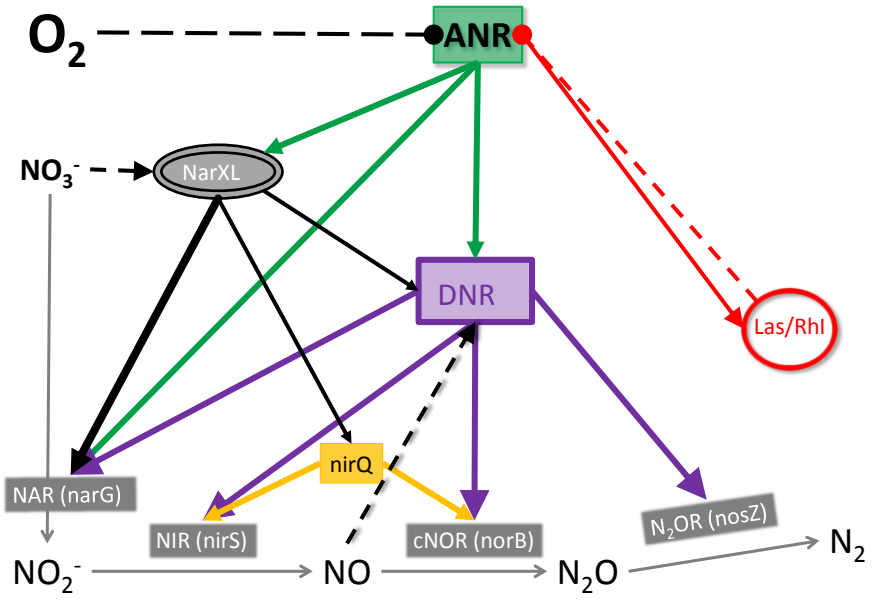

(Arai et al., 2011)

Figure 5: *Regulatory network controlling expression of denitrification genes in P. aeruginosa. Arrows = activtions; Circled arrow = inhibitions. Grey arrows = chemical reachion of denitrification. ANR is repressed by osygen. When oxygen is depleted, ANR becomes active and the events of a signal cacade begin. ANR activates DNR expression under anaerobic or low oxygen conditions. In respons to NO precense, DNR activates the transcription of all core genes of denitrification. Under enhancement by nitrate via NarXL, the DNR increases all expressions, especially nirS. NarXL complex activates nirQ to balance nirS and norB expression, as well as narG,. That way, only when NO_3^- is reduced to NO_2^- and NO, DNR can be fully activated by NO presence, leading to full onset of all denitrification genes. The schematic figure is found in Vasil and Clark (2011).*

MATERIALS AND METHODS

Bacteria

The initial phenotypic experiments were done on two strains from Germany: *P. aeruginosa* PAO1wild type (DSM 22644) and the type strain (DSM 50071) (Klockgether et al., 2010). Based on preliminary results, further experimentations were done with a double deletion mutant (PAO1 *rhlI*–*lasI*–) and its parent strain (PAO1 wild type). The mutant and its parent strain, PAO1 wild type (PAO1-UW) (Wang et al., 2015), came from the laboratory of Professor Peter Greenberg (Department of microbiology, School of medicine, University of Washington: http://depts.washington.edu/epglab). The deletions were confirmed by PCR using primers flanking *rhlI* and *lasI* (tab.4.; Results, fig.19).

The PAO1 *rhlI*–*lasI*– mutant is deficient in AHL synthesis, but the AHL receptors, *rhlr* and *lasr* are intact and thus it responds to exogenous AHL signals through RHLR and LasR.

The type strain is a reference for deciding whether a new organism belong to the *Pseudomonas aeruginosa* species. In this case, the type strain[5] is a comparable "scaffold" when characterizing denitrification physiology and other metabolic phenotypes of other strains, like PAO1.

P. aeruginosa ssp. is a Biosafety Level 2 (BSL-2) pathogen, and caution had to be taken by following institutional guidelines for handling and safety (LaBouve and Wargo, 2012). Plating of cultures on TSA medium (Tryptic soy agar: general medium), LB medium (Luria-Bertani: general medium) and Sistrom´s medium (defined medium) assured that strain specific growth curves were not contaminated (Appendix, fig.I).

All strains were stored in 25% glycerol at -80°C. 0.7 mL of overnight bacterial culture was added to cryogenic vial with 0.3 mL 85% glycerol. In preparation for experiments, glycerol stocks of 1 mL were transferred directly to liquid medium for aerobic pre-culturing.

[5] A type strain is defined in the "International Code of Nomenclature of Bacteria" as the "nomenclatural type of the species", and is the "reference point" to which all other strains are compared in order to know whether they belong to that species or not.

Media and culturing conditions

All experiments were performed in batch cultures with slightly modified Sistrom´s medium (Sistrom, 1962). This is a defined growth medium, which contains 34 mM succinate (carbon source) and 3.6 mM ammonium chloride (nitrogen source). For complete composition, see table I, Appendix. Stock solutions of 10 X Sistom´s medium were brought to 1 x concnetration, adjusted to pH 7 with KOH, and autoclaved before use. Sterile techniques in biosafety cabinets[6] were practiced during all culturing steps to avoid contamination. Since *P. aeruginosa* is an opportunistic pathogen, open cultures were always handled in a sterile bench, with air-flow system that protects both worker and sample.

The optimum growth temperature of *P. aeruginosa* is 37°C (LaBauve and Wargo, 2012). The growth temperature must be lower than optimum growth temperature in order monitor denitrification regulatory phenotype in this organism (Appendix, fig.IV). However, it survives at a wide range of temperatures from 4°C to 42°C. Here, 20˚C was used consistently for all growth curves and experiments. That way, biological parameters, like specific growth rate μ, which depends on temperature as well as medium components, will be assumed to be one constant during aerobic respiration, and another constant during anaerobic respiration at standard conditions (tab2.).

Cells were cultured under oxic conditions at 20˚C in 120 mL serum vials containing 50 mL autoclaved medium and triangular magnetic bars for continuous stirring. When cultured in anoxic conditions, 2 mM KNO_3 was added before the media were autoclaved. For standard experimental conditions, see table 2 (Gas and nitrite measurements).

All cultures were continuously and vigorously stirred (500 or 700 rpm: depending on magnet bar size) in order to minimize cell aggregation and ensure proper gas exchange between liquid and headspace. Vials used for aerobic cultures were closed using cotton plugs and aluminium foil, while vials for anaerobic growth were made gas tight by sealing with butyl rubber septa and aluminium caps (by sterile technique: flame, 70% ethanol, and LAF[7] bench). The atmosphere in headspace was then replaced by

[6] Biosafety cabinets: the air flow protects both sample and operating personnel.

[7] LAF: Laminar Air Flow cabinet.

Helium in a series of evacuations and gas fillings (fig.6). This "He-washing" routine typically resulted in O_2 concentrations of 150-300 ppm (versus 210000 ppm in ambient air). Experimental flasks were also pre-adjusted to water-bath temperature and lab-pressure (fig.6). Optimally, pressure in experimental flasks must be equal to the pressure in the needle of the robotic headspace sampler, which is equal to lab-environment. Pre-adjusting the pressure is done to avoid having over-pressure or under-pressure affecting volume or content of sampling during incubation experiments. High pressure in flask is let out through septum with a syringe coupled to the needle filled with 70% ethanol. The high gas pressure in the serum flask will leave through the ethanol, seen as bubbles. When pressure is equal to the surroundings, the bubbles appear no more and the gas syringe is removed.

Following gas-pressure adjustments, oxygen is manually added to flasks in 4 % initial oxygen concentrations (3,5 mL) with a sterile gas syringe, and finally inoculated with 1 mL aerobic pre-culture at OD 0.067 OD_{600} (initial cell number: 2.56×10^7). In order to control the inoculum injected into the experiment, certain biological parameters at standardized conditions must be characterized for each strain: biomass (mg/mL), maximum specific growth rate ($\mu\ h^{-1}$) and cell number (cells/mL). The method utilized to bring together these parameters were in units of optical density (OD_{600}).

Figure 6. *Helium-wash and pressure adjustment.* ***Left:*** *Experimental flasks being Helium washed after autoclaving.* ***Middle:*** *Bubbles forming during evacuation are shown on magnet bars at bottom of the serum flasks.* ***Right:*** *Headspace in a serum flask being adjusted to pressure equal to lab-environment.*

Estimating Biological Parameters

Before *P. aeruginosa* PAO1 and the type strain were brought into large physiological investigation, critical biological parameters were estimated that cannot be measured during, but are crusial for set-up and analyses of larger physiological experiments. Biological parameters consist mainly of: cell number/mL; initial biomass (mg/mL); and growth curves to determine the cultures´ growth rates ($\mu\ h^{-1}$) and generation times (T_d).

Growth curves and optical density versus cell number/biomass

Growth curves were made for aerobic and anaerobic cultures of PAO1 and the type strain through optical density (OD) by spectrophotometry. Log linear growth curves were used to estimate growth rate ($\mu\ h^{-1}$) and generation time (T_d). Cell numbers and cell mass versus OD_{600} were determined from aerobic cultures, by the DAPI cell count method from continuous growth and biomass by dry weight method, respectively. An "OD to cell number" conversion factor allows the estimation of cell yields (cell/flask), per cell respiration rates and transcripts-concentration of specific genes in growing cultures. This "OD to Biomass" conversion factor describes the weight of the culture at a given state of growth.

Optical density spectrophotometry is principally a measure of the intensity of light transmitted through a solution. Normal light intensity of a given wavelength (colour) by spectrophotometry scales from 200 nm (ultraviolet) to 0.3 mm (infrared). The wavelength for measuring cell density is often used at 600 nm optical density (OD_{600}).

The number given by the spectrophotometer is Abs_{600}, or the amount of light absorbed by a specific compound in the sample. For example, 0.15 Abs_{600} reflects the amount absorbed from 600 nm light waves, and contains more of the compound compared to a lower optical density, like 0.05 Abs_{600}. That way, absorbance measured by spectrophotometry is proportional with the concentrations of the absorbing compound (i.e. *P. aeruginosa* cells and their culture density at a given growth stage). A control is purposeful in spectrophotometry because it cancels out the absorbance readings from Sistrom´s medium reagents. Spectrophotometry by OD_{600} is frequently used to measure cell densities on prokaryotes, and leads to an efficient way for calculating $\mu\ h^{-1}$ and T_d.

DAPI (4′,6-diamidino-2-phenylindole) is a popular counter stain with maximum excitation/emission at 358 and 461 nm, respectively, thus emitting blue fluorescence. This dye stains the cell DNA through binding to AT regions. Detection is done by fluorescence microscopy using a blue/cyan filter. DAPI also binds to RNA, although its

fluorescence is not as strong. Since DAPI is a DNA-binding dye, it is considered mutagenic. Therefore, caution must be taken for safe handling and disposal.

DAPI cell count was used to determine the conversion factor cells/mL/OD_{600}. This, in the end, will facilitate per cell estimations of transcript numbers and specific activities during aerobic and anaerobic growth.

Preparing the DAPI cell count

Aerobically growing cells of *P. aeruginosa* PAO1 (28˚C) were harvested at different cell densities, vacuum filtrated and stained by DAPI[8].

Filters (Whatman Anodisc, 0.2 µm pore size) were placed on the vacuum filtration apparatus that had been pre-washed with 70 % ethanol. Cells were added onto filter in volumes according to OD_{600} (Calc. 1.c, below), and followed by a washing step with 1 mL filter-sterilized PBS and filter-sterilized 15 mM NaCl through vacuum filtration. Cells on filter were stained in dark surroundings by: adding 100x culture volume of 3 µM DAPI working solution (Calc.1.d), incubating for 5 minutes, followed by vacuum filtration. Filters were then washed 3-4 times with 5 mL filter-sterilized PBS and 15 mM NaCl (Appendix, tab.IV). Filter with stained cells was then fixed on an object glass between two drops of paraffin and a cover glass on top. A microscopic BCZ square was used to count the fixed cells on filter at 100x objective (fig.7A). Both the filter and the BCZ square have a known areal. Cells are counted within the BCZ square a number of times at arbitrary places on filter until approximately 200 cells are reached. Average of cells/BCZ squares are multiplied with the filter`s complete areal (F-factor).

Wanted cells/ BCZ square

Before staining and make a cell/BCZ square count, a practical aid is to make a wanted average cell/BCZ square prediction. Wanted cells/BCZ square could be seven cells. Firstly, if choosing the objective 100x, an F-factor (fig. 7B) is multiplied with 7cells/BCZ square (Calc.1.a). Secondly, the parallel between OD, X, and wanted cell/mL is converted to find the volume of wanted cell number (Eq.1). X is a typical representative cell number of exponential growth phase, and is used as a rule of thumb where X becomes10^9 cells. Thirdly, the volume from OD=0.014 to add on filter in order is given as 1 mL culture to reach 7 cells/BCZ square (Calc.1.b). Finally, because this culture volume depends on cell density, the volume is also used to find the amount of DAPI to add onto filter (Calc.1.c).

[8] DAPI is an UV-fluorescent dye that can be seen under UV illumination, and thus must be protected from strong light upon staining and storage.

$F = 2.01x10^6 \times 7 \text{ cells} = 1.41 \times 10^7 \text{ cells}$ Calculation 1.a

$$\text{Cells/mL} = OD * X \quad \text{Eq.1}$$

Example: Calculation 1.b

If OD = 0.014

1.41×10^7 cells/ (10^9cells * 0.014) *1000≈ 1 mL culture at OD_{600}=0.014 is added onto filter.

A thumb rule: DAPI volume =100x culture volume added onto filter.

Since the filter contain a thin culture density OD_{600}=0.014 of such high volumes (1000µL), the thumb of rule sais the staining requires a lot of DAPI:

100*1mL of culture = 100 mL DAPI Calculation 1. c

Therefore, thumb of rule is excluded.

Here, the DAPI volume was reduced by 20 times:

→ (100mL/20)*1000 = 5 mL of 3 µM DAPI was added to catch all the cells.

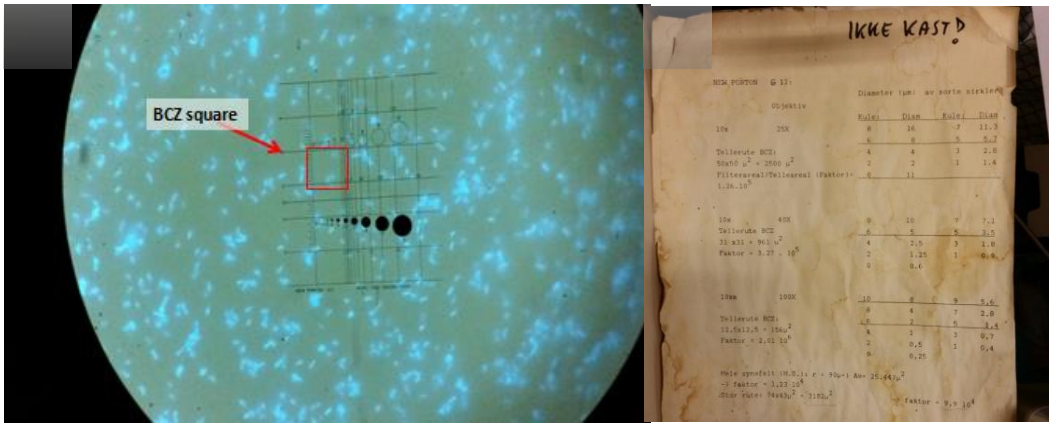

Figure 7. A) *P. aeruginosa rods shaped cells from 1000 µL of culture at OD_{600}=0.014 was added onto filter (Whatman Anodisc, 0.2 µm pore size) stained with 5000 µL of DAPI dye, and seen under 100x objective with immersion oil (type F) by fluorescence microscopy (LEICA DMRE) with blue/cyan filter.* ***B****) Paper belonging to LEICA DMRE microscopy and its factor (F) describing total number of BCZ squares on filter at 100x objective.*

Microscopic cell count

The purpose of microscopy cell count is to find "OD to cell/mL" linear regression relationship with a conversion factor: the slope. Finding the "OD to cell count" linear graph depend on OD of culture on filter and the associated counted cell number on that

specific filter.

Microscopy cell count was done in dark environments under UV-light by *LEICA DMRE* microscope with 100x objective with oil immersion (*Leica*, type-F without auto-fluorescence). Visible cells were counted within BCZ-squares, until reaching approximately 200 cells in total. This made the basis for average cell number/mL culture through equation (Eq. 2), and an example that followed numbers from calc. 1.(a-b) is illustrated in Table 1.

Table 1. *Example values from calculation 1(a-d) that make out the linear relationship "cell count to OD". The final goal is shown in bold as "Cells/mL".*

Calculation Units	Example value	(Calculations by conversions)
BCZ Square*:	**33**	
F-factor:**	2010000	
OD:	0,014	OD_{600}
SUM:	205	cells
AVG:	6,21212121	cells/BCZ square
	1,25E+07	F*cells/BCZ
	1,25E+07	**cells/mL**

**BCZ squares are Counted until SUM of cells reaches ~200*

*** Total number of BCZ-squares on filter at100x objective.*

$$\text{Cells/mL} = \frac{(\text{SUM cells/BCZsquares}) * \text{F-factor}}{\text{culture volume on filter (mL)}} \quad \text{(Eq. 2)}$$

Dry weight (Biomass)

P. aeruginosa PAO1 and *P. aeruginosa* the type strain was cultivated, washed, pelleted and dried before determining their initial biomass (mg/mL/OD_{600}).

3 L of autoclaved Sistom`s Medium was inoculated with 50 mL culture and incubated under oxic conditions with continuous stirring (extra large magnetic bar, 500 rpm) at room temperature for approximately five days. Cell density was followed by spectrophotometry, and cells were harvested during exponential growth (OD_{600}=0.45). The culture was split and weighted into equal volumes of 3x 1L. This was pelleted by centrifugation at 10, 000 x g (6330 rpm) for 40 minutes at 4˚C, and OD_{600} of supernatant was determined and discarded. The centrifuge was set at max acceleration and slow deceleration (Avanti™ JLA-26S XP, Beckman®). Three washing stages followed, where the four cell pellets were resuspended in 300 mL sterile isotonic salt solution (15

mM NaCl) and distilled water, and centrifuged at 10, 000 x g (6330 rpm) for 40 minutes at 4˚C (rotor JS-rotor,Avanti™J-25, Beckman®). After confirming that the supernatant was cell free (OD_{600}), it was discarded and the cell pellets were collected in a final volume of 200 mL H_2O and left in an 70˚C hot air oven until weight was stable. The dry biomass was weighted for 5 minutes to correct for water-absorption from ambient air during transport from hot air oven to weighting area, and during the weighting.

Growth curve

The purpose of performing growth curves is to determine μ and doubling time from the growth curve`s log linear exponential phase (Appendix, fig.II). Pre-cultures were raised under oxic conditions in nitrate free medium, or under anoxic conditions with 2 mM KNO_3, at 20˚C. 1 mL of exponentially growing cultures (OD_{600} 0.09) were then transferred to new aerobic or anaerobic vials in triplicates with 0 or 7 mM KNO_3, respectively. Before all measurements, a control, containing 1 mL milliQ-H_2O in a cyvette was used to set the zero-absorbance at 600 nm. Frequent sampling (0.8 mL) and determination of OD_{600} by specrophotometry was used to monitor subsequent growth. Optical density with time gave log linear relationship with slope as μ.

Specific growth rate and generation time

Specific growth rate (μ d^{-1}, h^{-1}, or min^{-1}) of a bacterium is the rate at which a cell divides. It is tightly connected to cell doubling, or generation time (t_d)[9] (Eq.3):

$$\mu = \frac{ln2}{t_d} \qquad Eq.3$$

and the number (N) of cells in a culture at a given time (t) is given by:

$$N = N_0 e^{\mu t} \qquad Eq.4$$

Where N_0 is the number of cells at time 0. Essentially, μ and T_d together make the slope in the log linear relationship of "OD to time" (Eq.4).The highest μ gives the shortest generation time, T_d. The μ and t_d from aerobic and anaerobic growth curves were determined at standard temperature (20˚C) for PAO1, the type strain. Doubling time was used to predict when early-exponential growth phase (0.05-0.09 OD_{600}) was

[9] Doubling time (t_d) means a doubling of Abs_{600}-value during that time.

reached during pre-cultivations and experimental inoculation.

Experimental systems

Robot incubation system and NOA-system

Gas and nitrite measurements

An in-house designed, semi-automatic incubation system for gas measurements were used for frequent headspace-sampling by an auto-sampler (robotic sampling-arm) connected to a gas chromatograph (GC) and an NO-analyzer (fig.8). The setup has two different channels: one is channelled to a micro GC with 15 stirred cultures in a thermostatic water bath, and the other channel is connected with a traditional GC (Agilent 7890A) and is connected with a larger thermostatic water bath with room for 30 stirred cultures (Molstad et al., 2007). NO_2^- is measured manually in the Sievers NOA 280i (fig.9). The setup yields rich datasets of all relevant substrates and products of aerobic respiration and denitrification: O_2, CO_2, NO_2^-, NO, N_2O and N_2 (Molstad et al., 2007).

During physiological experiments, the depletion of O_2 and accumulation of relevant gaseous products (CO_2, and NO, N_2O, N_2,) are monitored by a Roboplot software in cultures during transitions from aerobic respiration to denitrification (Appendix, fig.III). In each experiment, 15 parallel batch cultures (120 mL serum flasks) fitting into a water bath, are single-sampled from headspace at specific time points managed by software programme (Python) connected to the robot arm. Every vial-headspace is sealed off from the environment by butyl-rubber septa and aluminium crimp caps. Then, they are made anaerobic and free form ambient nitrogen by replacing the atmosphere with Helium in a series of evacuations and gas fillings. Sealed flasks cleared from air should not leak any significant amounts of ambient air or gas produced during an experiment.

In addition, standard calbration is made by running three gas-controls (ambient air, N_2O and NO) to assure a set of responsefactors that are used to calibrate and correct for minor leakages (High standard, or 10000 ppm (1%) CO_2 and 150 ppm N_2O in Helium), and dilution (low standard, or ambient air 210000 (21%) O_2 and 780000 (78%) N_2). An additional NO standard for responsfactor on NO contains 25 ppm NO in N_2.

Helium washed flasks with Sistrom´s medium were put in the water bath at 20˚C for 30 minutes, to adjust pressure against the experimental temperature. 3.5 mL oxygen

was added with a gastight syringe to make 4 % initial oxygenic atmosphere. This condition is used to investigate adaptations, which denitrifying organisms must make when experiencing the transition from oxic to anoxic enviroment.

Nitric Oxide-Analyzer (NOA) (fig.9) measures the nitrite. This technology consists of a chemical set up containing reducing reagent (for converting NO_2^- to NO), and detects NO with an accuracy of nanomolar concentration. The system is sealed off from lab-the environment with glass, septa and plastic weirs. A continuous flow of nitrogen gas (N_2) (in 5 psi; 0,5 bar; 5.2 Torr) is bubbling through the reducing agent. As a result, any nitrite injected with the metal syringe (typically a 10 µL sample of cell culture) will be reduced to nitric oxide gas (NO), which becomes transported by the inert N_2 through the system, and perceived by chemiluminescence by the NO-Analyzer.

A dilution series of KNO_2 in H_2O (2000 µM; 200µM; 20 µM; and 2 µM) was used as standards. These were injected into the NOA system at regular intervals between injections of samples to get a response factor for assuring correct nitrite estimations per sample (Appendix, tab.II).

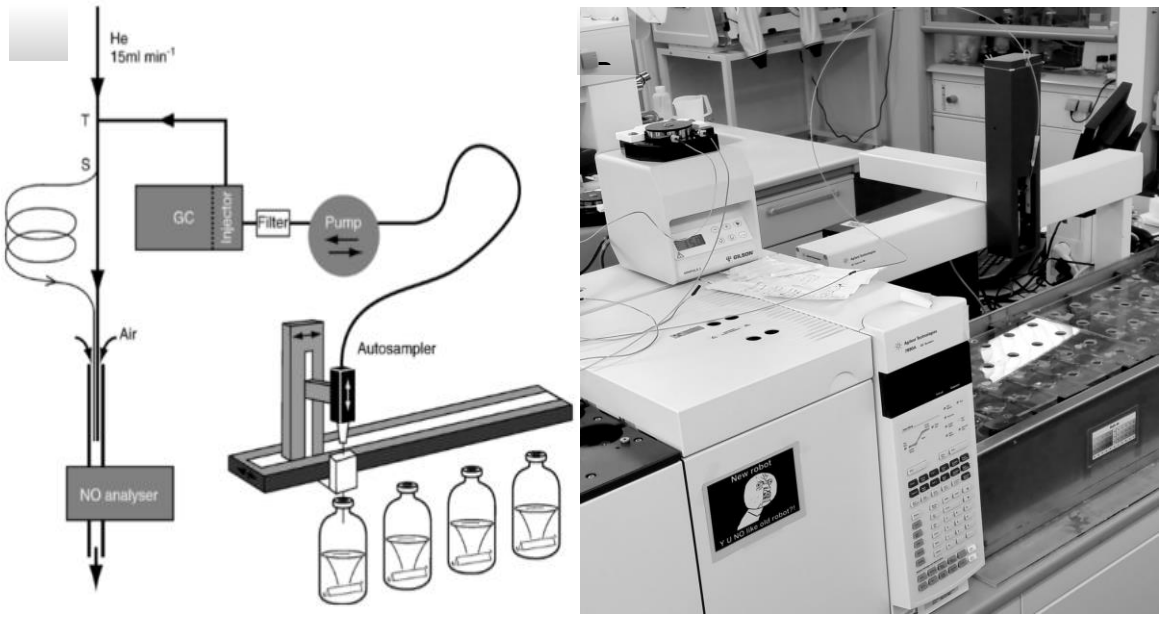

Figure 8. *The robotic incubation system (schematic diagram to the left (**A**), and photograph to the right (**B**)), used for measuring gasses (O_2, N_2O, N_2O, N_2, and CO_2). Transported gases carried by Helium gas, flow from the autosampler and is channelling either through a traditional GC (Agilent 7890A) or the microCG (Molstad, et al. 2007).*

Figure 9. *The nitric oxide (NO)-Analyzer (NOA) (Sievers NOA 280i) and its chemical set up. Left panel: Gas – over, and – under pressure through plastic & glass tubes make out the system for determining the nitrite concentrations (nM to mM concentrations). To the right: the NOA (the tallest, white box with blue display). A sample is injected manually into a rubber-sealed glass-system. There, nitrite traces in sample will react with a reducing agent (NaI in 50 % acetic acid) which converts nitrite into NO. Inert N_2 bubbles through the reducing agent, and thus carries the NO through the glass- and plastic wires. At the endpoint, the NOA detects NO through chemiluminescence.*

Table 2: *Standard conditions during physiological experiments performed in the micro GC, unless otherwise mentioned in the experimental protocol.*

PROTOCOLL ISSUE	SPECIFIED ISSUE	DETAILED ISSUE
Cultivating Technique	Batch culturing	Pre-cultivation and experimental incubation
Growth medium	Sistrom´s medium (Sistrom WR., 1962)	1 X dilution of Stock solution (10X Sistrom`s Medium)
pH	7.02±0.02	10 M KOH
Volume (mL)	50	
Stirring (rpm)	500	Large magnetic bars
Oxic conditions (mL)	3.5	4 % initial O_2
	6	7 % initial O_2
Anoxic conditions (mM)	2	100µmol-N total, KNO_3
Temperature (˚C)	20	

Designing primer pairs

Primers are necessary to amplify denitrification genes (*napA*, *narG, nirS, norB*, and *nosZ*) and QS circuit genes (*lasR-lasI and rhlR-RhlI*) through the Polymerase Chain Reaction (PCR). Primers suitable for traditional PCR as well as quantitative PCR (real-time and droplet digital PCR) were designed using NCBI`s Primer-Blast (Ye et la., 2012), and a Primer3 software. For practical purposes, I attempted to design one primer pair that fitted both strains (PAO1 and the type strain). All primer pairs were then purchased from ThermoFisher Scientific AS, Norway. The primer`s specificity and accuracy (product length) were tested by running a control with ordinary PCR followed by gel electrophoresis and viewed by UV imaging system (Molecular Imager® Gel Doc™XR Imaging System). In addition, PCR efficiency as well as specificity was tested using real-time PCR with melting curves.

When designing primer pairs, annotated denitrification genes and genomes of *P. aeruginosa* PAO1(DSM 22644) were found as FASTA sequences and blasted against the type strain genome (DSM 50071). Genomes were downloaded from NCBI as GenBank (.gz): files that are readable in the genome browser *Artemis*-program (Sanger Institute) (NCBI, 27.11.2016). However, both Artemis and NCBI lacked any genome annotation in the type strain DSM 50071 (Accession number for FASTA sequence in NCBI: NZ_CP012001.1/CP012001.1). Therefore, only the PAO1 genome annotations were used as reference for finding similar sequences in the type strain genome.

The original platform at NCBI is called Primer-Blast, which made a suggestion list of primer pairs, resulted in unspecific *napA* and *nirS* PCR products when checked by real-time PCR and melt curve.

A clean melt curve should give only one T_m for PCR product. Because the type strain and PAO1 have different genomes, they did not align well at *napA*gene. Real-time PCR gave a melt curve that revealed impurity from *napA* primer pair on PAO1 DNA, and it was concluded that low homology made unspecific primer pair design for *napA*gene. Gel picture of *napA* PCR product in the type strain revealed weak bands: i.e. poor PCR product yield, which also Qubit confirmed by low measurements (ng/mL).

As there was little accuracy in primer pair designed for *napA* and *nirS*, one new attempt was made in another platform, "Primer3". A new attempt was also performed for *nirS*, where resulting primer pair (Psa_nirS) is presented in Table 3, below.

However, melt curve of PCR product revealed secondary products from reactions with this Psa_nirS F/R primer pair. Hence, new primer pair for nirS was made (nirS_PAO1)(tab.3), and melt curve was considered to not contain any secondary structure.

LasR-lasI and *rhlR-rhlI* primer pairs derived from Wang et al., (2015) and were used to confirm deletions in PAO1 *lasI⁻rhlI⁻* mutant vs PAO1-UW before performing the two larger physiological experiments (tab.4).

Troubleshooting:

When blasting genome of PAO1 with the type strain (making a sequence-alignment algorithm BLASTP44), I looked for the best hits above a stringent comparison threshold (an expect value of 10-5) (Stover et al., 2000). This test confirms that the type strain should be a sensible comparison partner for PAO1 when designing one primer pair for both (Stover et al., 2000). Therefore, PAO1 gene FASTA sequence from Artemis was used to find gene FASTA sequences of *narG, nirS, norB* and *nosZ* in the type strain. CLUSTALW (Primer3-platform) and NCBI Primer Design Tool was used to design a list of relevant primers by aligning gene FASTA sequences of the two strains. The appropriate primer pairs (forward and reverse) were chosen from the list according to a set of rules (PrimierBiosoft, 25.11.2016). This list also agreed with rules listed by the platforms and Primer designing tools, and contained: Primer stability, primer specificity, the resulting base pair length, how to avoid stabile secondary structures, and GC content.

Primer Stability: The melting temperature (T_m) a of primer pair is the melt temperature of the less stabile primer-template. To maximize the PCR product yield, the stability of the two primer-template pairs should be as equal as possible in accuracy towards a region. The difference of 5°C or more can lead to no amplification. Where too high T_m produce insufficient hybridization between primer-template with low PCR product yield, too low T_m may lead to non-specific products caused by a high number of base pair mismatches. Because mismatch tolerance is found to have the strongest influence on PCR specificity, it was therefore important to find as equal temperature between the two primer templates.

Primer specificity was tested by a score ID from blasting reverse and forward primer sequence against *P. aeruginosa* PAO1 genome in NCBI ("Alignment tool for two or more sequences using BLAST"). The Score revealed a 99-100% ID (Expected value, E=0,00004), which means high specificity, where the chance is one per hundred thousand, of primer template binding somewhere else in that genome. Furthermore, to improve specificity of the primers it is necessary to avoid regions of homology. Most importantly, homology between and within primer pairs were checked in order to avoid any self-dimerisation or cross-dimers during annealing. However, none of the primer pairs were put into the same mastermix, so homology between primer pair were

considered irrelevant.

The resulting base pair length of primers was 20 bp (tab.3). This is a normal length for PCRprimers: a length that accurately bind specific genome region, while keeping the melting temperature within the desired range. Repeated base pairs in a primer was avoided as they more readily bind elsewhere to the genome, and no more than 4 repeats in a primer could be tolerated.

To avoid stable secondary structures, the designed primers must originate from a template region that does not form stable secondary structures during PCR reactions. The potential of secondary structures from designed primer pairs were predicted using self-complementarity through Biotools, 03.02.2016.

A primer can be located near the 5' end, the 3' end or anywhere within specified length of the gene-sequence of interest. Generally, the sequence close to the 3' end of a gene is known with greater confidence (Premierbiosoft, 25.11.2016). However, that depends on the algorithms during sequencing, which are trimming the reads according to a given threshold. Whether they work at the 5' end or the 3'end, or both will give a statistical level of confidence to that end sequence. If it works at the 3' end, this end is more confident. For example, the Sickle algorithm, which reads from 5' end towards 3'end, identify the cut position when the threshold quality of reads are less than a given value (Del Fabbro et al., 2013). When it comes to the primer`s own 3' end, there are stability criteria, which say that the 3'-end should actually be a bit unstable to ensure less false priming. However, the primer`s clamp (within the last 5 bases from the 3'end) if containing G or C, will help promote specific binding due to stronger bondage within DNA structure (but more than three should be avoided).

The G+C content in a primer should be between 40-60 % of the total bases (DNA BASER, 11.11.2016). The G+C content is the number of G's and C's in the primer as a percentage of the total bases. Primers contains between 50 and 60 % GC (tab.3).

Table 3. *Primer pairs designed to amplify denitrification genes (napA, narG, nirS, norB, and nosZ). They were used in traditional PCR (end-point analysis by gel electrophoresis: fig. 8,9,10, Results), and quantitative PCR techniques.*

Sequence (5'->3')	Template strand	Length	Tm	GC%	Product length (bp)
TP_napA_F: CAGACCGACCTGATCATCCT	Plus	20	49	55.00	
TP_napA_R: CAGGGTATAGGGCTTGACGA	Minus	20	49	55.00	
					234

Psa_narG_F: GACGAGAAGATCCGCTTCCG	Plus	20	51	60.00	
Psa_narG_R. CTGAGCCAGATGATCGGACC	Minus	20	51	60.00	
					389
Psa_nirS_F: GATCCGAAGAACCATCCGCA*	Plus	20	49	55.00	
Psa_nirS_R: GTTCCACACCGAGAACCAGA*	Minus	20	49	55.00	
					297
nirS_PAO1_F: AGAAAGTCGCCGAACTACAG	Plus	20	49	50.00	
nirS_PAO1_R: AGGTTCTTCAGGTCGAACAC	Minus	20	49	50.00	
					125
Psa_norB_F: TACTTCGTGTTCGCCCTGAT	Plus	20	47	50.00	
Psa_norB_R: GTACAGCTCGCAGTCGCTCT	Minus	20	51	60.00	
					212
Psa_nosZ_F: CGGCAAGTACCTGTTCATCA	Plus	20	51	50.00	
Psa_nosZ_R: GTACAGGGTGAAGGCGTTGT	Minus	20	47	60.00	
					243

*Psa_nirS was used only on preliminary studied PAO1 and the type strain, due to poor melt curve.

Table 4. *Primer pairs designed to amplify quorum sensing regulator genes (rhlI, rhlI$^-$, rhlr, lasI, lasI$^-$, and lasr).*

Sequence (5'->3')	Strain	Template strand	Length	GC %	Product length (bp)
RHLI_F: GTCTTCCCCCTCATGTGTGT		PLUS	20	55	
RHLI_R:CCGCAGAGAGACTACGCAAG	**WT**	MINUS	20	60	850
	MUT				~400
RHLR_F: GAATTGTCACAACCGCACAG	**WT+**	PLUS	20	50	
RHLR_R:CACACATGAGGGGGAAGACT	**MUT**	MINUS	20	55	1040
LASI_F: TCTCTCGTGTGAAGCCATTG		PLUS	20	50	
LASI_R: ACCCACAGCATCGATCTACC	**WT**	MINUS	20	55	999
	MUT				~500
LASR_F: GTGGGCTGACTGGACATCTT	**WT+**	PLUS	20	55	
LASR_R: TCAGAGCAATGGCTTCACAC	**MUT**	MINUS	20	50	1115

DNA extraction

Genomic DNA (gDNA) was extracted from culture sampled at end of exponential growth with the DNA extraction kit called QIAamp DNA Mini Kit (Qiagen).

Washing steps followed by three eluation steps was performed according to manual from QIAamp DNA Mini Handbook 02/2015 by QIAGEN. Additionally, 96-100% ethanol was added during isolation of DNA (fig.10).

Extracted DNA was stored in Eppendorf tubes at - 20˚C for subsequent PCR and primer pair check.

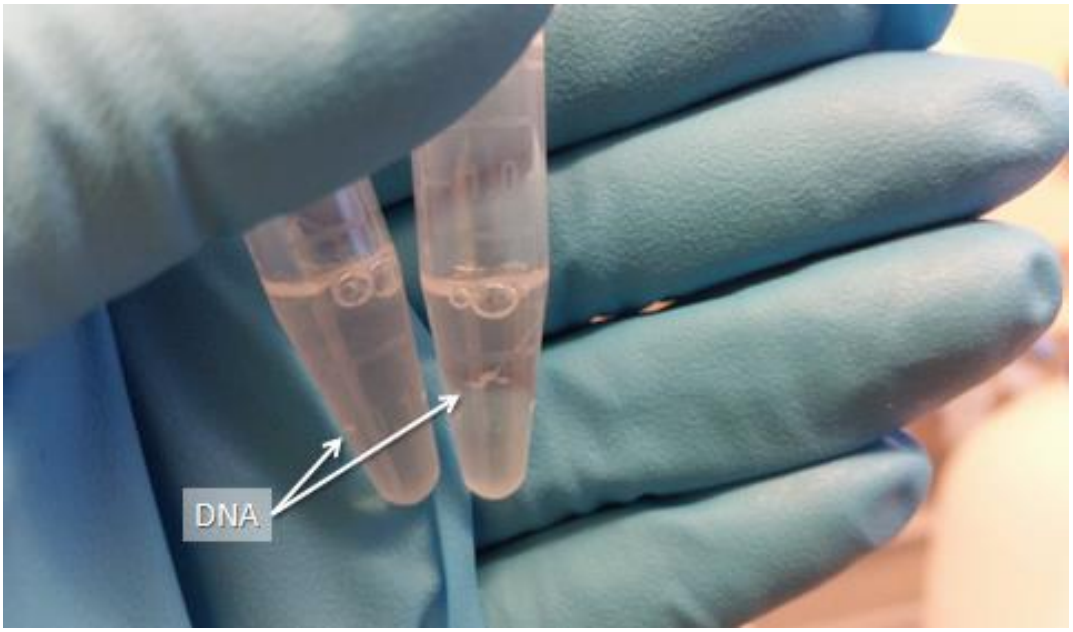

Figure 10. *DNA from DNA extraction of P. aeruginosa PAO1. Cold 96-100% ethanol shields the charge of negative phosphate group (PO_3^-) in DNA in order for dissolved positively charged salts to more easily bind with negatively charged DNA, which then becomes hydrophobic and precipitates into visible threads in the liquid.*

PCR and gel electrophoresis

The primer pairs were tested on isolated genomic DNA from PAO1 and the type strain, as well as PAO1-UW and PAO1 *rhlI*$^-$*lasI*$^-$ mutant by following protocol from TaKaRa Bio-Inc. Kits (tab.5).

Subsequent gel electrophoresis was performed to identify the expected gel band size of the respective sequences from the denitrification genes and the LasI$^-$RhlI$^-$ deletion in the mutant.

2 % Agarose gel was made by adding 1 or 2 gram Agarose (SIGMA, Life Science) in 50 or 100 mL 1X TAE buffer (depending on the electrophoresis apparatus). This was mixed by heating and gentile boiling. Upon cooling to ~50˚C, 3 or 5 µL DNA/RNA dye was added (peqGREEN Dye from peQlab). Ladders were made of 7 or 14 µL of 100 bp ladder (NEW ENGLAND Biolabs®). Wells were filled with 7 or 14 µL PCR product with 3 or 5 µL loading dye (NEW ENGLAND Biolabs®). PCR products were separated between plus and minuse electrodes by gel electrophoresis at 90V, for 35 minutes (PowerPac300, BIORAD). PCR products, present in gel-bands were visualized (Gel Doc™XP, Molecular Imager®) and adjusted to proper light intensity through a gel picture (Quanta One 4.6.7 Software, BIORAD).

Table 5. *Mastermix per reaction and PCR conditions during traditional PCR following the TaKaRa Bio-Inc. Kits (Takara Ex Taq™ and TakaRa PrimeSTAR GXL DNA).*

Component	µL in 50 µL rxn	Program		Cycles
TakaRa PrimeSTAR GXL DNA Mastermix				
PrimeSTAR GXL DNA Polymerase (1.25 U/µL)	1	98˚C denaturation	10´´	30
5X PrimeSTAR GXL Buffer (Mg^{2+} plus)	10	60˚C annealing	15´´	
dNTP Mixture (2.5 mM each)	4	68˚C elongation	1 min	
primer F (0.2 µM)	1	4°C	∞	
primer R (0.2 µM)	1			
DNA template (50-500 ng/µL)	2			
ddH_2O	Up to 50			
Component	**µL in 25 µL rxn**	**Program**		**Cycles**
Takara Ex Taq™ mastermix				
Takara Ex Taq Poluymerase (5 units/µL)	0.125			
10X Ex Taq Buffer (with Mg_2^+)	2.5	98˚C denaturation	10´´	30
dNTP Mixture (2.5 mM each)	2	60˚C annealing	30´´	
primer F (10µM)	1	72˚C elongation	30´´	

primer R (10µM)		1	4°C	∞
DNA template (50-500 ng/µL)		2		
ddH2O	up to 25			

Experimental protocol

Investigating DRP in *P. aeruginosa* involved three incubatory experiments: a first experimentation with two different initial oxygen concentration to define DRP; two secondary experiments with AHL systems effect on DRP; and gene expression during DRP. The first, preliminary study contained two different strains: PAO1 and the type strain so as to compare DRP between them and characterize DRP in *P.aeruginosa* PAO1. However, based on the preliminary results, DRP by PAO1 strain needed further investigation, as the N_2OR activity was unexplainably slow in its N_2O reduction activity. Therefore, the AHLs systems study was made to characterize the phenotype of PAO1-UW and PAO1 *rhlI-lasI-* mutant by inhibiting QS and inducing QS (AHLs), respectively. The third experiment with gene expression would investigate regulatory phenotype difference at the transcriptional level of *narG, nirS, norB* and *nosZ* in PAO1-UW and PAO1 *rhlI-lasI-* mutant.

Pre-cultivation and inoculation

All pre-cultivations and experimental inoculations of PAO1, the type strain, as well as PAO1 *rhlI-lasI-* mutant, and PAO1-UW followed standard conditions, unless otherwise mentioned (tab.2). T_d at standard temperature (20°C) was used to predict when early-exponential growth phase (0.05-0.09 OD_{600}) was reached during pre-cultivations in order to perform controlled experimental inoculation (every inoculums should contain the same amount of cells). Two reasons for predicting when early exponential growth phase is reached: *i)* to predict density of aerobic cultures by their doubling time in order to avoid aggregation. *P. aeruginosa* have a great tendency to aggregate during mid-exponential growth (OD_{600}=0.2). Aggregation creates uncontrolled microenvironments of potential hypoxia (oxygen-depletion). Cells experiencing hypoxia during aggregation may induce expression of denitrification proteins.

ii) Importantly, predicting early-exponential growth (0.05-0.09 OD_{600}) by doubling time gives thin inoculum that dilutes potential old denitrification apparatus. Therefore, all pre-cultivations occurred from two to three sequential thin inoculations (0.05-0.09 OD_{600}) with aerobic inocula.

The reasons i) and ii) are both to important to avoid inoculating experimental

flasks with denitrification proteins that represent potential confounding variables[10].

1. First experimentations

To determine DRP of *P. aeruginosa* ssp., two strains (the type strain and PAO1) were exposed to different initial oxygen treatments (0, and 7 %). O_2 consumption and accumulation of NO_x (CO_2, O_2, NO, N_2O, and N_2) were monitored by a by the semi-automatic GC-incubation system (Agilent 7890A) during the transition from oxic to anoxic conditions in batch cultures (fig.8). 200 µL liquid samples were manually separated for quantification of nitrite through reduction to NO and detection by chemiluminescence (NOA-system) (fig.9). Nitrite was subsequently calculated as µmol NO_2^- by a nitrite standard (Appendix, tab.II). This set-up yielded rich datasets of all relevant substrates and products of aerobic respiration and denitrification for comparing *P. aeruginosa* PAO1 and the type strain under standard conditions.

2. AHLs systems experiments

To test QS-effects on denitrification, flasks with sterile Sistrom´s medium were added a QS inhibitor, N-Decanoyl cyclopentylamide (C10-CPA; Ishida et al., 2007), to PAO1-UW and N-(3-oxododecanoyl)-L-homoserine lactone (3-oxo-C12-HSL) and N-butyryl-L-homoserine lactone (C4-HSL)(Toyofuku et al., 2007) to PAO1 *rhlI- lasI-* mutant cultures (tab.6).

AHLs and C10-CPA were dissolved in sterile filtered (0.2 µm Acrodisc® Syringe Filters with PTFE Membrane, PALL corporation) DMSO[11] to 2mg/mL and 290 mM, respectively, and stored under Helium atmosphere at 4˚C. AHLs and QS inhibitor were serial diluted from stock and finally added with sterile syringes before sealing and He-washing of autoclaved Sistrom´s medium flasks (tab.6).

Stock solutions of C10-CPA were 290 mM and diluted into final concentrations of 250 with sterile syringe by a serial transfer of ~150 µL to sterile Eppendorf tube. 43 µL

[10] Confounding variable: a statistical term on an extraneous (additional) variable that explains away (significantly correlates with) both the dependent and independent variable in a statistical model (experiment) (Løvås, 2004).

[11] DMSO: Dimethyl-sulfoxide. DMSO solvent has a melting point of ~18˚C, and when solved in water has a freezing point at 15˚C, and does not need to be stored in freezer and will be kept well under refrigerated conditions.

from Eppendorf tube was injected directly into 50 mL medium flask.

Stock solution of C4HSL was stored as 2 mg/mL and transferred in exact volumes used with C10-CPA.

Stock solution of 3-oxo-C12-HSL was also 2 mg/mL. After transfer to sterile Eppendorf tube, a sterile syringe was used to dilute 26 µL stock solution in 124 µL DMSO. 43 µL of this directly diluted into 50 mL medium flask.

Table 6. *Concentrations of AHL signals and inhibitor during experimentation with P. aeruginosa PAO1*-UW *and rhlI*$^-$*lasI*$^-$ *mutant.*

Signal molecule	Action	Final concentration (µM)	Source:
C10-CPA:	Inhibits both quorum systems (*rhl* and *las*).	250	(Ishida et al., 2007)
C4-HSL:	Activates receptor of the Rhl system.	10	(Toyofuku et al., 2007)
3O-C12-HSL:	Activates receptor of the Las system.	1	(Toyofuku et al., 2007)

Experimental setup

The AHL systems experiment was setup in the micro GC incubating 6 vials of PAO1-UW and 9 vials PAO1 *rhlI*$^-$*lasI*$^-$mutant, with the expectation that their respective phenotypes under QS-inhibition (C10-CPA) and QS-induction (AHLs), respectively, would be characterized (tab.7). These were incubated at standard conditions in sterile Sistrom´s medium with 4 % initial O_2 (3,5 mL 100% O_2) (tab.2).

The experimental set-up is designed with the assumption that the same phenotype observed at 0 % initial O_2 in preliminary results is expected at 4 % initial oxygen. This ensured a higher cell density that resulted in the expected phenotype of N_2O accumulations without having as high a rate as the anaerobic respiration rate that followed from 7 % initial O_2 respiration. Respiration of 7 % initial O_2 tended to produce a DRP that was abruptly over within the five first robot measurements. A better resolution of the phenotypes will follow in this particular set-up (tab.7). Expected N_2O accumulations from functional QS systems in PAO1-UW (treatment control, n=3) will be identical in phenotype with N_2O accumulations from cultures treated with exogenous AHLs. The phenotype of PAO1 *rhlI*$^-$*lasI*$^-$mutant lacking the functional QS systems (treatment control), will be identical in phenotype with the phenotype from PAO1-UW added a QS-inhibitor (C10-CPA). Gas measurements were performed using the Micro-GC, and nitrite was measured every 3rd hour from 2 out of 3 replicate vials. Cell density

(OD_{600}) was measured in the aerobic inocula and in experimental cultures after depletion of electron acceptors (end of experiment).

Table 7. *QS-experiment: AHL signals and QS inhibiotors on PAO1*-UW (wild type) *and PAO1 rhlI⁻lasI⁻ mutant.*

***P. aeruginosa* PAO1**	**Replicate flasks**	**Treatment**	**Expected result**
wild type	3	Control on functional QS	The N_2O reductase (encoded by *nosZ*) is blocked, and the available nitrate-N recovered as N_2O-N.
rhlI⁻lasI⁻	3	Control on non-functional QS	Minimal N_2O accumulation and full recovery of nitrate as N_2.
wild type	3	C10-CPA	Both systems of las and rhl are blocked and we expect minimal N_2O production, and nitrate fully recovered as N_2.
rhlI⁻lasI⁻	3	C4-HSL	C4-HSL activates RhlR (receptor), while no stimuli on LasR will occur. We expect minimal N_2O, even though it might become higher than *rhlI⁻lasI⁻*mutant alone, and full recovery of nitrate as N_2.
rhlI⁻lasI⁻	3	3O-C12-HSL	The LasR will be stimulated and we expect a phenotype closely similar to the wild type: i.e. N_2O accumulation.

3. Gene expression experiments

In order to further compare DRP of PAO1 *rhlI⁻lasI⁻*mutant and PAO1-UW, denitrification phenotypes were monitored for each of them while gene transcripts were sampled and cell densities measured to find the gene expression/cell. This experiment occurred under the assumption that the QS-experiment (tab.7) went as expected. The set-up design for RNA sampling from PAO1-UW and PAO1 rhlI⁻lasI⁻mutant contained six different sampling times with biological replicates of three vials that subsequently were discarded after sample preservation (tab.8). Nitrate and cell density (OD_{600}) were measured simultaneously with sample preservation.

Every run occurred in standard conditions of 4 % initial O_2, 2 mM nitrate (KNO_3), at 20˚C (tab.2). Experimental setup was first restricted to the PAO1-UW incubating in

the micro GC. The PAO1 rhlI⁻lasI⁻ mutant incubated in the microGC during second setup run. Both runs followed the same set-up design (tab.8). RNA samples were taken by harvesting culture directly from flasks, which were subsequently discarded (†), or put back into micro GC (∘). Last sampling time included both sampling for RNA preservation (5 mL) and gDNA isolation (2 mL). While preserving samples for gene analysis, 1 mL culture from each vial was put aside on ice, for simultaneous measure of immediate OD and nitrite.

Sampling procedure and preservation

Samples for gene expression analysis, collected from different time points (1) Semi-aerobic; 2) Declining O2; 3) Increasing NO; 4) NOmax/N_2Oincrease; 5) N_2Omax/N_2increase; 6) End) were treated as efficient as possible with RNA protect to stabilize intracellular RNA from mRNA degradation. Oxygen exposure inhibits ANR transcriptional regulator in the cells. The sudden stop of transcription does not stop the RNAdegradation time as well, which for mRNA is quite short. To not loose high levels of transcripts produced during anoxic condition, between RNAsampling from culture through centrifugation until cells are protected by RNApotect, the time is of essence. Cooling cells down to 4°C (on ice) will aid in lowering all biological processes, including the mRNAdegradation time.

Vials were collected on ice, and sample volumes from flasks were balanced upon transfer to pre-cooled falcon tubes by weighting. RNAsamples were pelleted by centrifugation the falcon tubes for 7 minutes, 10 000 x g at 4˚C using an Avanti ™ Beckman centrifuge with JA-12 rotor. Acceleration and deceleration were set to MAX to minimize time, under the assumption that cell pellets would not be significantly disturbed under a shortened the time between sampling and RNApreservation before adding RNA protect. The inocula (2 mL in duplicates) were centrifuged into pellets for 7 minutes, 10 000 x g at 4˚C in another centrifuge (KUBATO 3500).

Cell pellets were mixed with 1 mL RNAprotect® (Qiagen)[12] by pipetting, and transferred to 1,5 mL sterile RNase-free Eppendorf tube, followed by incubation at room temperature for 5 min. Subsequently, the tubes were centrifuged at room temperature for 5 min, at 8000 rpm. Pellets were not always visible; at least it never was in the first sampling time (1 and 2). Although supernatant was discarded, 100-200µL of the

[12] RNAprotect reagents are used and stored at room temperature in order to avoid precipitation at low temperatures.

supernatant remained with cell pellet to avoid loss of cells while discarding supernatant. Pellets were stored at -80˚C.

Table 8. *Gene expression: sampling for RNA extraction from batch cultures of P. aeruginosa PAO1 -UW and PAO1 rhlI-lasI-mutant.*

Sampling time	Biological replicates	Sample volume (mL)	Final action on flasks
0) Inoculum	2	2	
1) Semi-aerobic	3	50	†
2) Declining O_2	3	30	†
3) Increasing NO	3	10	†
4) NO max/ Increasing N_2O*	3	5	∘
5) N_2O max**/ increasing N_2	3	5	†
6) End	3	5	†
		2	

* Increasing N_2O: PAO1-UW. NO max: *rhlI-lasI*-mutant.

** N_2O max: PAO1-UW. Increasing N_2: *rhlI-lasI*-mutant.

†Exception from destroyed triplicates: same flasks are used in the next round of sampling. To account for the leakage and under-pressure created from sampling, volume loss was replaced by adding Helium before sampling of cell culture (for the PAO1-UW this occurred at stage 5 to 6. While for the double mutant this occurred, as planned from stage 4 to 5).

Sample processing

RNAextraction

RNA is easily degrades by enzymes called RNases, which exist ubiquitously in air, and on surfaces: glassware, plastic surfaces, benches, pipettors, gloves and skin. mRNA is particularly vulnerable to degradation and it is therefore essential to minimize the risk of contaminating samples with RNases from the surroundings. This was done by wiping all possible contaminating surfaces (except skin) with RNase AWAY® spray[13] (Molecular Bio-Products Inc): a surface decontaminant that inactivates RNases.

Cells are full of RNases, which degrades intracellular RNA, why RNAprotect® (Qiagen) was added immediately during RNAsampling. Here, I used the RNeasy® Mini Kit

[13] RNase AWAY® should not be used as a reagent: take care when cleaning plastic ware and tube-equipment that is used for reactions.

(Qiagen), with Quick-StartPrtocol, RNasey®Mini Kit, Part 1(Appendix, tab.III). This kit contains RNase degrading reagents for extracting total mRNA in a cell culture. The RNeasy Mini Kit provides silica-membrane RNeasy spin columns with a binding capacity of 100 µg RNA.

Finally, RNA concentrations in a small selection from each time series were measured by NanoDrop (NanoDrop®Spectrophotometer ND-1000) to confirm that RNAextractions were successful and samples (60µL) stored at -80˚C.

All samples were subsequently treated simultaneously with DNase, and isolated RNA concentrations were finally measured by Qubit, and reverse transcribed into the more stabile complementary DNA (cDNA).

RNA purification

Avoiding false positives is important when quantifying gene expressions. Genomic DNA (gDNA) is a false positive in cDNA synthesis (downstream protocol). DNase enzymes improve the RNA sample by digesting (cutting) remaining levels of gDNA, which potentially came as carryover from overloaded filers in spin columns, or with interfaces of RNA eluations.

All samples were thawed on ice after storage at -80˚C. TURBO DNA-free™ Kit (Thermo Fischer Scientific) containing DNase (TURBO DNA-free™ reagents) was used to destroy gDNA from RNA preparations. 2 µL TURBO DNase (2 Units/µL) was added to 30 µL RNA, and mixed gently together with 3 µL buffer (10x TURBO DNase buffer). Unlike what the protocol suggests, digestion was incubated at room temperature for 20-30 minutes with occasional, carefully up-ending of Eppendorf tubes, so as to keep the solvents mixed while not unnecessarily disturbing this, somewhat, fragile DNase activity.

To inactivate the DNase-enzyme, 3 µL (0.1 volume) DNase inactivation reagent was resuspended and mixed well with 5 minutes incubation at room temperature.

RNA quantification

RNA quantification by NanorDrop (NanoDrop®Spectrophotometer ND-1000) was utilized to confirm that RNA extractions were successful before storage (-80˚C).

NanoDrop is used to measure absorbance in the UV-Vis spectrum and can thus be used to quantify nucleic acids and proteins. All nucleotides (ssDNA, dsDNA and RNA) all absorb light at 260 nm, and the nanodrop does not discriminate between them. The ratio between the absorbance at 260/280 nm reflects the purity of DNA and RNA in the sample. DNA purity is good at ~1.8 ratio, while pure RNA has a ratio at 2.0. Lower ratios

in either case indicate impurities (protein presence, phenol, or other contaminants), which absorb strongly near 280 nm spectre of UV-light. Expected 260/230 values are commonly in the range of 2.0-2.2 for "pure" nucleic acids. If ratio is lower than expected, the "pure" sample contains contaminants (ThermoFischer Scientific, 26.11.2016).

Additionally, RNA needs to be quantified to normalize samples before cDNA synthesis. Qubit quantifies detected fluorescence from interaction between nucleic acid and Qubit reagents. Because it detects target-specific fluorescence instead of UV absorbance-based, like the NanoDrop, it is thought to be a more sensitive method for rapidly quantifying nucleic acids. Optimally, reverse transcription runs with the same amount of RNA templates (ng/µL) in each reaction. Therefore, RNA concentrations were quantified by Qubit to evaluate whether samples needed dilutions to avoid overloaded cDNA synthesis (i.e. normalization).

To measure purified RNA or DNA by Qubit®fluorometer (Invitrogen™) requires an RNA HS or dsDNA BR assay kit (Qubit® by Invitrogen), respectively, which provides working buffer, light sensitive reagents and pre-diluted standards. The Qubit protocol was performed as described by Invitrogen™Qubit™ assasy according to the target molecule of interest (RNA or DNA).

In this preparation part for cDNA synthesis, all qubit measurements had even RNA amounts, and therefore no additional dilution step for normalising samples was necessary.

cDNA synthesis

cDNA synthesis occurs by reverse transcription, which synthesizes complementary DNA (cDNA) from mRNA. All residual gDNA had to be removed with DNase treatment a second- or even third round, before any cDNA synthesis, which meant when until the real-time PCR of purified RNA gave zero positive signals from RNA samples. This, however, may lower the RNA concentration due to degradation both during prolonged storage, and incubation at 37°C during treatment with DNase reagents (TURBO DNA-*free*™ Ki).

To secure that sufficient RNA templates are included into the cDNA synthesis reaction, concentrations of RNA in all samples were checked by Qubit (ng/ µL). Optimally, reverse transcription (cDNA synthesis) of samples is run with the same amount of RNA templates (ng/µL) in each sample. Any normalization found necessary after Qubit measurements, were be done by dilution before proceeding to cDNA

synthesis. However, this was not found necessary due to even numbers from Qubit measurements.

The kit, Maxima First Strand cDNA Syntesis Kit (Thermo Scientific), contains a maxima Enzyme mix (transcriptase enzymes and RNase inhibitors), 5X Reaction Mix (reaction buffer, dNTPs, oligo $(dT)_{18}$ and random hexamer primers) and nuclease free Water[14]. Thermostabile Reverse Transcriptase (1 ng–5µg) and RNase inhibitor protects RNA template from degradation. In addition, the kit contains oligo $(dT)_{18}$ and random hexamer primers used to prime synthesis of first strand cDNA. The kit is made to ensure primers with high sensitivity towards RNA (low copy number transcript assays).

In order to asses for cDNA synthesis and assume it was 100% efficient, negatives in real-time PCR and cDNA synthesis are crusial to add. Negative control contains all reagents, except for the Maxima Enzyme Mix. This verifies the results of the first strand cDNA synthesis by assessing for gDNA contamination of the RNA sample. During real time PCR, a No Template Control (NTC) is used to assess for reagent contamination, and should contain all reagents for the reverse transcription reaction except for the RNA template. In addition, the Qubit concentrations of purified RNA samples were even (40 – 60 ng/µL), which assumes an optimal cDNA synthesis.

Mastermix reagents (Maxima, Thermo Scientific) had to be thawed, mixed, briefly centrifuged to remove drops form lid, and stored on ice (4°C). Mastermix per reaction were prepared in sterile, RNase free tubes on ice in the following order; 4 µL 5X Reaction mix; 2 µL Maxima Enzyme Mix; 1 pg–5 µg Template RNA (i.e. 14 µL extracted and purified RNA); and nuclease free water up to 20 µL total. Thus, the first dilution factor (14/20 µL) was noted for correction during final RNA concentrations/cell estimates. IN accordance to Maxima kit (ThermoScientific) PCR conditions for cDNA synthesis were: incubation for 10 minutes at 25˚C, followed by 15 minutes at reaction temperature 65˚C (chosen due to GC-rich genomes of *P. aeruginosa*)[15]. Reactions terminated by heating at 85˚C for 5 minutes.

---

[14] Nuclease free water is water free of endo-, exodeoxyribonucleases, ribonucleases and phosphatases.

[15] *P. aeruginosa* the type strain (DSM 50071) genome (6.32Mb) has only 95.8 % identical sequences with *P. aeruginosa* PAO1 (DSM 22644) or AE004091 (6.26 Mb)(DSMZ, 07.12.2016). Their difference is also reflected in GC content: PAO1 genome contains 66.6 % GC, while the type strain has 66.5 % GC, but both are considered GC rich organisms (>50% GC) (NCBI, 27.11.2016).
(>50% GC)(Khuu et al., 2007).

In preparation for ddPCR, cDNA was diluted as follows: time series: 0), 1) and 2) were diluted as 1:5. cDNA from time series 3), 4), 5) and 6), were diluted 1:10. All samples were then stored at -20˚C, ready for digital droplet PCR (ddPCR) preparation and quantification.

Preparation for ddPCR (dilutions)

When preparing cDNA samples for droplet generator, samples were diluted as not to be overloaded during reading by the digital droplet reader. Time series (already 1:5 dilutions) 0), 1) and 2) were diluted 1:5; time series (already 1:10 dilutions) 3), 4), 5) were diluted 1:100, and 6) was diluted 1:10. The dilution exception was for nirS, time series 3), as it was diluted 1:10. All these dilutions were accounted for, when calculating back towards final RNA/cell.

Quantitative PCR (qPCR)

Both real-time PCR and droplet digital PCR (ddPCR) are denoted the name: quantitative PCR (qPCR). The real-time PCR was used as an evaluation on RNA purity to confirm that all residual gDNA (flase positives) had been digestively treated by DNase. ddPCR was used to quantify cDNAcopies of all the denitrification genes (*narG, nirS, norB* and *nosZ*).

Both techniques are based on fluorescence signal sent by an unspecific intercalating agent (SYBR®Green I or EvaGreen) upon binding to DNA (fig.11). Another type of frequently used assay are product specific fluorescence signal sent by primers or probes (TaqMan) upon contact with nucleases at the specific DNA sequences. This creates more specific PCR products with less false positives (primer-dimers) in comparison to the sequence-unspecific agents. Overall, the fluorescence accumulates until it reaches a threshold above baseline[16] (background signal).

In real time PCR, this threshold is the first detection of PCR product and occurs in a specific PCR-cycle, called threshold cycle (C_T). Thus, this C_T-score is inversely proportional to the amount of template in the sample: i.e. the earlier detection the lower C_T-score and the higher template amount in the respective sample. Thus, the C_T-score

[16] Baseline is the background signal from sample. The mastermix reagent in real-time PCR, ROX, which is supposed to be equal in all samples, is used by StepOne Software v2.3 by Applied biosystems, to correct for pipett-mistakes (during mastermix-preparation).

is critical in quantifying the initial amount of amplified template. The fact that amplification is followed in real-time (*in situ*) and C_T-score is in strong correlation with the initial concentration of fragments enables the technical aspect of quantitative PCR (qPCR)[17]. Traditional PCR gives endpoint analysis where amount of product is not in consequence to initial concentration and cannot be used quantitatively. In these experiments, though, the real-time PCR C_T is simply used semi-quantitatively, which means that a sample`s concentration is determined as above/below the C_T score of a relative external standard. Procedure for mastermix and PCR condition was followed as described by SYBR® (Premix Ex Taq ™ II (Tli RNaseH Plus), by TaKaRa BIO) kit containing reagents for master mix and the intercalating dye SYBR® Green I reagent[18] (tab.9). Each sample`s amplification curve and melting curve was qualitatively checked against positive standards (10^3 and 10^2 copies/µL) and negative (nuclease free water).

The QX200 Droplet Digital PCR (ddPCR™) System (BIO-RAD) consists of two systems: QX200 Droplet generator, and a QX200 droplet reader (fig.12). Quantification of mRNA by ddPCR is an end-point analysis that gives absolute concentrations of *narG, nirS, norB* and *nosZ*, without the use of a standard. The droplet generator utilizes oil reagents and microfluids to partition each PCR reaction into ~20,000 nanoliter-sized droplets. In those partitions, a fewer number of template molecules are distributed (fig.13). Each droplet contains zero, one or more copies of the template as well as all components necessary to carry out PCR. Following PCR amplification, the droplet reader (second system) counts the number of positive droplets (containing amplified templates) and negative droplets (contain no amplified templates). The instrument analyzes each of the individual droplets in one sample using a two-color fluorescence detection system. A fluorescence threshold assigns positives and negatives for each sample. The absolute quantification by ddPCR does not require a standard curve as positive droplets[19] in each sample is statistically evaluated by QuantaSoft™ software with a total error from Poisson

[17] As C_T-scores are relative numbers, a standard curve, made of known amounts of template (10^2,10^3,10^4, 10^5 copies/µL), is required for template quantification. The log C_T-scores of a standard curve gives a linear regression that is used to calculate the initial concentration of templates

[18] SYBR® Green I reagent is an asymmetric cyanine dye, and requires care to avoid exposures to strong light when preparing the reaction mixtures.

[19] Droplets cannot be saturated in order to make a good Poisson confidence, and final ddPCR reaction mix must not exceed 5,000 copies of target/µL.

95% confidence limits (Applications guide for QX200, 01.12.2016). The Poisson distribution algorithm corrects for positive droplets among total number of accepted droplets and designate a Poisson confidence to the final absolute number of original fragments (fig.13). The mastermix and PCR conditions were performed according to QX200™ ddPCR EvaGeen Supermix[20] kit (BIORAD) (tab.9). One reaction was prepared as 20 uL and loaded into cartridges, which separately were filled 70 uL Droplet generation oil for EvaGreen per well (x8), and finally covered with a gasket (DG8™ Cartridges and Gaskets for QX200™ Droplet Generator). The droplet generator work with eight samples at a time in about 2 minutes (~30 min for a 96-well plate), where the appropriate droplet generator oil (70µL) is mixed with 20 µL reaction-mix containing 2 µL diluted cDNA.

After the droplet generator, samples are transferred and sealed (PX1™ PCR plate sealer foil) to avoid evaporation, into 96-well plate that fits both the ordinary PCR machine (for amplification), and the droplet reader (for quantification). The absolute quantification data are measured in copies/µL by QuantaSoft™software.

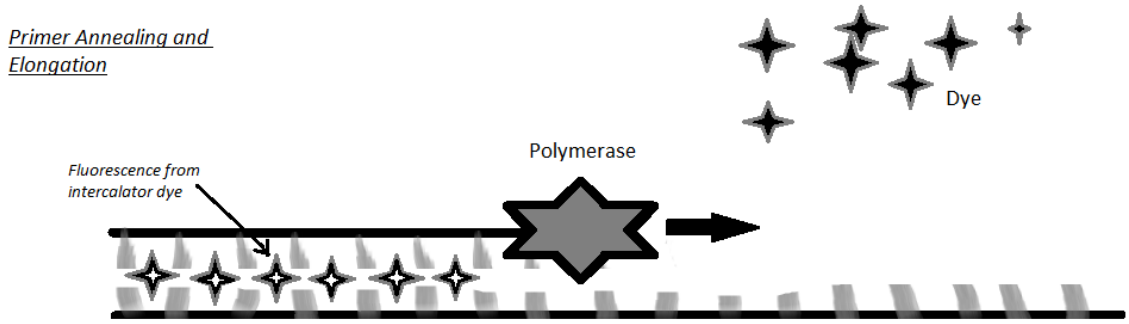

Figure 11. *The intercalating dye (SYBR® Green I) binds to dsDNA and emit fluorescence, which the real-time PCR system detects as signals. The dsDNA elongates by polymerase activity when designed primer pair and ssDNA (template) anneals. The subsequent events of PCR cycles allow an amplification that accumulates fluorescent signal, which is the real-time PCR system detects as an amplification curve. (Source: SYBR® Premix Ex Taq ™ II (Tli RNaseH Plus) Cat. #RR820A).*

[20] Supermix (reagents in the mastermix), after storage at -20 or 4°C, requires to be homogenized by vortexing, and brief centrifugation/spin-down before dispensing it into samples. This ensures that bottom contents are collected.

Figure 12. *QX200 digital droplet reader (left) and QX200 droplet generator (right). (Source: Instruction Manual for QX200, 01.12.2016).*

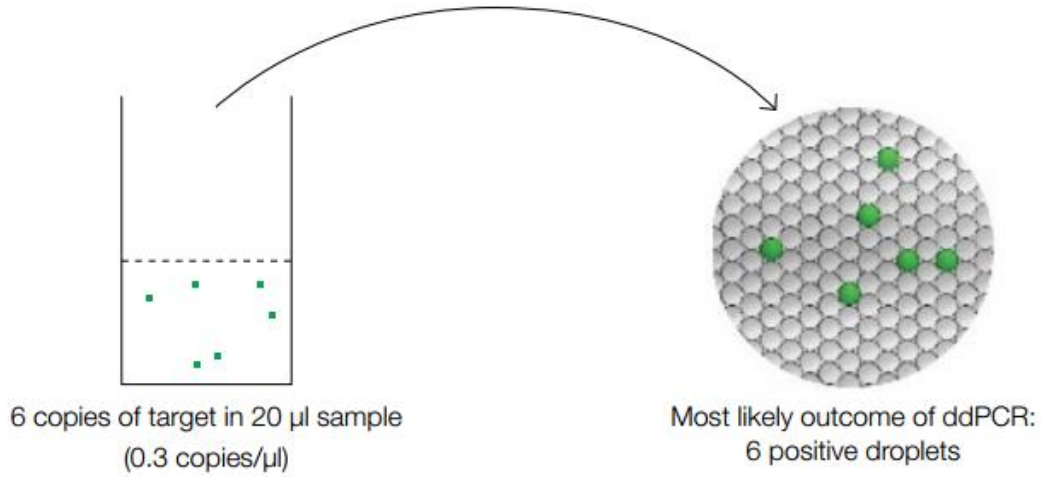

Figure 13. *Outcome of ddPCR in two modes of analysis: partition distribution in volumes of sample, and partition distributions among the 20,000 nanolitre-sized droplets (Source: Application guide for QX200, 01.12.2016).*

Table 9. *Mastermix and PCR conditions for qPCR following TaKaRa BIO-kit (real-time PCR), and BIO-RAD QX200™ ddPCR EvaGeen Supermix-kit (ddPCR).*

qPCR				
Real-time PCR				
Component	**µL in 20 µL rxn**	**Program**		**Cycle**
SYBR® (Premix Ex Taq ™ II (Tli RNaseH Plus), by TaKaRa BIO) mastermix				
(1X) SYBR® Premix Ex Taq II (Tli RNaseH Plus; 2X)	10	95°C denaturation	30´´	40
(0.4 µM) PCR F Primer (10 µM)	0.8	60°C annealing/elongation	30´´	
(0.4 µM) PCR R Primer (10 µM)	0.8	4°C	∞	
(1X) ROX Reference Dye (50X)	0.4			
Template ("pure" RNA)	2			
ddH2O	6			
ddPCR				
Component	**µL in 20 µL rxn**	**Program**		**Cycles**
QX200™ ddPCR EvaGeen Supermix (BIO-RAD) mastermix				
EVA (2x) supermix	11	95°C denaturation	30´´	
(0.2 µm) F primer	1	60°C annealing	30´´	40
(0.2 µm) R primer	1	72°C elongation	30´´	
Template (cDNA)	2	4°C stabilizing	5´´	
ddH2O	5	90°C stabilizing	5´´	
		12°C	∞	

Melt point curve

A melt curve was used to evaluate designed primer pairs 'specificity by analysing melting points derived from the PCR products. In addition to monitoring amplification *in situ*, the real-time PCR system performs a melt curve of the PCR products (T_m -curve). The PCR products (amplicons) are typically longer than secondary, unspecific products

and are thus expected to melt at a higher temperature. The purity of a compound is determined by its melting point range: if wide, and many melt-points, then impurity exists; and if short and singular (for example: 125 – 125.5˚C), the compound is considered pure. That way, it is possible to test for false positives, such as primer-dimers or unspecific products.

To confirm if unspecific products exist in the PCR products, real-time PCR system (StepOnePlus™, Applied Biosystems) performs a melt curve (T_m -curve) immediately after amplification. The melting curve by the real-time detects decreasing fluorescence when DNA denatures as temperature increases. The intercalator (SYBR® Green I) stops its emission detached from denatured/melted PCR products. The melting point is the point where the curve starts to drop to zero fluorescence, i.e. the negative first derivative of the melting curve. If pure, the 1st negative derivative gives one clear identifiable peak for the PCR product. This is at the specific temperature which indicates PCR product purity (and primer specificity). If any peak occurs below this temperature, the derivative curve is not even, but consists of several small peaks and PCR product sample is impure.

Computational tools

Data analyses

mRNA/cell

The QuantaSoft™software data are exported for analysis as *.csv file and into spreadsheet (Microsoft excel), where the Poisson algorithm has predetermined the starting concentration of target cDNA in units of copies/ µL input from sample. The absolute quantification of mRNA is given in copy numbers per 20 (copy/µLcDNA). Those 20 µL includes 2 µL of diluted cDNAsample, and this is the basis µL for calculating concentrations of templates back to the absolute numbers of mRNA/cell. Dilutions made in cDNA synthesis and DNase treatments were corrected for when estimating the number of transcripts per ng RNA, which was used in estimating the final gene copy/cell.

Final ddPCR reaction mix that exceed 5,000 copies of target/µL is considered saturated. If all 20,000 droplets in ddPCR contain target, the QuantaSoft™software will

not give good estimate on transcript numbers, which needs both positive and negative events (droplets) to make poisson distribution estimate (95 % conf. interval). To avoid such saturated samples into the ddPCR, cDNA samples had to first be estimated through Qubit measurements. *nar, nir, nor* and *nos* genes were assumed to have 100-1000x higher copy numbers at anoxic compared to oxic samples. To be sure that the samples put into ddPCR were never overloaded, several test-runs with different dilutions in the ddPCR was performed in order for making a final safe run on absolute quantification for all gene copies.

Excel-Spreadsheet for analysis of gas data

A specially designed Microsoft Excel spreadsheet ("Spreadsheet_april 2014", by Lars Bakken, Nitrogen group at IMV, NMBU in Ås) was used to sort and analyse the output (time and peak areas) from the incubation experiments. This Spreadsheet (Excel file) is used to plot together gas data, with timing of mRNA/cell according to timing of sampling from gas-experiment. However, the most important feature is that this ensures a correct depiction of phenotypic data by taking into account important parameters such as solubility of gases, pH, temperature, transport rate from headspace to liquid, leakage, dilution by sampling and ppm to peak area (response factors). The output includes, but is not restricted to, concentrations and reduction/accumulation rates of relevant gases, electron flow to O2 and NOx, cumulative O2 reduction and N2 and CO2 accumulation for each sampling time point or interval.

Concentrations of gases (N2O, CO2, and N2) are calculated in µmole of headspace (120-50 mL). O2 and NO are calculated as nmolar concentrations in liquid (50 mL). The nmolar concentration in liquid builds on a parameter called the transport coefficient (kt), a constant that describes the equilibrium of molecule between gas and liquid phase, depending on magnetic bar size stirring the volume of liquid. This is why standard conditions include standard magnetic bar size and rpm (tab.2). CO2 in liquid is a function of pH and temperature, with variations in species, dissociating constants, and concentrations (mol/l*atm) (Appelo and Postma,1993); also heat conductivity of some gases (He, H2, N2, O2, CO2, N2O) are constants that are used as basis during calculating concentrations of gases against time.

RESULTS

Initially, the *P. aeruginosa* type strain and PAO1 were characterized with respect to their specific growth rate ($\mu\ h^{-1}$) during aerobic and anaerobic growth, and their initial biomass vs OD_{600} and cell number, followed by a physiological incubation experiment characterizing denitrification phenotype during their transition from aerobic respiration to denitrification.

The results from the initial physiological incubation experiment indicated a correlation between N_2O accumulation and cell density (thus possibly quorum sensing) in PAO1. This phenomenon was further explored in a *rhlI*$^-$*lasI*$^-$ mutant and its parent strain PAO1-UW originating from USA (Wang et al., 2015), which were also characterized with respect to transcription of *narG, nirS, norB,* and *nosZ* during their transition from aerobic respiration to denitrification.

Estimation of Biological Parameters

The empirical estimation of some basic parameters was done to facilitate set-up and analyses of larger physiological experiments. These include OD_{600} vs cell number/mL vs biomass, and specific aerobic and anaerobic respiration rates (μ_{oxic} and $\mu_{anoxic}\ h^{-1}$) of different strains. Ultimately, these present conversion factors for determining specific knowledge. For instance, the conversion factor from "cell number/mL to OD_{600}" was required for estimating gene transcripts/cell.

Biomass and cell numbers

From a necessity to convert cell density into actual cell number/mL, a regression line from "cell number/mL to OD_{600}" was made, and its slope provided the needed conversion factor: cell/mL/OD_{600}. In addition, it was necessary to convert OD_{600} to biomass (mg/mL). These conversion factors made it possible, from gas data with start- and end-OD_{600}, to estimate cell yield per mol electron acceptor (O_2 and NO_3^-). Additionally, the conversion factors made it possible to normalise for cell numbers in analysis for transcriptional data (gene transcripts/cell).

The regression line "cell number/mL with OD_{600}" resulted in the slope that represents conversion factor $4*10^8$ cells/mL/OD_{600} (R^2=.97) (fig.14). The given slope indicates that OD_{600}=0.1 corresponds to $4*10^7$ cells/mL.

The dry weight of *P. aeruginosa* PAO1 was found to give 0.427 mg/mL/OD_{600}

biomass. The same dry weight estimate for the type strain gave a 20 % heavier biomass (0.553 mg/mL/OD_{600}). The predicted weight if OD_{600}=0.1 of PAO1, is 0.043 mg/mL biomass, and 0.055 mg/mL biomass for the type strain.

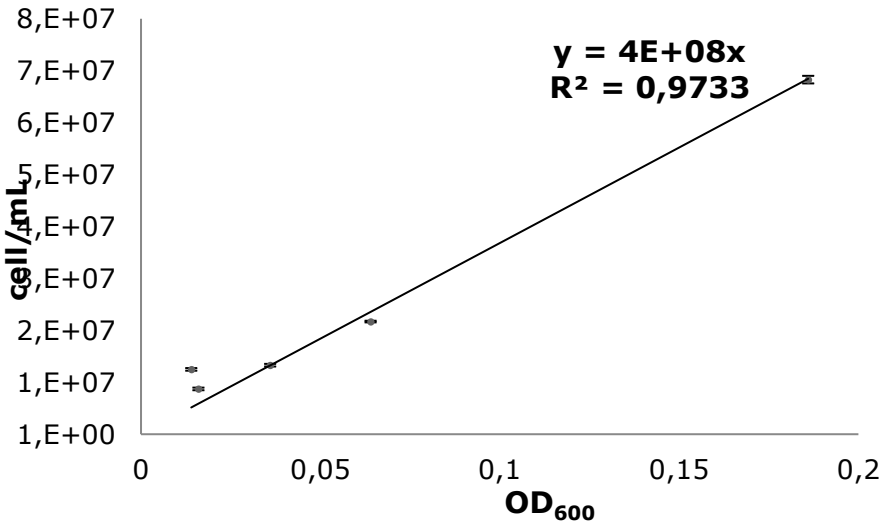

Figure 14. *The linear relationship between "cell number/mL to OD_{600}"* from estimations of DAPI stained cells/mL from aerobically grown *PAO1-UW* monitored *by spectrophotometry. Slope is 4*10⁸ when forced into origo (R^2=.97).*

Growth curve

Aerobic and anaerobic growth curves were characterized in *P. aeruginosa* type strain and PAO1. These growth curves[21] show the average optical density (OD_{600}) as a function of time from inoculation to stationary phase via lag- and exponential growth phases (fig. 15 and 16). Death phase was not monitored, as only exponential growth was experimentally relevant.

P. aeruginosa, grown with succinate (34 mM) as carbon source, showed exponential growth that levelled out at stationary phase. Under oxic conditions, the type strain reached a maximal OD_{600} of 0.4, half that of PAO1 (OD_{600} = 0.8) (fig.15 A,B). Likewise, anaerobic cultures of PAO1 reached maximal optical density at 0.2 OD_{600} and the type strain reached the half by OD_{600}=0.1 (fig.15. C, D).

[21] (n=5, the type strain under oxic conditions; n=4, the type strain and PAO1 under anoxic conditions, and PAO1 under oxic conditions).

When PAO1 grew at 30 ˚C, it reached the log (exponential) phase earlier and with a steeper curve compared to under 20˚C (fig.16).

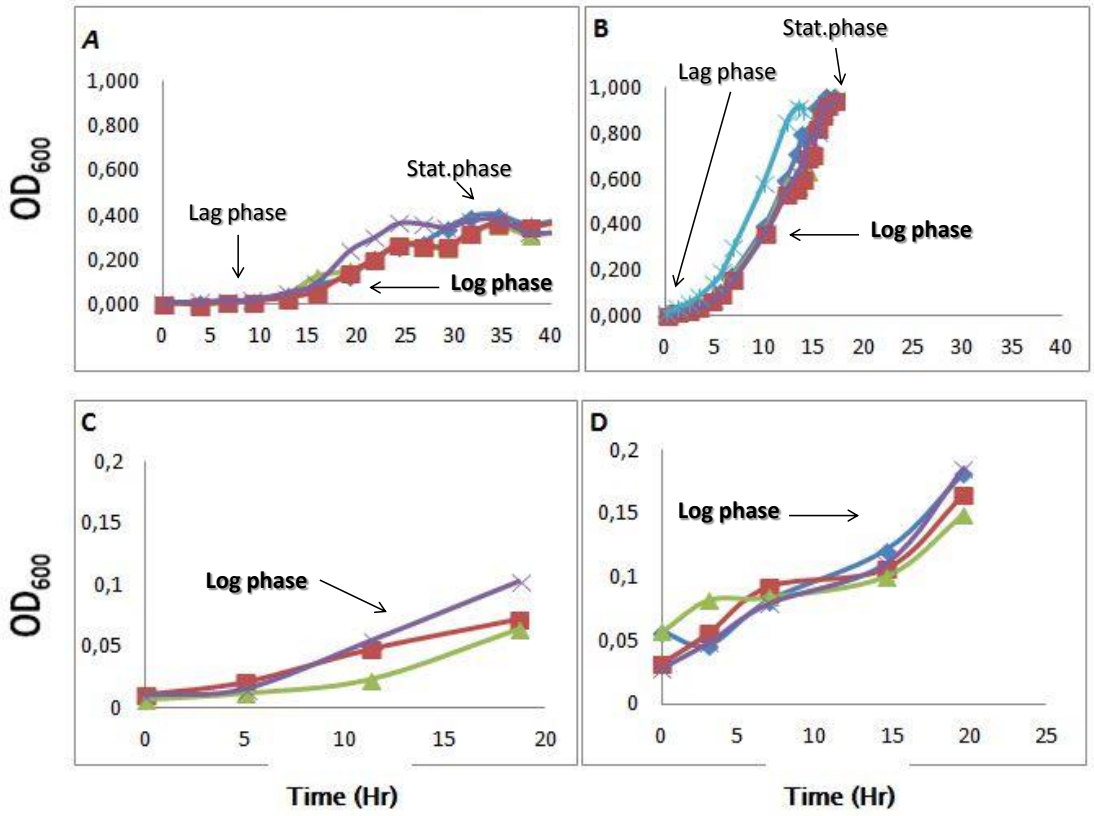

Figure 15. *Growth curve of Pseudomonas aeruginosa strains as a relationship between optical density (OD600) and time.* The different growth phases are defined for *conditions in Sistrom `s medium at 20 ˚C.* ***A)*** *P. aeruginosa the type strain: oxic conditions with continuous stirring (small magnets, at 700 rpm) in half strength Sistrom `s medium (n=5).* ***B)*** *P. aeruginosa PAO1, oxic conditions with continuous stirring (large magnets, at 500 rpm) in Sistrom `s medium (n=4).* ***C)*** *P. aeruginosa the type strain, anoxic conditions with continuous stirring (large magnets, at 500 rpm), 7 mM $KNO_3$, in Sistrom `s medium (n=4).* ***D)*** *P. aeruginosa PAO1, anoxic incubation with continuous stirring (large magnets, at 500 rpm), 7 mM KNO_3, in Sistrom `s medium (n=4).*

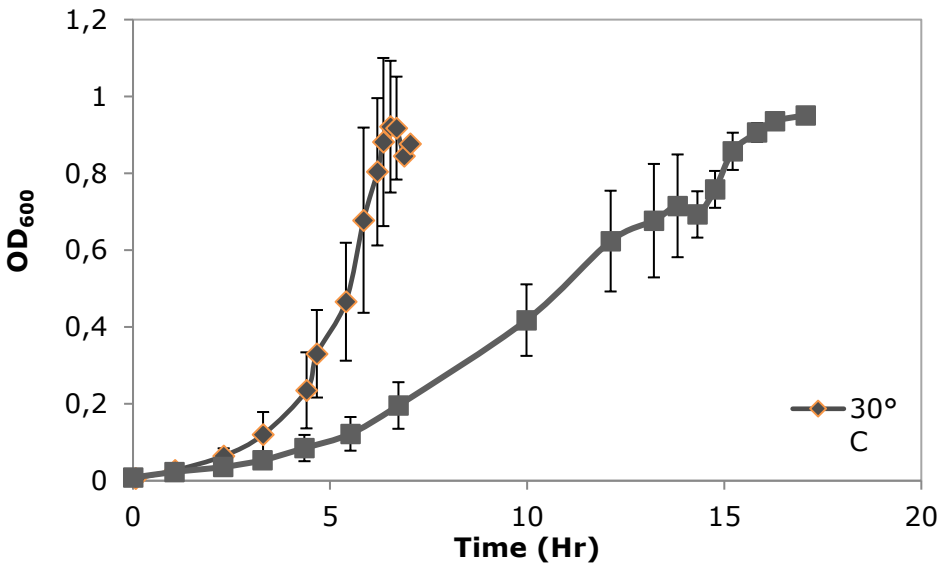

Figure 16. *Aerobic growth curves of P. aeruginosa PAO1 at 30 ˚C and 20 ˚C in Sistrom `s medium with continuous stirring (small magnets, at 700 rpm).*

Specific growth rate (μ) and doubling time (T_d)

Log linear growth curves from oxic and anoxic conditions at 20˚C were used to estimate specific growth rates (μ h^{-1}) and generation times (T_d) for the PAO1 and the type strain (*Eq.3;* tab.10).

The two strains were different with respect to μ $h^{-1}$and T_d during oxic conditions: *P. aeruginosa PAO1 had a* 0.385±0.022 μ h^{-1}, with 1.8 T_d, while the type strain was slower with 0.193±0.012μ h^{-1}, and 3.58 T_d. During anoxic conditions the type strain was faster with 0.096±0.048 μ h^{-1} (7.22 T_d) compared to PAO1, which had 0.067±0.019 μ h^{-1} (10.35 T_d).

Table 10. *The Specific growth rate (μ h^{-1}) and doubling time (T_d) from log linear growth curves of PAO1 and the type strain under oxic and anoxic conditions at 20 ˚C. Number of replicate (n) ranges from 3 to 5.*

Strain and type of respiration		Average specific (μ h^{-1})	Standard error SD	Replicates (n)	Generation time T_d in (T_d)	Temperature (˚C)
PAO1	aerobic	0.385	0.022	(n=5)	1.8	20
PAO1	anaerobic	0.067	0.019	(n=4)	10.35	20
TS	aerobic	0.193	0.012	(n=4)	3.59	20
TS	anaerobic	0.096	0.048	(n=4)	7.22	20

Testing of primer pairs for quantitative PCR and confirmation of lasI/rhlI deletions

Gel pictures

The gel pictures confirm expected gene fragment sizes from designed primer pairs during transcriptional analysis, and deletions in PAO1 lasI⁻rhlI⁻ mutant vs PAO1-UW before the two larger physiological experiments.

Fragments from designed primer pairs had expected sizes without any visible unspecific products: *napA (243 bp), narG (389 bp), nirS (297 for* Psa_nirS, fig.17)) and 125 for nirS_PAO1, fig.18)), *norB (212 bp),* and *nosZ (243 bp)*) (fig.17; 18). Quorum sensing genes *rhlI/R* and *lasI/R* with respective deletions also had expected sizes without any visible unspecific products: *lasI* (999 bp wild type; ~500 bp muant), *rhlI* (850 bp wild type; ~450 bp mutant), *lasR* (1115 bp) and *rhlR* (1040 bp) (fig.19).

Additionally, primer specificity was confirmed by targeting the denitrification genes trough real-time PCR where primer pairs gave fragments with single melt points that confirm pure PCR products (Appendix, tab.V.).

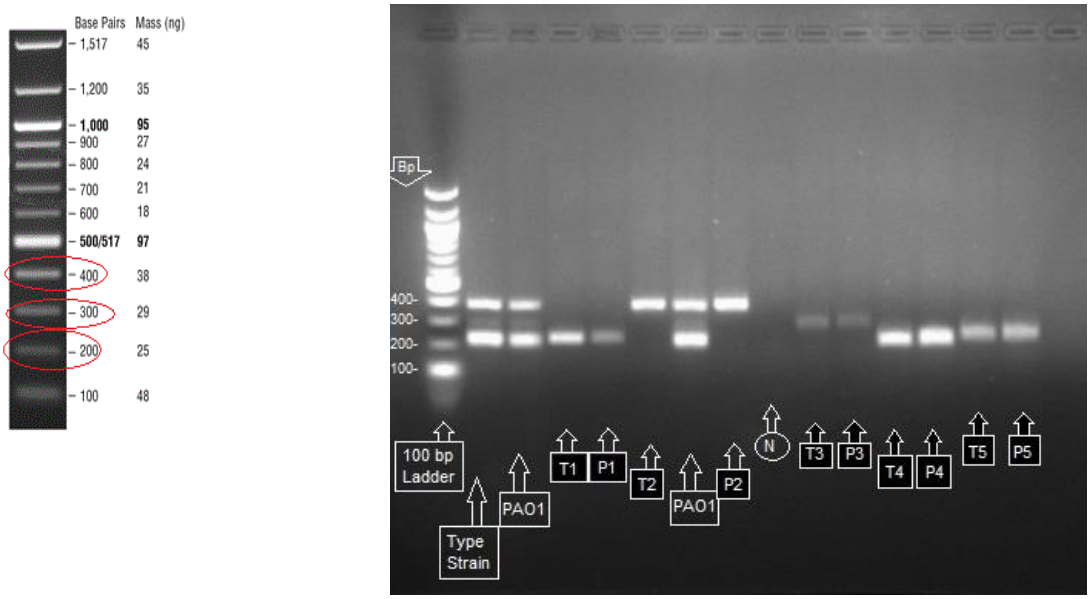

Figure 17. *Different band sizes of PCR products in gel electrophoresis, from PAO1 and the type strain. From left to right: 100 bp ladder; the Type strain (**T**) multiplexed all 5 primer pairs; PAO1 (**P**) multiplexing all 5 primer pairs; napA of the Type strain (**T1**); napA of PAO1 (**P1**); narG (**T2**) and (**P2**); negative (with primernpair for nosZ); nirS (**T3**) and (**P3**); norB (**T4**) and (**P4**); nosZ (**T5**) and (**P5**). The gel consists of 2 % agarose, stained with* peqGREEN Dye (peQlab*).*

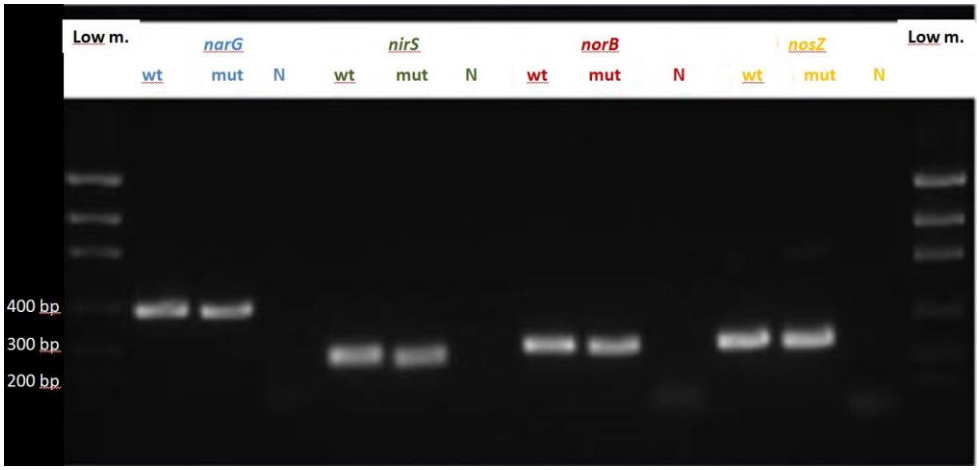

Figure 18. PCR products from primer pairs used on both PAO1-UW (wt) and PAO1 rhlI⁻ lasI⁻ mutant (mut). A different nirS primer pair was used, which had a cleaner melt curve during real-time PCR. The gel (2 % agarose), stained with peqGREEN Dye (peQlab) *shows fragments of expected size for narG, nirS (new), norB and nosZ, in both QS-mutant and PAO1-UW.*

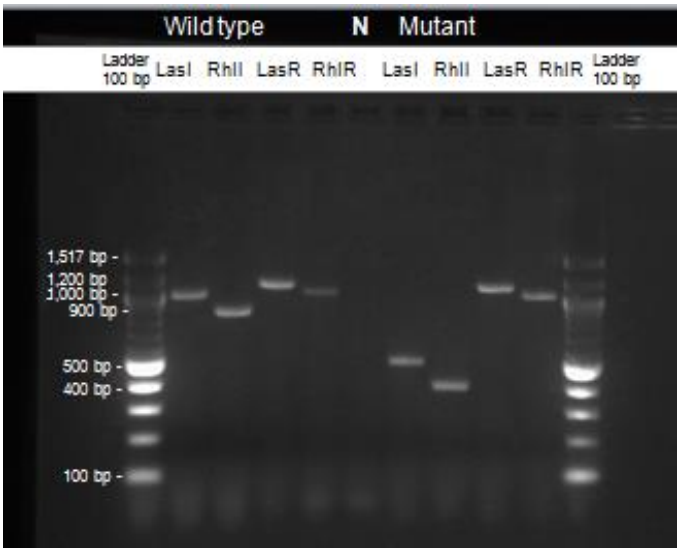

Figure 19. *Gel electrophoresis confirming deletions within lasI and rhlI in the lasI/rhlI double mutant. Templates were DNA extracted from endpoint samples taken from the "gene expression experiment". Gel consists of 2 % agarose, stained with peqGREEN Dye (peQlab).*

Physiological experiments

All incubation experiments with gas measurements were performed at 20˚C, with variations in the initial concentration of electron acceptors (0, 1, 4 or 7% initial oxygen and 1 or 2 mM NO_2^- or NO_3^-). Additionally, measurements were done on their final cell densities during normal DRP and after AHLs systems under standard conditions (Materials and Methods, tab.2).

Pre-experimentation – initial oxygen concentration

The first physiological incubation experiment was done to characterize the gas kinetics (CO_2, O_2, NO_2^-, NO, N_2O, and N_2) during the shift from aerobic to anaerobic respiration under standard conditions (0, and 7 % initial O_2 and 2mM NO_3^-) (fig.20 and 21). (CO_2

levels are shown in the Appendix, fig.VI) [22]. Based on the gas measurements, the μ_{oxic} and μ_{anoxic} h^{-1} were calculated for comparison between aerobic and anaerobic respiration rates (tab.11). (Final cell densities were measured in PAO1 cultures for comparison between oxygen treatments, Appendix, fig.V).

In either of the oxygen treatments (0 and 7 %) PAO1 showed very little nitrite accumulation. In comparison, the type strain accumulated over 60 µmol vial-1 (initial NO_3^- was 100 µmol) before reducing it further to NO (fig. 21). NO was kept at low nanomolar concentrations (~15-40 nM NO in liquid) in both strains throughout the anoxic phase (tab.11). Although transiently accumulating N_2O (max 0.2±0.1 at 0% O_2 and 37.0±28.4 at 7% O2) (tab.11), the type strain completed denitrification by releasing a total of 100 µmol N_2 regardless of initial O_2 concentration (fig.21A). In contrast, when treated with 7 % initial oxygen PAO1 did not complete denitrification, but stopped at 112.7±2.8 N_2O max (tab.11), without any further reduction to N_2 (fig.21B). Denitrification was only partially completed in cultures with 0 % initial oxygen (fig. 2C). Here, PAO1 recovered 2 mM NO_3^- as 74.2±3 µmol N_2O_{max}, which was further reduced to N_2 (tab.11). PAO1 had a 26 % higher specific rate at oxic conditions with 2mM KNO_3 (μ_{oxic}=0.289±0.025 h^{-1}) compared to the type train (μ_{oxic}=0.213±0.015 h^{-1}) (tab.11). When given 2mM KNO_2, the type strain increases its μ_{oxic} with 10 % compared to when given 2mM KNO_3. Also, the PAO1 has only 10 % higher specific growth rate (μ_{oxic}=0.265±0.007 h^{-1}) compared to the type strain (0.238±n.a. h^{-1}) under 2mM KNO_2. At anoxic conditions PAO1 have approximately 17 % higher μ_{anoxic} (0.136±0.009 h^{-1}) compared to the type strain (0.113±0.002 h^{-1}) under 2 mM KNO_3 (tab.11).

Table 11. *Maximum concentrations of accumulated intermediates (NO, N_2O-N, CO_2, NO_2^-) during 0 and 7 % initial oxygen treatments with 2 mM potassium nitrate (2NA) or 2 mM potassium nitrite (2NI) in P. aeruginosa PAO1 and the type strain. Included are hours from inoculation to N2 max and Cell yield per mol e^- acceptor (based on final OD600). Few replicates for the type strain (7% 2NI; n=1 and n=2, 0 % 2NI).*

[22] CO_2 is potentially useful when gaining insight into growth, however, the solubility of CO_2 in liquid is strongly dependent on pH. Thus CO_2 accumulation is never a safe estimate on its own, of growth and activity.

Strain	Treatment		Replicates	NO_{max} (nM in liquid)	$N_2O\text{-}N_{max}$ (µmol-N $vial^{-1}$)	$CO_{2\ max}$ (µmol $vial^{-1}$)	$NO_2^-{}_{max}$ (mM)	O2 (µM) at first NO	Δt (t_{end}-t_0, h)	Cell yield per mol e-acceptor	μ_{oxic} (h^{-1})†	μ_{anoxic} (h^{-1})§
PAO1 (DSM 22644)	7% 2NA	AVG	n=4	15,3	112,7	183,5	n.d.[1]	27,4	25,8	n.d.	0,289	n.d.
		SD		5,1	2,8	15,4		8,8	6,2		0,025	
	0% 2NA	AVG	n=4	28,6	74,3	42,7	n.d.	n.a.	34,4	n.d.	n.a.	0,136
		SD		2,7	2,2	1,3		n.a	1,8			0,009
	7% 2NI	AVG	n=3	22,3	138,4	144,8	n.a.[2]	33,6	23,1	n.a.	0,265	n.d.
		SD		24,3	9,0	16,4		28,2	1,1		0,007	
	0% 2NI	AVG	n=3	30,6	49,8	25,6	n.a.	n.a.	35,6	n.a.	n.a.	0,098
		SD		4,3	85,9	19,4		n.a.	0,8			0,041
Type strain (DSM 50071)	7% 2NA	AVG	n=4	22,6	37,0	208,0	0,705	18,0	22,1	4,88E+10	0,213	n.d.
		SD		9,2	28,4	47,6	0,142	4,7	1,9	7,26E+10	0,015	
	0% 2NA	AVG	n=2	31,5	0,2	52,5	1,337	n.a.	25,5	4,18E+10	n.a.	0,113
		SD		0,1	0,1	2,1	0,011	n.a.	0,1	2,11E+11		0,002
	7% 2NI*	AVG	n=3	38,6	59,6	195,0	n.a.	18,0	23,5	4,40E+10	0,238	n.d.
		SD		n.a.	n.a.	n.a.		n.a.	n.a.	n.a.	n.a.	
	0% 2NI	AVG	n=1	35,5	0,2	28,0	n.a.	n.a.	35,7	1,83E+10	n.a.	0,092
		SD		3,6	0,0	5,3		n.a.	8,4	3,65E+12		0,033

*n = 1 for Type strain with 7% 2NI

[1] Not determined (n.d.) were not found in the data or data did not allow good estimations.

[2] Not applicable (n.a.) were not relevant under the given condition.

† Oxic growth rates in cultures with 4 vol % initial concentration in headspace.

§ Anoxic growth rates were determined in cultures with initial oxygen near zero.

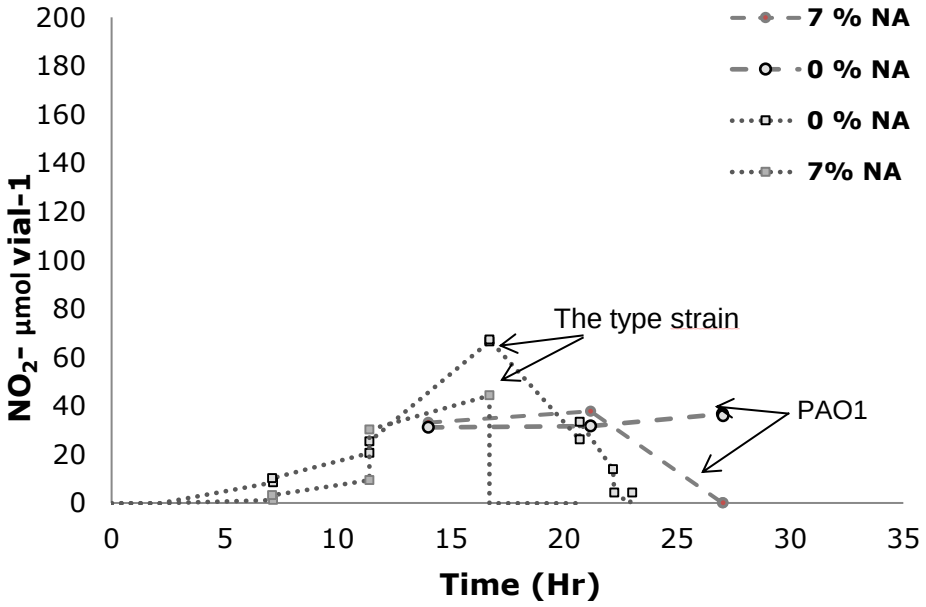

Figure 20. Nitrite accumulation in P. aeruginosa and the type strain at standard conditions, given 2 mM KNO_3 (100 µmol $vial^{-1}$).

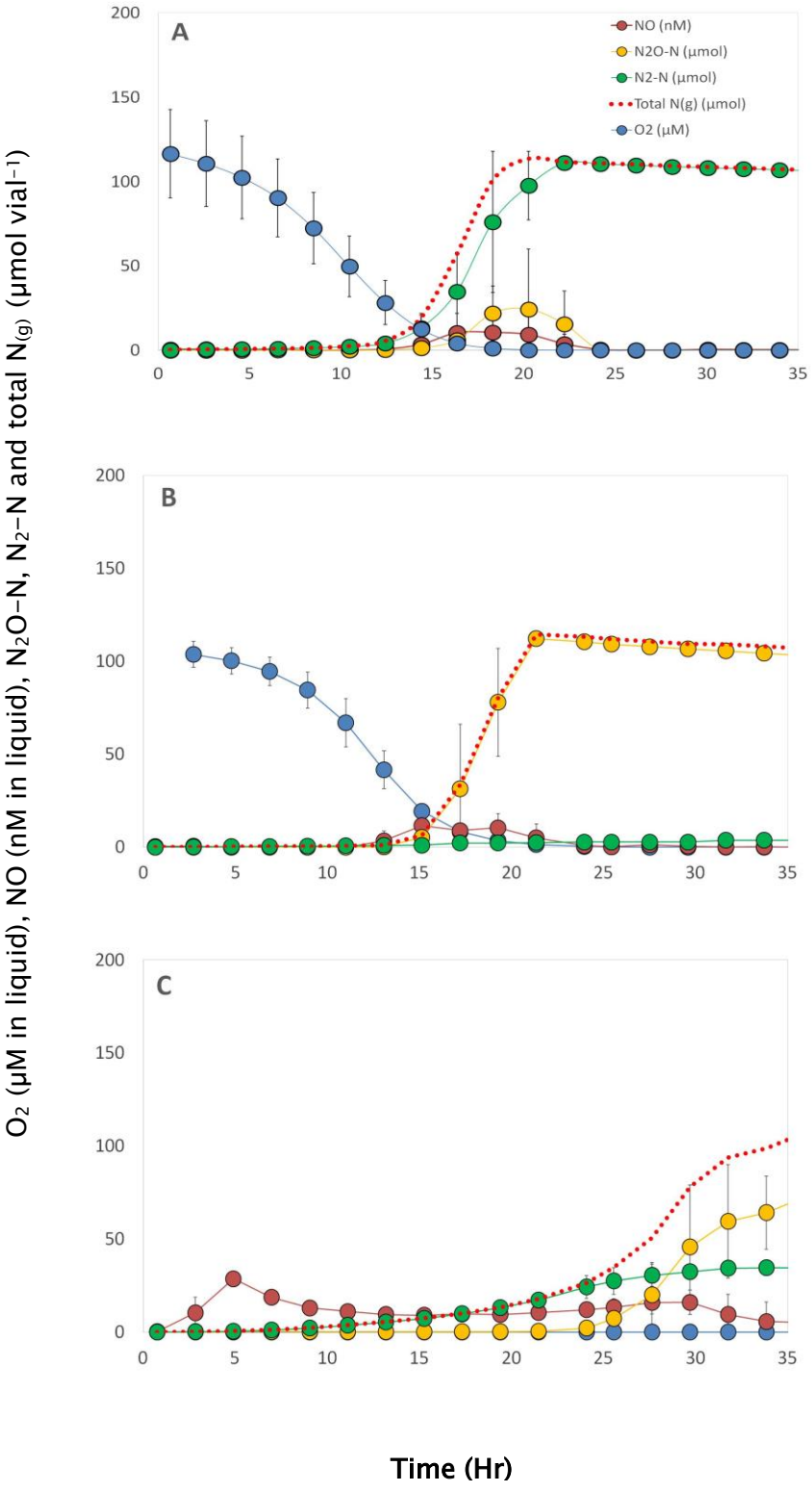

Figure 21. *Transition to denitrification: oxygen consumption and accumulation of N-oxides in cultures with 0 (C) or 7% (A and B) initial O_2 and 2 mM (100 µmol) NO_3^-. A) Full recovery of available NO_3^- as N_2 in P. aeruginosa the type strain at intermediate cell*

density; B) Full recovery of NO_3^- as N_2O in P. aeruginosa PAO1 at intermediate cell density; and C) Partial recovery of NO_3^- as N_2 in P. aeruginosa PAO1 at low cell density.

DRP and AHLs systems experiment

Two larger physiological incubation experiments were done with PAO1-UW and PAO1 *rhlI*$^-$*lasI*$^-$ mutant under standard conditions given 4 % initial oxygen concentration and 2 mM NO_3^-.

PAO1-UW and PAO1 *rhlI*$^-$*lasI*$^-$ mutant showed different denitrification phenotypes during the transition from aerobic to anaerobic respiration (fig.22). Both strains kept NO_{max} below 5.2 nM in liquid during denitrification. However, whereas PAO1-UW accumulated all the available NO_3—N as N_2O-N (103.9±2.3 µmol-N vial^{-1}) before reducing it further to N_2, the mutant reduced NO_3^- to N_2 with only negligible accumulation of N_2O (0.7±0.8 µmol-N) (tab.12).

The denitrification phenotype also differed between AHL treatments, but not with QS-inhibitor (fig.23). PAO1 *rhlI*$^-$*lasI*$^-$ mutant treated with 3O-C12-HSL (1 µM), accumulated N_2O (96.7±12.2 N_2Omax µmol-N vial^{-1}) followed by full recovery to N_2 exactly like the PAO1-UW phenotype (tab.12). Under C4-HSL-(10 µM) PAO1 *rhlI*$^-$*lasI*$^-$ mutant fully recovered 2 mM nitrate to N_2, with a minor N_2O accumulation (31.5±22.8), which differed from its normal phenotype (fig.22B). C10-CPA addition (250 µM) had no discernible effect on the gaseous intermediate accumulation during denitrification in PAO1-UW (fig.23C).

E-flow (µmol e$^-$ vial^{-1} h^{-1}) to O_2 and NO_x showed similarities in PAO1-UW and *rhlI*$^-$*lasI*$^-$ mutant during the transition from aerobic to anaerobic respiration (fig.24). Both showed a smooth transition with no dramatic drop in total electron flow. However, during the anoxic phase, the PAO1-UW had an overall lower e-flow rate (µmol e$^-$hr^{-1}) (fig.24A). When excluding N_2OR and comparing the respective e$^-$-flow to NAR, NIR, NOR only, the rates were comparable between mutant and parent strain (fig. 25A). While e-flow towards N_2OR in the LasI/RhLI negative strain is simultaneous and comparable to the upstream reductases (34.5 µmol e$^-$ vial^{-1} h^{-1}), N_2OR activity is severely delayed in PAO1-UW (fig.25B). When the e-flow towards N_2OR eventually occurred, the rate was slow and constant (11.4 µmol e$^-$ vial^{-1} h^{-1}).

Table 12. *The maximum concentrations of accumulated intermediates (NO, N_2O-N, CO_2, NO_2^-) that were monitored during QS experiment with P. aeruginosa PAO1-UW and PAO1 rhlI$^-$lasI$^-$ mutant. Included, the time-span from inoculation to N_{2max} and cell yield per mol e$^-$ acceptor (based on final OD_{600}) (n=3).*

Strain	Treatment		μ_{oxic} (h^{-1})	NO_{max} (nM in liquid)	N_2O-N_{max} (µmol-N $vial^{-1}$)	$NO_2^-{}_{max}$ (mM)	Δt (t_{end}-t_0, h)	Cell yield per mol e-acceptor
PAO1 (UW) [1]	WT	AVG	0,27	7,4	102,3	0,580	35,5	2,28E+10
		SD	0,01	2,5	2,1	0,016	1,2	8,42E+10
	WT-C10-CPA	AVG	0,31	4,0	0,8	0,760	36,2	2,72E+10
		SD	0,06	2,3	0,7	0,010	2,3	1,32E+10
PAO1 *rhlI-lasI-* (UW) [1]	*rhlI-lasI-*	AVG	0,28	11,2	107,7	0,464	28,2	2,61E+10
		SD	0,03	3,4	1,5	0,009	0,2	4,19E+09
	rhlI-lasI-C4-HSL	AVG	0,30	6,2	40,7	0,617	30,9	1,95E+10
		SD	0,06	2,8	12,6	0,057	0,1	1,13E+10
	rhlI-lasI- 3O-C12-HSL	AVG	0,27	3,9	98,3	0,327	34,8	2,01E+10
		SD	0,00	3,8	8,5	0,145	1,1	8,73E+10

[1] *The PAO1-UW (USA strain) is a different strain from the PAO1 (DSM 22644) with the phenotype: max N_2O-N = N_2O-N at the end of experiment, and was never reduced further to N_2 in the initially studied PAO1 (DSM 22644) strain (Klockgether et al., 2010).*

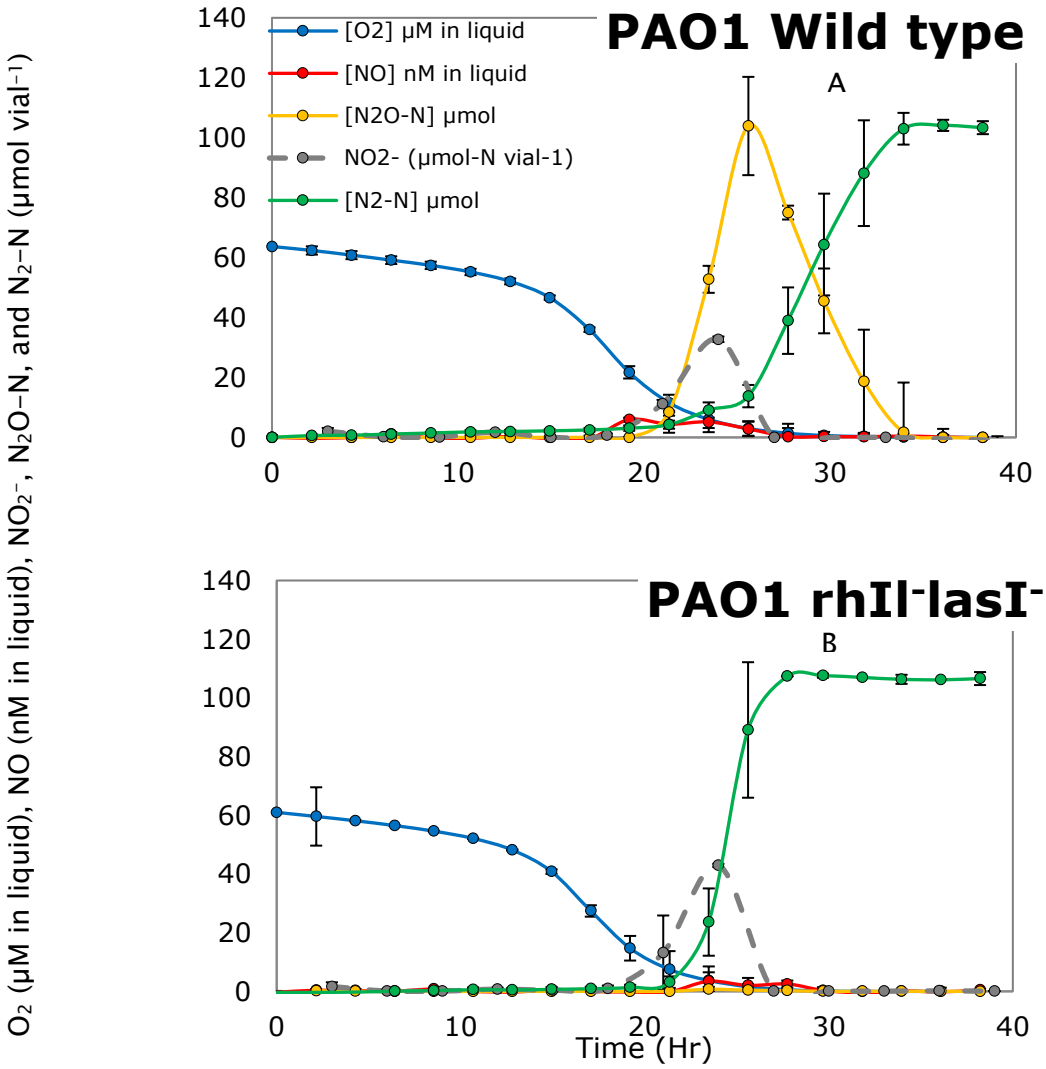

Figure 22. *O_2 depletion and accumulation of N-oxides during the transition from aerobic respiration to denitrification **A)*** PAO1-UW *and **B)** PAO1 rhlI-lasI- mutant during a 40 hour experiment with 4 % initial oxygen and 2 mM KNO_3 (See standard conditions, tab.2).*

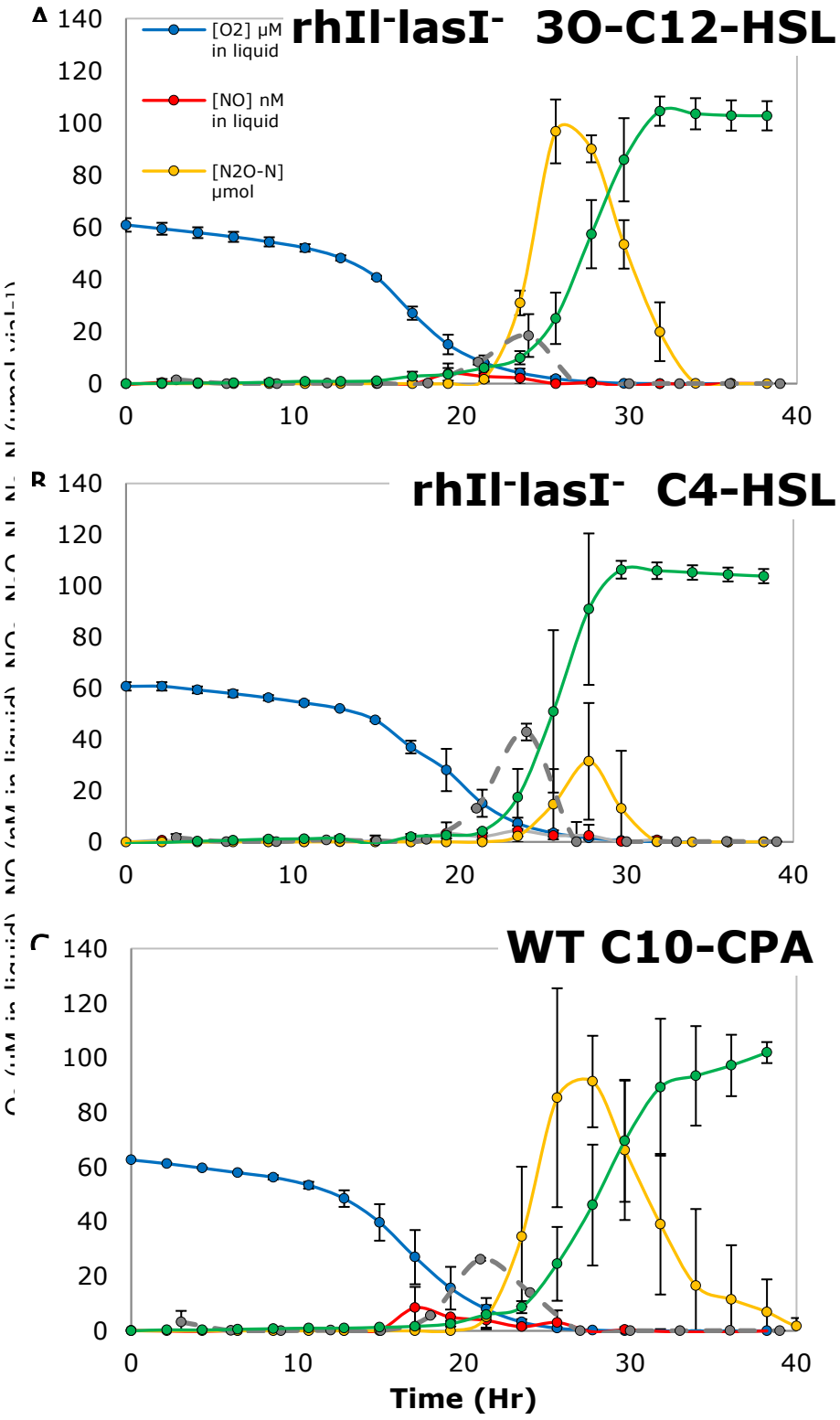

Figure 23. *Denitrification phenotype of PAO1 rhlI- lasI-* mutant and PAO1-UW (wild type, WT) *treated with AHLs and LasI-inhibitor.* ***A****) Accumulation of N_2O followed by full recovery to N_2 when LasR receptors are induced by 3O-C12-HSL.* ***B****) Full recovery of*

*2mM NO_3^- to N_2 when RhlR receptors are induced by C4-HSL. **C**) Accumulation of N_2O and full recovery to N_2 when LasR is inhibited by C10-CPA.*

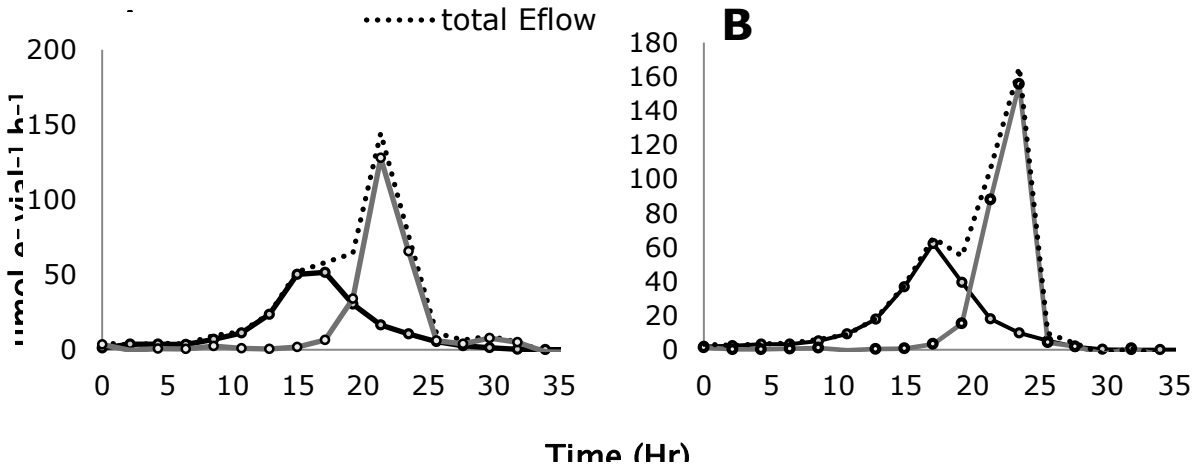

Figure 24. *Electron flow to O_2 and N-oxides (Nox) in **A)*** wild type (WT) *and **B)** PAO1 rhlI⁻ lasI⁻ mutant.*

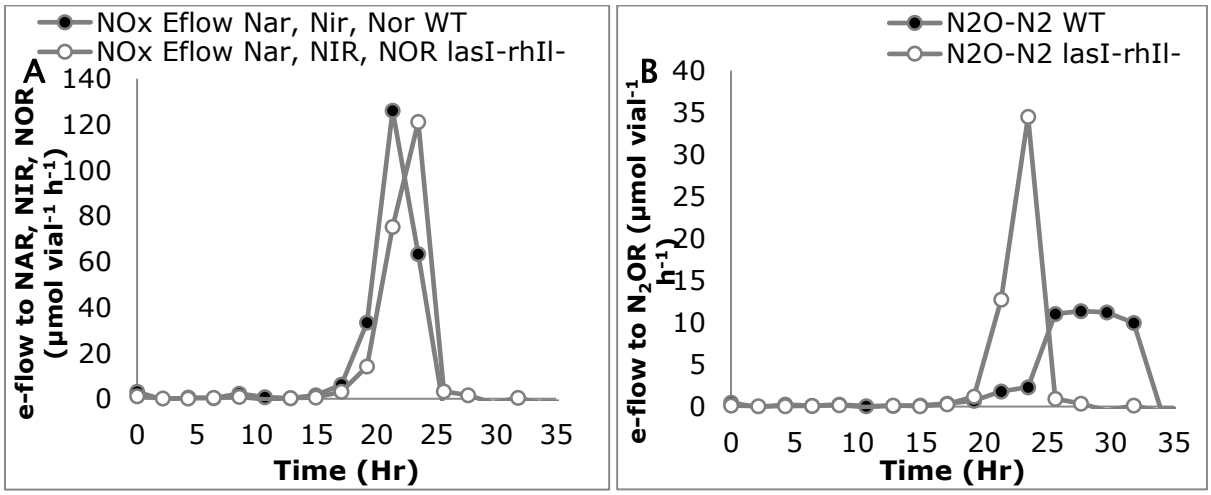

Figure 25. *Examples of electron flow **A**) to NAR, NIR and NOR in PAO1 wild type (WT) (•) and PAO1 lasI⁻rhlI⁻ mutant (○); and **B**) to N_2OR in PAO1 wild type (WT) and lasI⁻rhlI⁻ mutant.*

Gene expression experiment

The transcription of *narG, nirS, norB and nosZ* was monitored during the transition from aerobic respiration to denitrification in the *rhlI*⁻*lasI*⁻ mutant and its parent strain. QuantaSoft estimated absolute transcript quantifications, after manually setting a threshold between positive and negative droplets (fig.26). The QuantaSoft fits the positive droplets to a Poisson algorithm to determine the starting concentration of fragments. The Poisson distribution depends on number of accepted droplets. The QuantaSoft return to NO CALL from wells with too many positive droplets (not enough empty droplets to apply Poisson statistics), or wells with fewer than 10,000 droplets (Application guide for QX200, 01.12.2016). The average number of accepted droplets in total (negative and positive) in these experiments were below 20,000 droplets (from lowest *nosZ*: 14280±13.5 CV% to highest *nirS:* 16933,8±11.4 CV%) (tab.13). Normally, they lay around 17,000±1000 accepted droplets (Appendix, tab.VI).

All types of transcripts were present in inocula (0.04-0.4 mRNA/cell) (fig.27). Generally, slightly higher transcript levels were found in the *lasI /rhlI* deficient strain. The exception was *nosZ,* which appeared to be more actively transcribed in the parent strain (fig.27, D). The main difference between PAO1 *lasI*⁻*rhlI*⁻ mutant and its parent strain was their overall level of *nir* and *nos* transcripts under anoxic conditions (fig.28). The PAO1-UW seemed to more strongly express the *nosZ* compared to *nirS*gene (1.23±1.29 *nosZ/nirS* ratio). This was also larger than by the mutant (0.24±0.2 *nosZ/nirS* ratio). The *nosZ/nirS* max transcript ratio in PAO1 *lasI*⁻*rhlI*⁻ mutant was 0.62 *nosZ/nirS* mRNA/cell, while the PAO1-UW had 4.24 *nosZ/nirS* mRNA/cell (tab.14)(fig.28) That is a difference of times 4 between PAO1-UW and the *lasI rhlI* deficient strain.

Although hard to reflect in one figure, the detailed transcriptional profiles in the two strains (PAO1 wild type and PAO1 *lasI*⁻*rhlI*⁻ mutant) are directly comparable against timing from the profile of gas measurements (fig.22; fig.27). All expressions occurred within the same window of time: they started at anoxic conditions and peaked at the mid-anoxic incubation period, exactly with NO_{max}. The low *narG* expression of both strains (<0.1 mRNA/cell) came before detection of nitrite. The highest expression of *nirS* occurred in PAO1 *lasI*⁻*rhlI*⁻ mutant with a peak-level (0.8 mRNA/cell) that rose while NO levels were held very low. *nirS* expression and NO production had no large difference in timing in the *lasI*⁻*rhlI*⁻ mutant and its parent strain.

A second large difference between the two strains is their *nosZ* transcript levels. During anoxic incubation, the PAO1 *lasI*⁻*rhlI*⁻ mutant prolonged its low, stabile expression (0.4 mRNA/cell) that was followed by a quicker, 5 hours reduction to N_2 (100

µmol-N), while the *nosZ* levels in the PAO1-UW were much higher (1 mRNA/cell) but was followed with a double slow, 10 hour reduction to N_2 (100 µmol-N).

The cell desnities that followed the two last physiological experiments reflect some difference between PAO1-UW and PAO1 *lasI*$^-$*rhlI*$^-$ mutant (average OD_{600}, n=3). The largest cell density difference during denitrification that occurred between PAO1 *rhlI*$^-$*lasI*$^-$ (OD_{600}=0.266±0.024) and PAO1-UW (OD_{600}=0.138±0.024) is of almost 50% at N_2O_{max} (fig.29). Under exogenous AHL, the PAO1 *rhlI*$^-$*lasI*$^-$ (0.147±0.004) and PAO1 *rhlI*$^-$*lasI*$^-$ with 3O-C12-HSL (0.097±0.010) differ most with 34 % difference (fig.30).

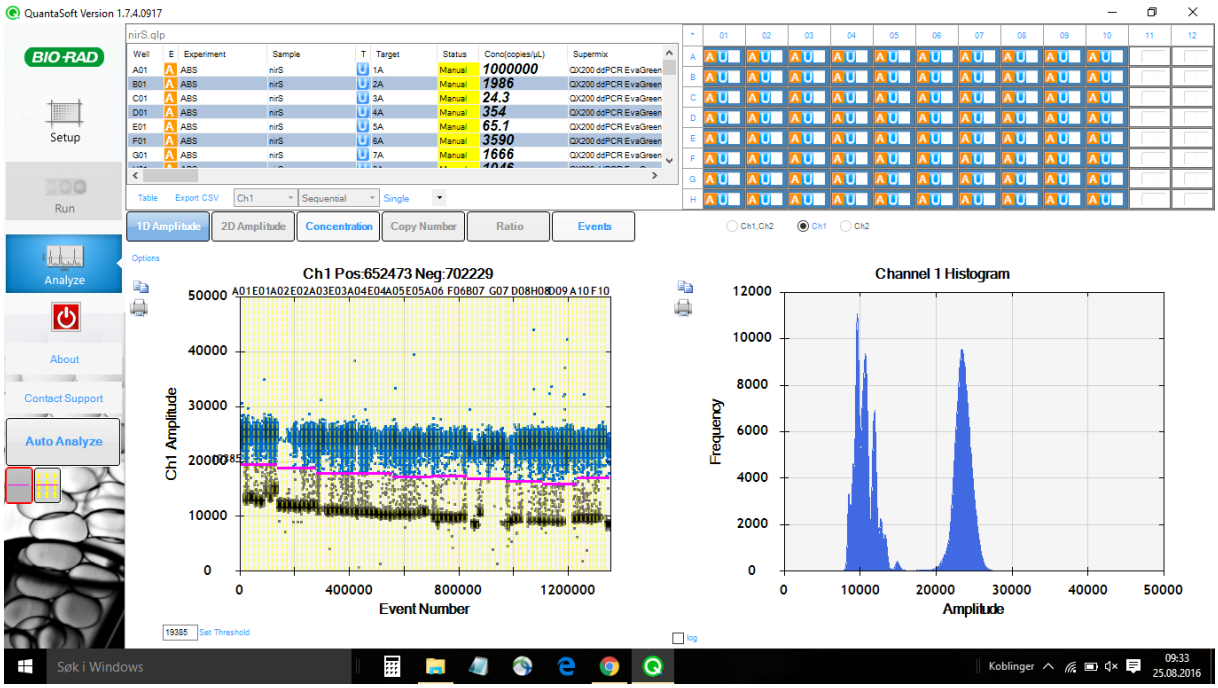

Figure 26. *Example of manual setting of threshold depending on number of positive droplets (blue) and negative droplets (black) detected by the ddPCR. Amplitude increases by the number of droplets that contain amplified products of nirS cDNA (illustration is derreived from QuantaSoft™ Software).*

Table 13. *Accepted droplets by droplet reader during the run of narG, nirS, norB or nosZ.*

Gene	Accepted Droplets		
	AVG	SD	CV%
narG	15073,4	2502,7	16,6
nirS	16933,8	1930,8	11,4
norB	15752,5	2461,3	15,6
nosZ	14280,1	1931,5	13,5

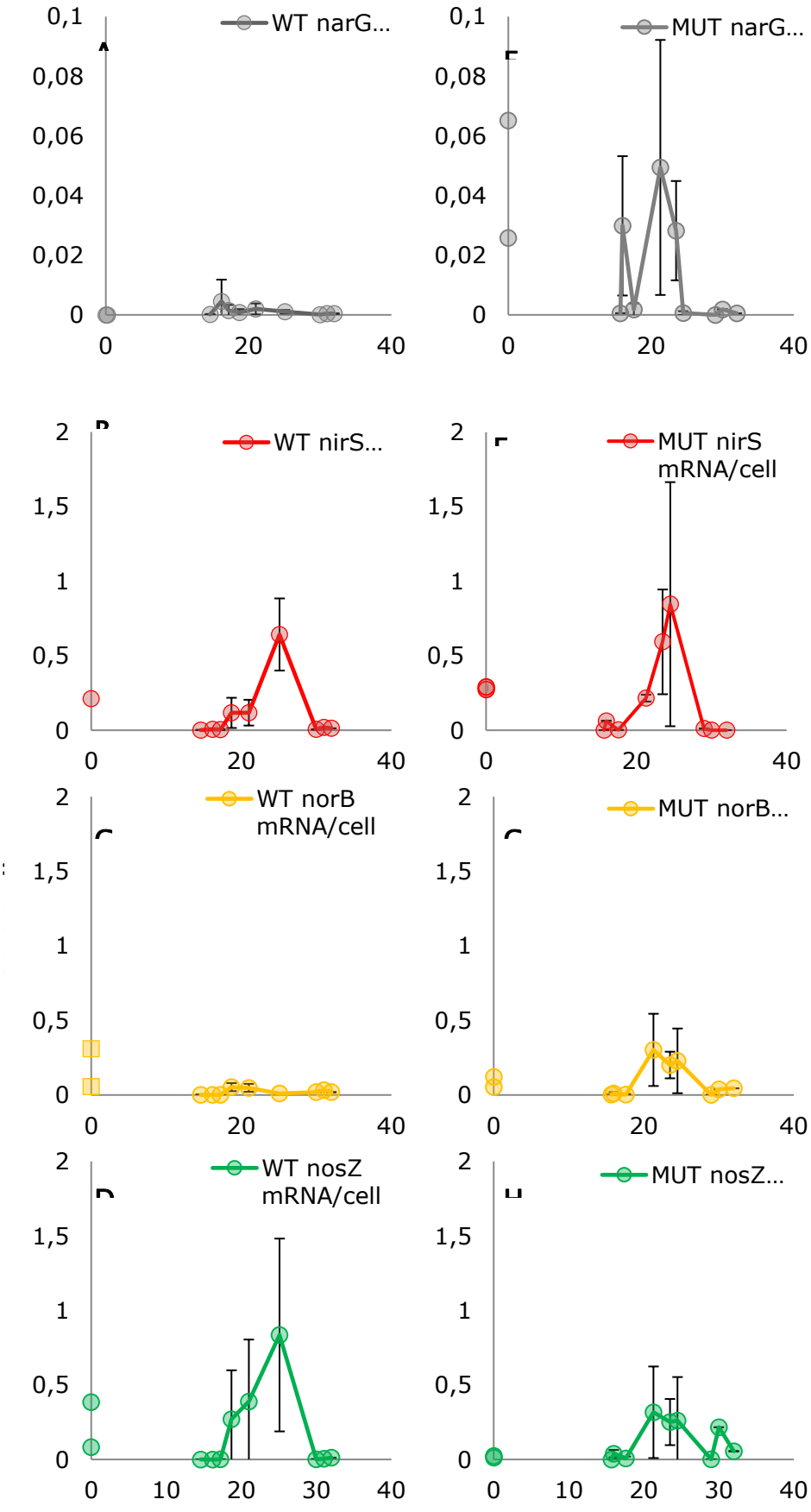
A
WT narG…
0,1
0,08
0,06
0,04
0,02
0
0
20
40
E
MUT narG…
0,1
0,08
0,06
0,04
0,02
0
0
20
40
B
WT nirS…
2
1,5
1
0,5
0
0
20
40
F
MUT nirS mRNA/cell
2
1,5
1
0,5
0
0
20
40
C
WT norB mRNA/cell
2
1,5
1
0,5
0
0
20
40
G
MUT norB…
2
1,5
1
0,5
0
0
20
40
D
WT nosZ mRNA/cell
2
1,5
1
0,5
0
0
10
20
30
40
H
MUT nosZ…
2
1,5
1
0,5
0
0
10
20
30
40
Time (Hr)

Figure 27. *Average narG, nirS, norB, nosZ transcription levels during the oxic–anoxic transition and subsequent denitrification in PAO1–UW (wild type, WT)(**A–D**), and the rhlI⁻ lasI⁻ mutant (**E–H**). Initial O_2 was 4 % and 2 mM (100 µmol) NO_3^- was added to the medium. Time 0 is the result for the inoculum prior to transfer. Standard deviations are shown as black bars (n=3;2).*

Table 14. *The transcript ratios are calculated as average±standard deviation (SD) and max between nosZ/nirS in rhlI⁻lasI⁻ mutant and PAO1–UW.*

Anoxic condition			
nosZ/nirS			nosZ/nirS $_{max}$
	AVG	SD	
MUT	0,24	0,20	0,62
WT	1,23	1,29	4,24

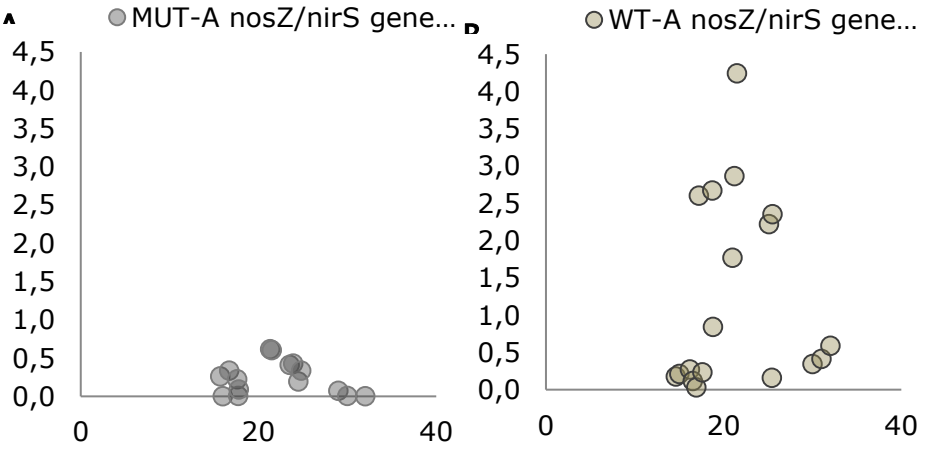

Figure 28. *nirS/nosZ ratio in **A**) PAO1 lasI⁻rhlI⁻ mutant, and **B**) PAO1–UW (WT)*, in all samples taken during the "transcription" incubation experiment.

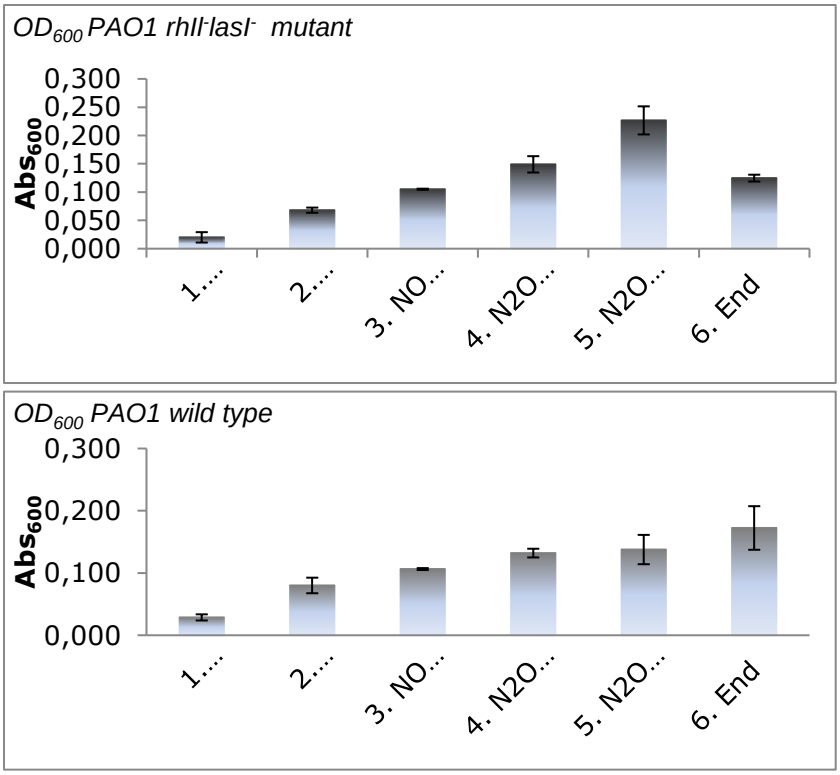

Figure 29. *Cell density of P. aeruginosa PAO1-UW* (wild type)*and PAO1 lasI-rhlI- mutant during denitrification at standard condition, treated with 4 % oxygen. Each bar in the histogram is measured by OD (Abs600) as mean±standard deviation (n=3).*

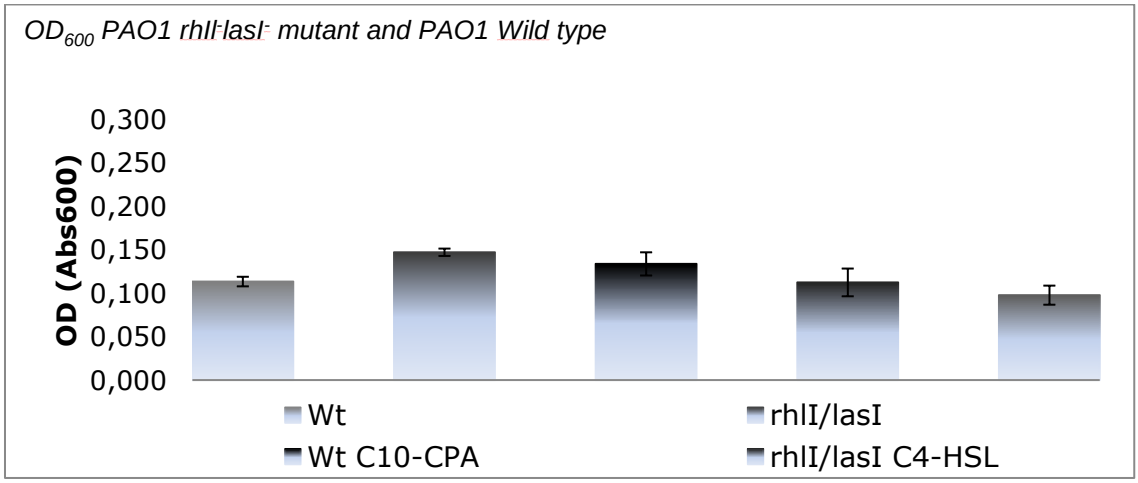

Figure 30. *Cell densities by P. aeruginosa PAO1-UW* (wild type) *and PAO1 lasI-rhlI- mutant at standard conditions treated with 4 % oxygen, AHLs and inhibitor during the QS-eksperiment. Each bar in the histogram is measured by OD (Abs600) as mean±standard deviation (n=3).*

DISCUSSION

I wanted to characterize *P. aeruginosa* with respect to its DRP. Early results indicated that cell density had a bearing on the accumulation of N_2O during denitrification. Thus, I also tested whether the AHL quorum sensing systems Las and Rhl regulated the expression of NO_x reductases, and N_2OR in particular.

The DRP of an organism encompasses transcriptional and post-transcriptional responses to oxygen depletion in the presence of NO_x. The initial physiological incubation experiment indicated that there was a correlation between N_2O accumulation and cell density (thus possibly quorum sensing) in PAO1. This phenomenon was further explored in *rhlI- lasI-* mutant and its parent strain PAO1-UW originating from USA (Wang et al., 2015). Additionally, these were also characterized with respect to transcription of *narG, nirS, norB,* and *nosZ* during their transition from aerobic respiration to denitrification.

However, before interpreting results there are some assumptions and troubleshooting to consider. These limit implications concerning QS-inhibitor (C10-CPA), dry weight and transcriptional results, mostly. In their wake follows a discussion on estimations of biological parameters, pre-cultivation and inoculation as well as statistics.

Finally, implications of physiological experiments are discussed: i) DRP during 0% and 7 % initial O_2: N_2O accumulation in correlation with cell density, and ii) AHLs system experiment: QS correlation with N_2O accumulation combined with gene expression analysis and cell density. In combination the results confirm that QS metabolically down-regulates denitrification, especially N_2OR by 3O-C12-HSL (LasR system) via post-transcriptional events.

Critical parameters and troubleshooting

Contamination

The possibility of contamination is relevant to all pure culture experiments, including those conducted in the present study. Several contamination-tests by plating were performed on cell stocks in order to ensure that cultures were pure (Appendix, fig.1).

QS-inhibitor

C10-CPA addition (250 µM) had no discernible effect on gaseous accumulation in PAO1-UW. The AHL analogue may have undergone decay during a three day suspension

in Sistrom´s medium solution before start of incubation experiment. Thus, any analysis on the Las and RhI systems is limited. Because C10-CPA binds to both RhIR and LasR receptor (Ishida et al., 2007), I would expect to see a phenotype exactly like the PAO1 *rhlI*$^-$*lasI*$^-$ mutant: full recovery of nitrate to N_2 without any pronounced accumulation of N_2O. Instead, the phenotype closely resembled that of the untreated wild type. The two AHLs, on the other hand, appeared to keep their stability in the Sistrom´s medium without any degradation limiting interpretations (Ishida et al., 2007).

Transcriptional results

The gene expression data are noisy. This could be explained by the inexperience of the experimenter (experimental weakness). Alternatively, transcription could occur in short bursts that are difficult to capture. Even so, certain trends protrude when timed with the gas data. The trick is to know if they differ due to a physiological response rather than extraction efficiency, RNA integrity or efficiency of cDNA synthesis.

mRNA produced in bacteria is continuously degraded at high rate (half time is most likely measured in minutes (Chen et al., 2015). When samples are taken from hypoxic or anoxic vials, the cells are exposed to ambient air. In response, the transcription of NO_x reductases stops, while degradation continues. Thus, degradation of mRNA could easily lead to underestimation of transcript numbers per cell. The time from exposure to oxygen and suspension in RNA protect (approximately 10 minutes at 4°C) probably resulted in some net decline in mRNA concentrations of denitrification genes. However, the abrupt temperature change (from 20°C to 4°C) should slowed down all reactions, including mRNA degradation. To know more about how much mRNA was lost to degradation, an endogenous mRNA control that is expressed at a constant level across samples would have been useful. However, under the relevant conditions, such a gene has yet to be identified. Thus, transcript levels could either be normalised against the concentrations of total RNA in the sample or, as was done here, against cells per sample. 16S RNA is not used in these experiments because total RNA mainly consists of ribosomal RNA, and since rRNA is also much more resilient to degradation than mRNA, the number of 16S RNA molecules in a sample does not give clues as to the amount of mRNA lost through degradation (Bergaust et al., 2008).

Every handling with mRNA-samples increases the risk of degradation. Especially, degradation could be occurring during DNase treatment. Two rounds of digestion incubation by TURBO DNase were performed because the first round gave very poor degradation results seen in real-time PCR. The method was considered inefficient, and thus, it was slightly changed from protocol of TURBO DNA-free™ Kit (Thermo Fischer

Scientific). Firstly, the temperature during second round was lowered from 37°C down to room temperature (~22˚C) during DNase digestion. Secondly, mixing was avoided and time of incubation was shortened into 20-30 minutes with occasional, carefully up-ending of Eppendorf tubes. This second round of Dnase digestion made successful gDNAdigestion, seen as insignificant levels of gDNA in the real-time PCR.

Normalization of cDNA is the practice of feeding equalized mRNA concentrations into each reaction mix in reverse transcription by making necessary dilutions on samples. There are two reasons for this: 1) avoid overloading reverse transcription, and 2) discover if specific genes´mRNA levels differ (Evrogen, 26.11.2016). Here, normalizations by dilutions were never necessary, since mRNA values extracted were in the same range (ng/µL). Even so, the amount of mRNA feeded into cDNA synthesis was known, so as to not overload reverse transcription. Then the specific genes´cDNA amount was corrected for by total RNA concentrations. Probably the cDNA synthesis is not 100 % effective for all RNA templates, but the reverse transcription efficiency will be approximately equal between samples as long as the mRNA inputs were not too high. Also, cDNA synthesis was conducted after a successful gDNA digestion had been confirmed by real-time PCR. Therefore, no false positives could exist among cDNA. Real-time PCR efficiency was never of interest, because it was never used for quantitative purposes. In addition for checking gDNA digestion result, the real-time PCR was used to test for primer pairs´ specificity before amplifying specific genes in the ddPCR.

In ddPCR, positive/negative droplets are assumed to be counted correct (absolute), so that Quantasoft estimates are exact representations of what exists in the sample, followed by manual corrections for threshold and dilutions. The average accepted droplet numbers are within the acceptable range for Poisson distributions algorithms (tab.13, Results; tab.VI, Appendix). These algorithms assume between 10,000 – 20,000 droplets (or 85 % Poisson confidence limit) (Applications Guide for QX200, 01.12.2016). The positive droplets counted during current qPCR were within this range and therefore, mRNA levels are assumed not largely affected by Poisson corrections.

Estimation of Biological Parameters

All physiological investigations that seek to characterize DRP require that we empirically estimate critical biological parameters. These facilitated set-up and analysis during the first and two following investigations on DRP. They include OD_{600} vs cell number/mL vs

biomass, and specific aerobic and anaerobic respiration rates of the strains (μ_{oxic} and μ_{anoxic} h^{-1}). Ultimately, these conversion factors make it possible for determining specific knowledge. From gas data with start- and end-OD_{600}, they estimate cell yield per mol electron acceptor (O_2 and NO_3^-), and make it possible to normalise for cell numbers in analysis for transcriptional data (gene transcripts/cell). By measuring cell density (OD_{600}), and by holding temperature at a constant, with initial oxygen and nitrate concentrations as "initially fixed standards levels", I can assume that μ and T_d will not be changing far from the resulting aerobic and anaerobic μ^{-h} during a given experiment.

Dry weight

Potentially, the type strain might be heavier of the two by 20 % mg/mL/OD_{600}. However, both biomass estimates are made from one single measurement, and are thus without statistical inference. Although the genome size of type strain (6.32 Mb) is larger than the PAO1 (6.26 Mb)(NCBI, 01.12.2016), this does not explain if the cell difference in mass is close to the truth, since biomass is highly dependent on amount of translated transcripts. Large genotype does not necessarily correlate with phenotype.

In addition, each single measurement derives from a 3 L culture that had problems, and even a full growth stop during this up-scaling of batch cultivation. Thus the dry weight may contain many cells starved for electron acceptors that will not represent relevant biomass and cannot be used during estimations of cell yield. As a suggestion, nitrate could have been given stepwise in a purely anaerobic grown culture.

More statistically trustworthy, is an estimate on mg/mL made from several, simultaneous batch cultivations of both strains. From these, further interpretation from initial biomass and its conversion factor (mg/mL/OD_{600}) could have been useful. For example, when combined with specific respiration rate (mol e- mg-1 dw h^{-1}), which describes moles oxygen used per mg of bacterial cells, or expressed transcripts per weight of culture at a given OD_{600}. Such yield coefficients provide useful factors that are valuable when modelling DRP, or N_2O emissions (Kim et al., 2012)[23].

[23]See tab.1 List of trials for modelling DRP, in Bergaust et al., (2011). For example, enzyme kinetics at aerobic and anaerobic respiration could be modelled by utilizing half-saturation constant of substrate and oxygen (mg/mL) converted into moles of substrate and oxygen used per mg cells, when modelling DRP, or N_2O emissions, or simply projecting transcripts per ng RNA (Kim et al., 2012).

Cell number estimate

Cell estimates are assumed safe due to the good regression of conversion factors from "OD to cell number" (R^2=.97). Pragmatically, as long as all cells derive from the same conditions, type of incubation is probably irrelevant. Therefore, time capacity of the current protocol can be shortened down by diluting one thickly dense vial into several different cell densities and count the cells from equal volumes under microscope. However, OD_{600} does not distinguish between live and dead cells. Therefore, this protocol was to count cells during their early growth (low- and mid-exponential growth). This should confirm that during experimental incubation, cells are alive at a given OD_{600}. Although the OD_{600} range counted seems low, it is equal to the final OD_{600} of every anaerobic growth curve of PAO1 and the type strain, and therefore highly relevant.

Additionally, DAPI stains the total bacterial population: both dead and live cells. Counting cell number from DAPI staining does not confirm whether a culture contains live or dead cells. For determining viable bacterial counts, the CFU/mL would have been a suggestion, as growth colonies are formed by live cells. However, as dead cells rarely exist at low- and mid-exponential growth, cell counts are assumed to involve viable cells only. Thus, the conversion factor cell/mL/OD_{600} is assumed to represent a robust estimate of living cell population in experimental flasks from which, ultimately, cell yield per mol electron acceptor (O_2 and NO_3^-) and mRNA transcripts per cell, derives.

Growth curves, μ^{-1} and T_d

Specific growth rate is a fundamental physiological parameter that should be reproducible when examined under a defined set of conditions (Egli, 2015). *P. aeruginosa* created different growth curves in response to: availability of electron acceptors, temperature and strain, (fig.4 and 5, Results). As expected, both PAO1and the type strain grow at slower rates during anoxic conditions. PAO1-UW is considered to be growing at the same rates and doubling times as PAO1 (DMS 22644), even though they come from different sources (Klockgether et al., 2010). The gas-based calculation of μ_{oxic} and μ_{anoxic} h^{-1} are slightly different from the empirically OD_{600} -based μ^{-1} by aerobic and anaerobic growth.

The growth curves were supposed to be measured under standard conditions. Instead, during anoxic conditions they were respiring 7 mM KNO_3. This concentration exceeds standard concentration of 2 mM KNO_3, and explains why no stationary phase is observed during anaerobic growth. However, the only implication is that the cultures

have grown and denitrified for prolonged time compared to experimental duration with 2 mM KNO_3. Specific growth rate (μ h^{-1}) is not changed by excessive concentration of electron acceptors.

The oxic conditions with excess electron acceptors (O_2) reveal a clear change from exponential to stationary growth, but the max OD_{600} was surprisingly low (OD_{600}=0.8). During growth, kinetic restriction causes an abrupt change from exponential to stationary phase (Egli, 2015). This means that stationary phase occurred due to a limiting nutrient of the Sistrom´s medium, like energy and C-source. However, succinate (C-source) was given in 34 mM concentrations and could not have been the explanation for the stationary phase at low OD_{600}. Since cell density is the object of curiosity in the overall study, this phenomenon of early halt in growth could be explained by quorum sensing regulation. Either that or another possible explanation for how cell density ended in surprisingly low levels may be due to pH. However, no changes in pH were found when measured in a few selected vials. Alternatively, one or more toxic accumulations in the Sistrom´s medium could have hindered growth, or some nutrient limitation other than carbon, like the lack of growth factors or trace elements. The important knowledge from the growth curves is still valid: difference in growth curves occurs in consequence to cells respiring different electron acceptors. Aerobic cultures grow fast from using high oxidation potential molecules (O_2) as terminal electron acceptor, and thus, gain a higher energy yield for growth. Anaerobic cultures are slow due to lower energy yield from utilizing alternative terminal electron acceptors (NO_x) (lower oxidation potential than O_2).

Additionally, temperature affects the growth curve, and thus also the μ^{-1} *and* T_d. Generally, the expected exponential doubling time for PAO1at optimal temperature (37˚C) is of 1 to 1.5 hours in minimal media (such as MOPS Glucose) and 25 to 35 minutes in a rich broth such as LB (LaBauve and Wargo, 2012). In consequence, PAO1 had an exponential growth much earlier at 30°C compared to 20°C (Sistrom´s medium), probably a result of increased kinetic rate of energy production and carbon source utilization. Thus, temperature is an important parameter to include into standard conditions when performing controlled physiological experiments.

μ^{-1} and T_d is species specific. For example, PAO1 showed a slower μ^{-1} than the type train at anoxic conditions. This was opposite during oxic conditions, where O_2 is the terminal electron acceptor. It is clear that different organisms accumulate intermediates (NO_x) differently during denitrification at standard conditions (Bergaust et

al, 2008). Fpr example, here, the type strain is an NO_2^- accumulator[24]. It is expected that NO_3^- respiration renders a different growth rate than the rest of the NO_x respirations occurring in an NO_2^- accumulator. Because μ^{-1} and T_d depends highly on type of terminal electron acceptor, organisms, which accumulate large amounts of nitrite may have different μ_{anoxic} (h^{-1}). The organism that is a "nitrite accumulator" accumulates between 60-80 % NO_2^-, at least, from reducing the initial 2mM KNO_3. This is a boundary set to classify different phenotypes from many denitrifies observations (Milligan et al., in prep.). In organisms that accumulate large amounts of nitrite, the compound starts having a toxic effect that renders inhibition on terminal oxidases, which may render poor growth (Williams et al. 1978). Reduced growth is never seen when a denitrifier is given 2 mM KNO_3, an thus the current experiments ´concentrations are considered non-toxic, even when they may accumulte100 % $nitrite_{max}$ (i.e. 2 mM NO_2^-). For example, *Paracoccus denitrificans* accumulates 100 % of the 2mM NO_3^- as NO_2^-, without any growth inhibition. *P. denitrificans* is known to have a largely split transition from aerobic respiration to denitrification when accumulating NO_2^-. This split may potentially be occurring if synthesis of nitrite reductases were slow. Depending on initial O_2 concentrations, this would then render only a small population-part to continue their growth; those that were successful in synthesizing enough nitrite reductases. The rest of the population is exposed to anoxia entrapment: i.e. lack of energy production for enzyme synthesis (Høiberg et la., 1997). Also, stop of growth is observed when aerobic grown cultures are exposed to sudden and large amounts of NO_2^- (Williams et al., 1978). This renders organisms to have an energetically difficult transition to denitrification if aerobic cultures are transferred immediately to 2 mM NO_2^- in hypoxic media (1 or 7 % O_2) (Bergaust et al., 2011). However, when the culture itself is the producer of accumulated NO_2^-, it most probably will have the required apparatus to handle the NO_2^- accumulation (like transport systems and nitrite reductases). Here, the results show that *P. aeruginosa* type strain barely accumulates between 60 and 80 % nitrite, depending on initial oxygen level and a start concentration of NO_3^- (2 mM). Thus, an eventual effect from NO_2^- on the terminal oxidases that may hinder growth is considered irrelevant. The exception in *P. aeruginosa* could be an inhibitory effect of hypoxic conditions on the high affinity oxidase during the 1% and 7 % initial oxygen

[24]In organisms which accumulate large amounts of nitrite during nitrate reduction (i.e. *P. denitrificans*), any inference on, e.g. the μanoxic/μoxic ratio, which is calculated based on electron flows derived from the measurement of gaseous intermediates, the nitrate reduction step is excluded and thus will underestimate the ratio when nitrate is the NOx initially available (Bergaust et al., 2011).

concentrations (cbb3-1 and cbb3-2) (unpublished data in Vasil and Clark, 2011). These terminal oxidases are maintaining the advantageous micro-aerobic respiration in *P. aeruginosa,* when surviving under oxidative stress conditions during pathogenesis. However, as the NO_2^- is a reactive radical, and is pumped out by $NarK_2$, there is the suggestion that the cells´ redox reactions and sensors, which provide the activity of these terminal oxidases, will maintain these oxidases in an active state, rendering efficient growth during NO_2^- accumulation (Green and Paget, 2004; Sharma et al., 2006).

The type strain has slower aerobic $\mu\ h^{-1}$ than PAO1. This could be due to NO_2^- accumulation hindering respiration of full oxygen potential (i.e. the terminal oxidases cbb3-1 and 2). Therefore, a suggested explanation is that PAO1 is more energetically successful during oxygen respiration down at lower levels (micro-aerobic respiration ability). This success might explain why PAO1 constantly have a thicker culture than the type strain at both oxic and anoxic conditions in the growth curves. However, the type strain grows slightly faster when it comes to denitrification. Maybe this is due to the already available NO_2^- accumulated and switch-off of aerobic respiratory apparatus. The survival strategy is always to be prepared with a response towards impending anoxic conditions, i.e. switch to denitrification. *nirS* is an energy expensive enzyme to build, and the hypothesis is that *nirS* transcription in *P. denitrificans* is delayed (low transcription probability) so that not all the culture surrenders to denitrification in the event of a sudden comeback of oxygen (Hassan et al., 2014). On the other hand, *P. aerugionsa* is known to transcribe *nirS* (NO_2^- reductase) during aerobic respiration, as a structural stabilizer for flagella movement (Borrero-de Acuña et al., 2015). Also, there is no trace of the difficult transition from aerobic respiration to denitrification in *P. aeruginoa* (Results, fig.24) as seen for *P. denitrificans* (Bergaust et al., 2011). Other speculative reasons as to how the type strain has a different aerobic and anaerobic $\mu\ h^{-1}$ than PAO1 are due to a difference in their denitrification apparatus efficiency, oxidase efficiencies, or even different preferences in temperature.

If the transcript numbers were higher and measured more frequently, transcription rates could have been calculated and compared with denitrification rate. If these were compared, it would tell the amount of enzymes translated. This could be used, for example, for modelling enzyme kinetics at aerobic and anaerobic respiration when predicing N_2O emissions (Bergaust et al., 2011). This would assume that all of the cells are actively transcribing, as seen by the even e-flow and cell density during in their transition from aerobic respiration to denitrification.

However, transcript rates and denitrification rates are not necessarily comparable, as the absolute quantification of mRNA may have been representing lower

than the actual mRNA copy numbers per active cell (Bergaust et al., 2010). Most probably, this occurs due to poor extraction efficiency, or short bursts of transcription. mRNA have short burst of transcription, as part of the process that regulate gene expression (i.e. being able to turn off transcription), and is completely normal as the already transcribed proteins have a longer life time that make constant mRNA production unnecessary (Lesk, 2012). When doing absolute quantification on mRNA from pure cultures, they tend to vary when comparing the same gene in different strains of bacteria (Liu et la., 2014). This complicates the comparison matter, simply because each transcript may give an immense difference in translation numbers (i.e. proteins), and thus making the mRNA/protein-ratio from protein to protein containing a large variation. Even when a gene is transcribed, it does not necessarily mean that fully functional enzymes will always be the result, but is immaturely ended in the majority of the cases. Therefore, a transcript number simply means that the cell is making an attempt at producing the protein. This illustrates how important it is to observe the products associated with the proteins catalytic activity, or other phenotype, when making a transcript analysis. As was done here, which shows a contrasting effect between *nosZ* transcript levels and N_2OR product absence, in the case of PAO1 (DSM 22644).

Pre-cultivation and inoculation

The inocula used for the incubation experiments should be kept at similar and low cell densities, which are fully dispersed and free of aggregates with anoxic micro-sites (Bergaust et al., 2011). As seen by the levels of transcript: presence of potential denitrification proteome in inocula is an issue that may present a possible weakness in data (Results, fig.27). However, it may also be that these genes are constantly expressed at the given concentrations, making a background level during aerobic respiration. Not necessarily, do the transcripts mean to end in functional enzymes (cf. discussion above). Instead, low transcript concentration during aerobic growth is explained as the bacterium`s natural background expression in case of sudden anoxia. It uses such a background to manage an escape from energy-entrapment between oxic and anoxic conditions (i.e. manage O_2 respiration to utilize energy for NO_x reductase production) (Højberg et al., 1997). Although all aerobic pre-cultivations with continuous stirring were assumed to expose equal oxic conditions to each cell, aggregations seem to have occurred. The problem with aggregation is its potential to create uncontrolled microenvironments with potential hypoxia (oxygen-depletion) (Wessel et al., 2014). Cells experiencing hypoxia through aggregation may induce expression of

denitrification proteins.

Now, because aggregation is known to be a common response of *P. aeruginosa*, the frequent subcultivation with thin inoculum was considered sufficient to dilute potential denitrification proteome and maintain aerobic pre-cultivation (Egli, 2015).

Statistics

The observed N_2O accumulations were highest in all the cultures with highest density (highest initial O_2 concentration), when compared to lower cell densities (lower initial O_2). In terms of statistics, a positive correlation between N_2O and cell density would require observations from this phenotype at several cell densities together with higher resolution: e.g. 0, 0.1, 0.5, 1, 2, and 5 % initial O_2. A regression line between cell density and N_2O accumulation would then be illustrating the positive correlation with a statistical confidence level ($R^2 > .95$). Despite their differences in source and phenotype (Klockgether et al., 2010), both the PAO1 (DSM 22644, Germany) and the PAO1-UW (USA) are providing evidence for this phenomenon of cell density and N_2O accumulation. With the current data resolution of two levels (0, and above 1 % initial O_2), this phenomenon still justified the hypothesis that quorum sensing could be involved in the regulation of N_2O reductase.

Anticipated results and their implications

Initial phenotypic experiment with 0% and 7 % initial O_2

N_2O accumulation in correlation with cell density

In the first physiological experiment, the response of the two *P. aeruginosa* strains was monitored during transition from oxic to anoxic conditions. The O_2 concentration at which denitrification is initiated (seen as a first appearance of NO) is highly variable between the two strains, but also across different treatments (tab.11). The sample frequency (660 seconds) was not considered high enough to make a reliable estimate of this parameter (O_2 µM at first NO; Results, tab.11). The organism changes from aerobic respiration to denitrification when oxygen becomes limiting and a switch of electron acceptors are necessary to continue respiratory growth. This is induced via ANR, which becomes active when released from O_2 suppression. Here, the step occurs where the *P. aeruginosa* switches into denitrification respiration mode. The cells utilizes NO_x (nitrate,

nitrite, NO and N_2O) as alternative terminal electron acceptors readily reduced in the electron transport chain.

The initial experiment demonstrate a tight regulatory control of NO_x reductases in P. aeruginosa, particularly NIR and NOR, whose activities are carefully balanced to avoid accumulation of the toxic intermediate NO. NAR, which produces NO_2^-, is controlled by ANR and is thus supressed by oxygen. Only when oxygen is low, there is a small detection of NO_2^- in the PAO1 and a slightly higher detection in the type strain. However, only the type strain reaches the required NO_2^- levels considered a characteristic of nitrite accumulators (60–80% of 100 µmol-N). The growth of the type strain seems unaffected by this accumulation. The type strain proceeds at a highly intense denitrification when given 7 % initial oxygen respiration that renders no detection of intermediates until N_2 production starts.

The main difference is that denitrification proceeds at higher intensity in cultures given higher initial oxygen. High initial oxygen concentration, by consequently providing large energy quanta, determines cell density to be large in the transition from oxic to anoxic environment. A contrasting example is where PAO1 in the wake of 0 % initial oxygen releases a low NO_2^- level that lasts longer, as a consequence of low cell density (Results, fig.20). If denitrification occurs faster due to increased cell density, then N_2O should be effectively reduced by the N_2OR. However, N_2OR does not effectively reduce N_2O in neither of the oxygen treatments with *P. aeruginosa* PAO1. Why is an extreme N_2O-product detected in the PAO1 culture during high cell density, as well as during anoxic conditions, albeit at a lower level?

Some hypothesis on how cell density affects denitrification has been made. For example, denitrification is negatively correlated with quorum sensing activity (Hammond et al. 2015). Even so, it is less understood what cell density might do against the N_2OR activity, specifically. The initial result infer that N_2OR is either non-active, inhibited or not even transcribed at high initial oxygen concentrations, while at 0 % oxygen it seems stabile, but at relatively low activity. Assuming a clear correlation between cell density and N_2O accumulation in PAO1: could N_2O accumulation occur due to regulation on transcriptional events or metabolic level?

Further investigation involved finding whether quorum sensing down-regulates the whole denitrification, or particularly reduction of N_2O in PAO1. If a culture of PAO1 reaches a certain density, then QS-signals (AHLs) should appear to interfere with denitrification on transcriptional or metabolic level.

AHLs system experiment & Gene expressions

QS Correlation with N_2O accumulation

Both gas accumulation, e-flow to N_2OR, cell densities and *nosZ/nirS* transcript ratio revealed a rate limiting effect, which is most probably caused by QS on N_2OR. The AHL effect on N_2O accumulation revealed that N_2OR is under LasR system regulation (3O-C12-HSL) during post-transcriptional events.

In most respects, the denitrification phenotypes of the *lasI⁻rhlI⁻* mutant and its parent strain were very similar. Despite their slight differences in NO_x accumulations, NAR, NIR and NOR enzymes seemed well coordinated by both organisms. The transitions from aerobic respiration to denitrification were finely regulated so that the cultures switched between electron acceptors without any dramatic delay or drop in total electron flow (Results, fig.24). In comparison, other studies have found that the e-flow during oxic-anoxic transition in *P. denitrificans* is known to drop dramatically in between the oxic-anoxic transition. Furthermore, they took this to illustrate that only a minor fraction of the population becomes full-fledged denitrifiers (Hassan et al., 2014). Here, though, *P. aeruginosa* PAO1-UW and *lasI⁻rhlI⁻* mutant display a tighter control. Their e-flow and cell density rate implies that the whole culture becomes fully fledged in the transition from oxic to anoxic conditions (Results, fig.24; 29). Also, their tight control on the metabolic transition is reflected in the strict control of the toxic intermediate NO throughout all incubation experiments (Result, tab.12; fig.22 and 23). When comparing NO and timing of transcription, all peak expressions occur at peak measurement of NO (Results, fig.22; fig.27). This illustrates the regulatory effect where NO via DNR enhances denitrification. Furthermore, these enzymes are tightly regulated at transcription level by O_2 on ANR (negatively and global) and nitrate/nitrite and NO on DNR (positively). The difference in their phenotype occurs at N_2O accumulations, which imply that the N_2OR enzyme is controlled in a different way than the rest.

N_2O accumulation was never reduced to N_2 during initial experiment with the PAO1 (DSM 22644) (at above 1 % initial O_2) (Appendix, fig.IV; Results, fig.21). PAO1-UW managed to produced N_2 eventually, but only after all the other electron acceptors are reduced to N_2O_{max} (at 4 % initial O_2)(Results, fig.22). Even though these two organisms differed slightly in phenotype, the tendency of N_2O accumulation with cell density still holds true for both of them. In contrast to these two, the PAO1 *rhlI⁻lasI⁻* mutant denitrified all the way towards N_2 without any pronounced N_2O accumulation (Results, fig.22 B).

The e-flow (μmol e^-h^{-1}) between NAR, NIR, and NOR are identical in both mutant

and wild type (Results, fig.24). This means that respiration rate upstream of N_2OR is the same. However, e-flow to N_2OR is defining a rate-limiting step during denitrification phenotype in the PAO1-UW. When looking at cell densities during denitrification, their growth are almost completely alike during all reduction steps, except during N_2O reduction (Results, fig.29). The cell densities during transition from oxic to anoxic conditions, which increases at approximately the same rate in both organisms until they reach the N_2O_{max}, illustrates that NAR is not the bottleneck in this system: that would be N_2OR (Results, fig.29).

When looking at transcripts that precede Nar (*narG),* Nir *(nirS)*, and NOR (*norB*), these are very alike, except for the level of *narG* expression. *narG* gene is subject to direct transcriptional regulation by ANR, NarXL and DNR, while downstream genes (*nir, nor* and *nos*) are DNR activated (Hammond et la., 2015). In the PAO1-UW *narG* transcription is low, but detectable. The high expression in the *rhlI*$^-$*lasI*$^-$ mutant, confirm what is already known: that *narG* is repressed by QS (Brackman et al., 2016)**.** However, high or low *narG* expression does not affect respiration rate, which was exactly alike in both organisms (Results, fig.24). Thus, *narG* expression becomes irrelevant, as it does not explain the observed N_2O accumulation with cell density phenotype.

The *nosZ/nirS* transcript ratio is a strong reflection of something peculiar occurring during denitrification in the *P. aeruginosa* wild type. The wild type is expressing *nosZ/nirS* ratio by 4 times more than the mutant (Results, fig.28). The peculiar thing is that the high *nosZ/nirS* expression ratio contradicts the slow gas reduction of N_2O to N_2 in PAO1-UW (Results, fig.22A). A rate limiting control on N_2O reduction in the wild type is obviously occurring, when looking at its e-flow to N_2OR in PAO1-UW (Results, fig.25). What this is telling is that the N_2OR was apparently present (due to N_2 production from electron flow), but largely inactive until N_2O_{max} peak was reached. Once no more electron acceptors were available (due to reduction to N_2O) the existing N_2OR enzyme pool must have started to reduce the available N_2O further to N_2. The low, but limited number of N_2OR enzymes is a reasonable explanation for a constant e-flow to N_2OR (Results, fig.25B).

The transcript levels indicate that there is not occurring any depression on transcriptional level. Although, N_2O reductases exist, the further *nosZ* transcription cannot compensate for N_2O accumulation. In comparison, the *nosZ* transcription is low in an organism freed of QS-systems. Still: its produced N_2OR enzymes display N_2O reduction rates just as effective as the upstream NO_x reductases (Results, fig.25).

N_2O is known to not induce any regulatory effect on denitrification. Many prokaryotes exist that uses all enzymes without exogenous N_2O reduction due to

enzyme-loss (Bryan et al., 1985; SooHoo and Hollocher, 1990). Here though, enzymes probably already exist in the culture before QS regulation kicks in. Most likely, QS depresses N_2OR activity through post-transcriptional regulation. For example, assembly in the periplasm: either by direct or indirect repression. As a suggestion, QS either inhibits new assembly, or represses the activity of intact enzymes through some unknown mechanism.

To confirm that N_2OR is fully assembled, but its activity repressed during reduction of nitrate to N_2O, it would be interesting to add chloramphenicol[25] the moment before the wild type begins to reduce N_2O. The antibiotic, when administered at the correct concentration, does not significantly inhibit the activity of already assembled proteins, but stops *de novo* protein synthesis (Wolfe and Hahn, 1965). Thus, if N_2O is not reduced further, it would indicate that QS controls the assembly of functional N_2OR. However, if N_2O is reduced to N_2 after addition of chloramphenicol, it would suggest that N_2OR is fully functional, but interacts with some QS controlled factor, suppressing its activity as long as nitrate, nitrite or NO are available.

This work is still quite open-ended, as we have only begun to scratch the surface of how quorum sensing regulates denitrification. The late activation of N_2O could be explained by some missing factor, controlled by the QS system. In that case, the experiment above would result in N_2 production. Obviously, this factor would interplay with N_2OR to maintain its function.

The addition of 3O-C12-HSL to *rhlI*$^-$*lasI*$^-$ mutant provided approximately three times the N_2O concentration compared to exposure by C4-HSL (Results, fig.23; tab.12). Additionally, the 3O-C12-HSL effect on the mutant is considerable when looking at final cell densities. Their difference is 34 % between the 3O-C12-HSL treated mutant and its untreated cultures (Results, fig.30). The 3O-C12-HSL responses strongly suggest that the Las-circuit is the major negative regulator of N_2O reduction rate.

However, the interconnections between LasR-RhLR circuits and denitrification are still not fully understood. The C4-HSL-RhIR complex is referred to in literature as the single repressor on denitrification, where the 3O-C12-HSL-LasR complex was not found to have any effect on NO_3^- reduction rate in a PAO1 *rhlI*$^-$*lasI*$^-$ mutant (Toyofuku et al., 2007). Possibly, that was to test repression of *narG* expression. Here, though, the 3O-C12-HSL-LasR complex occurs to have the greatest effect on respiration at the N_2O

[25] Chloramphenicol inhibits the ribosomal peptidyl transferase, and thereby, preventing protein chain elongation (Wolfe and Hahn, 1965).

reduction rate.

At this time, we are left with more questions than answers. What are the mechanisms of QS-controlled inhibition of N_2O reductase? It is not the concentration of AHLs *per se*, but rather the activated LasR population that shape the AHL-QS regulon (Heurlier et al., 2006). During the growth of a culture, LasR/3O-C12-HSL is produced at low concentrations as long as the cell density is low. At a critical concentration their autoinduction on LasI starts. This also starts the induction of the RhLR/C4-HSL system, which does not reach effective thresholds until reaching higher cell densities (Heurlier et al., 2006). Thus it seems strange that C4-HSL could depress denitrification at the early stage of *narG* transcriptional events. The cultures at that particular experiment must have been very rich in electron acceptors. In fact they were. The *rhlI*- mutant cells were anaerobically grown with 100 mM NO_3^- (Toyofuku et al., 2007). That explains how the cultures could reach a higher cell density in order for catching the QS repressing effect on NO_3- reduction by RhLR/C4-HSL circuit. Another, similar description is that QS controls function at a *continuum*: i.e. AHL signals are continuously produced, but the amount of receptors are the limiting factor for cell density signalling (Schuster and Greenberg, 2006).

Most targets are not transcriptionally activated before sufficient LasR and RhLR levels are induced by AHLs (Schuster and Greenberg, 2006). Therefore, it could be said that LasR, at a certain cell density, changes the amount of active N_2OR. LasR then acts directly on promotors of genes. The QS controlled promotor (*las-rhl* box-like sequences) that exists in 15-25 % of all QS-controlled promoters, are regulated indirectly (Schuster et al., 2003; Schuster and Greenberg, 2006; Wagner et al., 2003). Therefore, LasR/3O-C12-HSL most likely inhibits N_2OR assembly or activity indirectly via factors within its regulon (fig.31). Additionally, RhIR and LasR are co-regulating their QS regulon with other regulators, like the ANR (positively) and QscR (negatively) (Chugani et al., 2001; Pessi and Haas, 2000).

The current results confirm that the LasR inducer, the 3O-C12-HSL signal, is the one mainly responsible for the low N_2O respiration rate effect seen in the wild type. The RhLR system is also involved, but not to the same degree. What is the purpose of a low N_2OR activity in an organism if it results in slower growth?

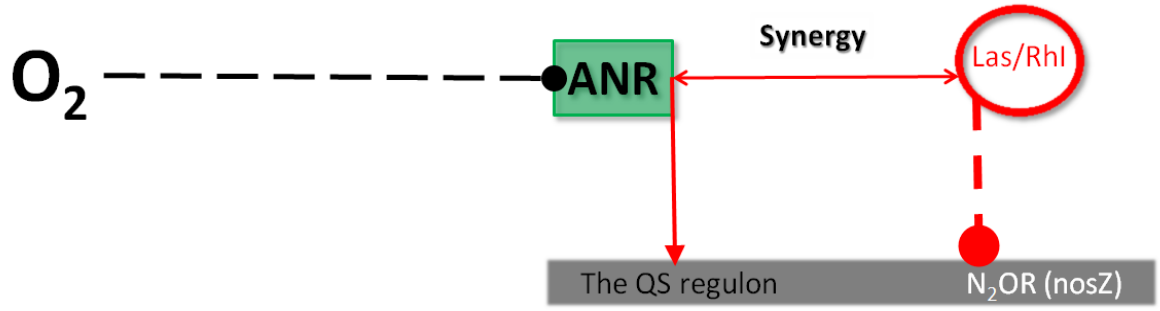

Figure 31. The QS regulon is defined as the collection of activated genes by LasR/3O-C12-HSL and RhlR/C4-HSL, directly or indirectly. Complete arrows=activation. Dots=inhibitions. Synergy: The interaction of two or more agents or forces so that their combined effect is greater than the sum of their individual effects (Arai et al., 2014; Schuster and Greenberg, 2006).

Both *P. aeruginosa* wild type (QS active) and a diversity of QS-mutants exist in the same biofilm (Zierdt and Schmidt, 1964). Apparently, QS receptor-mutants[26] are common examples of loss of QS-machinery because loss of functional LasR and RhLR has a larger phenotypic consequence compared to mutations in LasI and RhlI in biofilms (Heurlier et al., 2006). LasR and RhLR mutants are found to outgrow the wild type during stationary phase, not with the rationale that they have a faster rate, but how they undergo cell division and cell lysis at a slower rate than the wild type (Heurlier et al., 2005). In the current results, the *rhlI*$^-$*lasI*$^-$ mutants and PAO1-UW grew almost at the same rate, albeit the wild type slowed down growth at N_2O reduction. Therefore, I say the quorum sensing systems are slowing down the wild types growth rate, while the *rhlI*$^-$*lasI*$^-$ mutants are cheating by keeping up their population growth at a constant rate (fig.29). In fact, the *rhlI-lasI-* mutants in biofilms are thought to exploit the cooperative behaviour of the wild types and at the same time avoid production of AHLs (Diggle et al., 2007). However, if current cell density effect from QS seem illustrative (Results, fig. 29; fig.30), the difference of their cell yield per e^- acceptor is not very large (tab.12). Still, the reduced population growth of the wild type, where N_2OR activity is repressed and the transcriptional activity ratio is high. In combination with AHL systems experiment

[26] The rationale is that perhaps mutations in LasI and RhlI, when receptors are intact, will not have large consequence since AHLs produced by wild types in the biofilm compensating for lack of AHL production by LasI or RhLI mutants (Heurlier et al., 2006).

result, which say that QS, most likely the LasI-LasR system in *P. aeruginosa* PAO1 is the underlying mechanism not understood, imply that further investigations are needed on N_2OR repression.

Humans

P. aeruginosa PAO1 have been repeatedly identified in clinical samples (Salunkhe et al., 2005). Within biofilm of hosts´ tissues, there exists a natural variety of wild types and mutants. The fitness trait of QS-mutants is that they grow together with wild types to produce biofilm during human infection of, for example, the respiratory tract in CF patients. There, the mutants grow without using energy to produce parts of (RhLI or LasI mutants), or the whole QS system (RHLR or LasR mutants) (Hassett et al., 2002; Heurlier et al., 2006).

QS circuits are understood to be the major regulator in *P. aeruginosa.* It is considered a fitness trait when *P. aeruginosa* can switch between growing in a variety of conditions. Through its broad metabolic range of respiration abilities it adapts rapidly to anoxic conditions. QS greatly contribute to fitness through production of the signals C4-HSL and 3O-C12-HSL. Through AHL induction, QS regulates expression of anaerobic cytochrome oxide reductases (coxAB and cyoABCD) during transitions from oxic to anoxic conditions (Heurlier et al., 2006). Also, its background levels of *nirS* transcripts, which aid in the growth of flagella (Borrero-de Acuna et al., 2015), and the swimming motility towards tissues for adhesion, are probably a function under QS control (Köhler et al., 2000). However, during their biofilm formation, a steep hypoxic gradient is produced, in which the rapidly respiring QS mutants and slower growing wild types exist side by side (Chambers et al., 2005).

A negative impact on fitness by QS occurs at start of biofilm production and infection. At these circumstances, being a QS mutant is beneficial due to its free utility of a Type III secretory system. This injects virulence factors into hosts systems and increases the amount of sessile cells (adherence to tissue): a fitness for survival in any environment (Goodman et al., 2004).

How widespread the QS-intervening mechanism of N_2OR oppression at post-transctiprional levels really is among denitrifiers, is unknown. The initially studied *P. aeruginosa* type strain is less prone to accumulate N_2O under the conditions tested. This can be taken to illustrate that the QS effect on N_2OR is variable even within strains belonging to the same species. Also, lab-cultures are more rich in both carbon and electron sources compared to natural soils. Therefore, it is not unlikely that this mechanism of depressed anaerobic growth rate is an adaptation to energy poor

environments. Also, the reduced respiration rate in the wild type seems more believable if this mechanism should provide a stabile biofilm formation in environments where electron acceptors are variably available. In that case, this QS-depressing N_2OR-mechanism is just another variation of DRP that provide survival in certain critical situations, like lack of energy source. Lacking energy to provide binary fission is one of the main limitations that provide a stationary and death phase of a culture (Egli, 2015).

Overcoming the innate/adaptive immune system, antibiotics or other stress factors, the QS circuits seems immensely important to *P.aeruginosa* ((Hassett et al., 2002; Skindersoe et al., 2009; Smith and Iglewski, 2003). However, how it possibly could benefit by spitting out the N_2O during denitrification, is unknown. N_2O is known to inactivate cob(I)alamin[27], an important ingredient in biosynthesis of Glutathione (antioxidant of every cell system)(Nunn, 1988; Schafer and Buettner, 2001). Low glutathione level is a marker of chronic infections and immunocompromised individuals, like in lung tisues of CF patients (Roum et al., 1993). Thus, N_2O could play a factor of virulence by the *P. aeruginosa* wild types. But this would imply that the organism take the risk of losing an energy source during denitrification, and probably other virulence particles, like pyocyanin are effective virulence factors as well (Appendix, fig.I) (Cox and Parker, 1979; Lau et al., 2004).

The elucidation of mechanisms employed by *P. aeruginosa* to thrive in niches such as the lung are providing new insights to treatment strategies for *P. aeruginosa* infections (LaBauve and Wargo, 2012).

Climate

The *P. aeruginosa* is also found in soil and water systems (Ringen and Drake, 1952). This successful survivor of soil is aided by its swimming motility and biofilm formation ability. Biofilm communities transmitting and receiving information by QS, are able to regulate many genes under QS-control, such as production of virulence factors, antibiotics, population size dynamics (biofilm formation and dispersal) (van Elsas et al. 2006). During QS control on oxic-anoxic transition, a denitrifying organism in soil has a great potential to accumulate and emit N_2O. For example, PAO1 (7 % initial O_2

[27] Cob(I)alamin is the active derivative of vitamin B12, and an essential cofactor for the transfer of the methyl group from methyltetrahydrofolate to homocysteine to form methionine (Nunn, 1988).

treatment) most likely had a N_2OR highly susceptible to population dynamics, implied by its end-product, N_2O (Results, fig.21B). Probably, QS controlled the crowded environments to act accordingly, with a more strict nutrient acquisition for a more cooperative nutrient metabolism (An et al., 2014). Increased cell density increases the QS regulatory circuits in action, and N_2OR was probably inhibited in the process. Therefore, PAO1 accumulated and even emitted N_2O. If it is not an isolated phenomenon, the QS-mediated accumulation of N_2O in *P. aeruginosa* may have implications for the understanding of N_2O release from hotspots in the environment (Zheng and Doskey, 2016). In the environment, the relative N_2O production rates are dependent on partial pressure of oxygen (pO_2) experienced by the given cells, including pH, nitrate and nitrite concentrations. O_2 supply provides increased energy for growth, and thus increased cell population. When oxygen is suddenly depleted, the N_2O production has its potential to reach maximum peaks, provided the QS mechanism is in action.

Soils are the primary source of N_2O emission (Galloway et al., 2004). A soil system's propensity to emit N_2O are influenced by a series of parameters such as pH and the availability of oxygen and/or NO_x. However, the major correlation between soil pH and the N_2O/N_2 product ratio in soil does not explain all the N_2O released (ŠImek and Cooper, 2002). Denitrifiers in soils, when exposed to fluxes from aerated to anaerobic microsites of moisturized soils, emit N_2O (Anderson and Levine, 1986). The mimicking of O_2 fluctuations in soil with, for example investigations of the PAO1 that emitted N_2O (1 % initial O_2), could evidently propose QS as an additional explanation for the total 17 Tg/y that is emitted of N_2O from denitrification alone.

Denitrification is found abundantly widespread round the globe, in areas where it contributes to prokaryote`s survival during fluctuation of oxygen concentrations. Microbial organisms are extremely versatile in surviving fluctuating conditions, and *Pseudomonas aeruginosa* is one such extraordinary example, supporting this QS regulatory mechanism when determining DRP.

With the current understanding of the nitrogen cycle, it is suggested that we benefit if we minimize our impact on the nitrogen cycle by a sustainable development of the agricultural management (IPCC, 2014; Machida et a., 1995; Montzaka et al., 2011). Future trends of N_2O emissions from denitrification could change if it all was depending on one parameter: pH. Lack of regulatory knowledge on how not all N_2O from denitrification is explained by pH, is a gap that may be filled by QS regulatory effects on N_2O reductase. Biologically, only N_2OR enzymes are known to reduce N_2O to N_2 as their primary function (Jones, et al. 2008). Here, the N_2O accumulation and emission is

evidently proposing QS as an additional explanation for the total 17 Tg/y that is emitted of N_2O from denitrification alone.

REFERENCES

ALMASRI, M. N. & **KALUARACHCHI**, J. J. (**2004).** Assessment and management of long-term nitrate pollution of ground water in agriculture-dominated watersheds. *Journal of Hydrology,* 295**,** 225-245.

AN, J. H., GOO, E., KIM, H., SEO, Y.-S. & HWANG, I. (**2014).** Bacterial quorum sensing and metabolic slowing in a cooperative population. *Proceedings of the National Academy of Sciences,* 111**,** 14912-14917.

ANDERSON, I.C., & **LEVINE**, J.S. (**1986).** Relative Rates of Nitric Oxide and Nitrous Oxide Production by Nitrifiers, Denitrifiers, and Nitrate Respirers. American Society for Microbiology. Appl. Environ. Microbiol. vol. 51(5): 938-945.

APPELO C.A.J. & D.**POSTMA:** Geochemistry, groundwater and pollution (**1993**), A.A.Balkema/Rotterdam. pp.536.

APPLICATION GUIDE for QX200. (01.12. 2016), 11:14 am. Retrieved from http://www.bio-rad.com/webroot/web/pdf/lsr/literature/Bulletin_6407.pdf , pp.111

ARAI, H., Y. IGARASHI, & T. KODAMA. (**1995).** Expression of the nir and nor genes for denitrification of *Pseudomonas aeruginosa* requires a novel CRP/ FNR-related transcriptional regulator, DNR, in addition to ANR. FEBS Lett. 371:73–76

ARAI, H., KODAMA, T. & IGARASHI, Y. (**1997)**. Cascade regulation of the two CRP/FNR-related transcriptional regulators (ANR and DNR) and the denitrification enzymes in Pseudomonas aeruginosa. *Molecular microbiology,* 25**,** 1141-1148.

ARAI, H., KAWAKAMI, T., OSAMURA, T., HIRAI, T., SAKAI, Y. & ISHII, M. (**2014).** Enzymatic characterization and in vivo function of five terminal oxidases in Pseudomonas aeruginosa. *Journal of bacteriology,* 196**,** 4206-4215.

ATSDR, Kim Gehle MD, MPH**. (2015)**. 17.10.2016, 8 pm. Case Studies in Environmental Medicine (CSEM). *Nitrate/Nitrite Toxicity: What Are the Health Effects from Exposure to Nitrates and Nitrites?* Agency for Toxic Substances & Disease Registry, U.S. Department of Health and Human Services. Retrieved from https://www.atsdr.cdc.gov/csem/csem.asp?csem=28&po=10; http://www.haz-map.com/methem.html; https://www.atsdr.cdc.gov/csem/csem.asp?csem=28&po=10.

BAKKEN, L.R., BERGAUST, L., BINBIN LIU, & FROSTEGÅRD, Å. (**2011).** Regulation of denitrification at the cellular level: a clue to the understanding of N2O emissions from soils. Published 26 March 2012. DOI: 10.1098/rstb.2011.0321

BEDZYK, L., WANG, T. & **RICK,** W. Y. (**1999).** The Periplasmic Nitrate Reductase inPseudomonas sp. Strain G-179 Catalyzes the First Step of Denitrification. *Journal of bacteriology,* 181**,** 2802-2806.

BERGAUST, L., SHAPLEIGH, J., FROSTEGÅRD, Å. & BAKKEN, L. (**2008).** Transcription and activities of NOx reductases in Agrobacterium tumefaciens: the influence of nitrate, nitrite and oxygen availability. *Environmental microbiology,* 10**,** 3070-3081.

BERGAUST, L., MAO, Y., BAKKEN, L. R. & FROSTEGÅRD, Å. (**2010).** Denitrification response patterns during the transition to anoxic respiration and posttranscriptional effects of suboptimal pH on nitrogen oxide reductase in Paracoccus denitrificans. *Applied and environmental microbiology,* 76**,** 6387-6396.

BERGAUST, L., BAKKEN, L. R. & FROSTEGÅRD, Å. (**2011).** Denitrification regulatory phenotype, a new term for the characterization of denitrifying bacteria. *Biochemical Society Transactions,* 39**,** 207-212.

BIOTOOLS. (03.02.16). 13:47pm.
Retrieved from
http://biotools.nubic.northwestern.edu/OligoCalc.html

BORRERO-DE ACUÑA, J. M., MOLINARI, G., ROHDE, M., DAMMEYER, T., WISSING, J., JÄNSCH, L., ARIAS, S., JAHN, M., SCHOBERT, M. & TIMMIS, K. N. (**2015)**. A periplasmic complex of the nitrite reductase NirS, the chaperone DnaK, and the flagellum protein FliC is essential for flagellum assembly and motility in Pseudomonas aeruginosa. *Journal of bacteriology,* 197**,** 3066-3075.

BOTHE, H., FERGUSON, S. & NEWTON, W. E. (**2006).** *Biology of the nitrogen cycle*, Elsevier.

BRACKMAN, G., BREYNE, K., DE RYCKE, R., VERMOTE, A., VAN NIEUWERBURGH, F., MEYER, E., VAN CALENBERGH, S. & COENYE, T. (**2016).** The Quorum Sensing Inhibitor Hamamelitannin Increases Antibiotic Susceptibility of Staphylococcus aureus Biofilms by Affecting Peptidoglycan Biosynthesis and eDNA * Release. *Scientific reports,* 6.

BRONDIJK, T. H. C., NILAVONGSE, A., FILENKO, N. & RICHARDSON, D. J. (**2004).** NapGH components of the periplasmic nitrate reductase of Escherichia coli K-12: location, topology and physiological roles in quinol oxidation and redox balancing. *Biochemical Journal,* 379**,** 47-55.

BRYAN, B., JETER, R. & CARLSON, C. (**1985)**. Inability of Pseudomonas stutzeri denitrification mutants with the phenotype of Pseudomonas aeruginosa to grow in nitrous oxide. *Applied and environmental microbiology,* 50**,** 1301-1303.

CASTIGLIONE, N., RINALDO, S., GIARDINA, G. & CUTRUZZOLÀ, F. (**2009)**. The transcription factor DNR from Pseudomonas aeruginosa specifically requires nitric oxide and haem for the activation of a target promoter in Escherichia coli. *Microbiology,* 155**,** 2838-2844.

CHAMBERS, C. E., VISSER, M. B., SCHWAB, U. & SOKOL, P. A. (**2005)**. Identification of N-acylhomoserine lactones in mucopurulent respiratory secretions from cystic fibrosis patients. *FEMS microbiology letters,* 244**,** 297-304.

CHEN, D., LAN, Z., BAI, X., GRACE, J.B. & BAI, Y. **(2013).** Evidence that acidification-induced declines in plant diversity and productivity are mediated by changes in below-ground communities and soil properties in a semi-arid steppe. *Journal of Ecology* 2013, 101, 1322-1334. British Ecological Society doi:10.1111/1365-2745.12119 http://onlinelibrary.wiley.com/doi/10.1111/1365-2745.12119/epdf

CHEN, H., SHIROGUCHI, K., GE, H. & XIE, X. S. (**2015).** Genome-wide study of mRNA degradation and transcript elongation in Escherichia coli. *Molecular systems biology,* 11**,** 781.

CHEN, J. & **STROUS**, M. (**2013)**. Denitrification and aerobic respiration, hybrid electron transport chains and co-evolution. *Biochimica et Biophysica Acta (BBA)-Bioenergetics,* 1827**,** 136-144.

CHUGANI, S. A., WHITELEY, M., LEE, K. M., D'ARGENIO, D., MANOIL, C. & GREENBERG, E. (**2001).** QscR, a modulator of quorum-sensing signal synthesis and virulence in Pseudomonas aeruginosa. *Proceedings of the national academy of sciences,* 98**,** 2752-2757.

CICERONE, R. J. (**1987).** Changes in stratospheric ozone. *Science,* Volume 237**,** Issue4810, pp. 35-42. (DOI: 10.1126/science.237.4810.35)

COX, C. D. & **PARKER**, J. (**1979)**. Use of 2-aminoacetophenone production in identification of Pseudomonas aeruginosa. *Journal of Clinical Microbiology,* 9**,** 479-484.

ČUHEL, J., ŠIMEK, M., LAUGHLIN, R. J., BRU, D., CHÈNEBY, D., WATSON, C. J. & PHILIPPOT, L. (**2010).** Insights into the effect of soil pH on N2O and N2 emissions and denitrifier community size and activity. *Applied and environmental microbiology,* 76**,** 1870-1878

DAIMS, H., LEBEDEVA, E. V., PJEVAC, P., HAN, P., HERBOLD, C., ALBERTSEN, M., JEHMLICH, N., PALATINSZKY, M., VIERHEILIG, J. & BULAEV, A. (**2015).** Complete nitrification by Nitrospira bacteria. *Nature,* 528**,** 504-509.

DEKIMPE, V. & **DEZIEL**, E. (**2009)**. Revisiting the quorum-sensing hierarchy in Pseudomonas aeruginosa: the transcriptional regulator RhlR regulates LasR-specific factors. *Microbiology,* 155**,** 712-723.

DEL FABBRO, C., SCALABRIN, S., MORGANTE, M. & GIORGI, F. M. (**2013)**. An extensive evaluation of read trimming effects on Illumina NGS data analysis. *PLoS One,* 8**,** e85024.

DEREN, J. J., ARORA, B., TOSKES, P. P., HANSELL, J. & SIBINGA, M. S. (**1973).** Malabsorption of crystalline vitamin B12 in cystic fibrosis. *New England Journal of Medicine,* 288**,** 949-950.

DIGGLE, S. P., GRIFFIN, A. S., CAMPBELL, G. S. & WEST, S. A. (**2007)**. Cooperation and conflict in quorum-sensing bacterial populations. *Nature,* 450**,** 411-414.

DNA BASER. (11.11.2016). 14:26 am. DNA nucleotide counter. Sequence assembly software. Retrieved from *http://www.dnabaser.com/download/DNA-Counter/*

DRISCOLL, J. A., BRODY, S. L. & KOLLEF, M. H. (**2007).** The epidemiology, pathogenesis and treatment of Pseudomonas aeruginosa infections. *Drugs,* 67**,** 351-368.

DSMZ, (07.12.2016). 19:37 pm. Retrieved from *https://www.dsmz.de/catalogues/details/culture/DSM-22644.html*

EGLI, T. **(2015)**. Microbial growth and physiology: a call for better craftsmanship. *Frontiers in microbiology,* 6.

ENGEBRECHT, J., NEALSON, K. & SILVERMAN, M. (**1983)**. Bacterial bioluminescence: isolation and genetic analysis of functions from Vibrio fischeri. *Cell,* 32**,** 773-781.

EVROGEN. (26.11.2016). 12.44 pm. Retrieved from http://evrogen.com/technologies/normalization.shtml.

FUQUA, W.C., WINANS, S.C., & GREENBERG, E.P. (**1994).** Quorum sensing in bacteria: the LuxR-LuxI family of cell density-responsive transcriptional regulators. Copyright © 1994, American Society for Microbiology MINIREVIEW Journal of bacteriology, 176 (2): 269-275.

GALLOWAY, J. N., DENTENER, F. J., CAPONE, D. G., BOYER, E. W., HOWARTH, R. W., SEITZINGER, S. P., ASNER, G. P., CLEVELAND, C., GREEN, P. & HOLLAND, E. (**2004).** Nitrogen cycles: past, present, and future. *Biogeochemistry,* 70**,** 153-226.

GONG, Z., & PING **XIE**, P. **(2001).** Impact of eutrophication on biodiversity of the macrozoobenthos community in a Chinese shallow lake. *Journal of Freshwater Ecology* 16(2):171-178.

GOODMAN, A. L., KULASEKARA, B., RIETSCH, A., BOYD, D., SMITH, R. S. & LORY, S**. (2004).** A signaling network reciprocally regulates genes associated with acute infection and chronic persistence in Pseudomonas aeruginosa. *Developmental cell,* 7**,** 745-754.

GREENBERG, E. P. & **BECKER**, G**. (1977)**. Nitrous oxide as end product of denitrification by strains of fluorescent pseudomonads. *Canadian journal of microbiology,* 23**,** 903-907.

GREEN, J. & **PAGET**, M. S. (**2004)**. Bacterial redox sensors. *Nature Reviews Microbiology,* 2**,** 954-966.

GREEN, S. K., SCHROTH, M. N., CHO, J. J., KOMINOS, S. D. & VITANZA-JACK, V. B. (**1974).** Agricultural plants and soil as a reservoir for Pseudomonas aeruginosa. *Applied microbiology,* 28**,** 987-991.

GUO, J., LIU, X., ZHANG, Y., SHEN, J., HAN, W., ZHANG, W., CHRISTIE, P., GOULDING, K., VITOUSEK, P. & ZHANG, F. (**2010).** Significant acidification in major Chinese croplands. *science,* 327**,** 1008-1010.

HAMMOND, J. H., DOLBEN, E. F., SMITH, T. J., BHUJU, S. & HOGAN, D. A. (**2015).** Links between Anr and quorum sensing in Pseudomonas aeruginosa biofilms. *Journal of bacteriology,* 197**,** 2810-2820.

HANKE, A. **& STROUS**, M. **2010.** Climate, fertilization, and the nitrogen cycle. *J. Cosmology,* 8**,** 1838-1845.

HÄRTIG, E., SCHIEK, U., VOLLACK, K.-U. & ZUMFT, W. G. (**1999)**. Nitrate and Nitrite Control of Respiratory Nitrate Reduction in Denitrifying *Pseudomonas stutzeri* by a Two-Component Regulatory System Homologous to NarXL ofEscherichia coli. *Journal of bacteriology,* 181**,** 3658-3665.

HASEGAWA, N., ARAI, H. & IGARASHI, Y. (**1998).** Activation of a consensus FNR-dependent promoter by DNR of Pseudomonas aeruginosa in response to nitrite. *FEMS microbiology letters,* 166**,** 213-217.

HASSAN, J., BERGAUST, L. L., WHEAT, I. D. & BAKKEN, L. R. (**2014).** Low probability of initiating nirS transcription explains observed gas kinetics and growth of bacteria switching from aerobic respiration to denitrification. *PLoS Comput Biol,* 10**,** e1003933.

HASSETT, D. J., CUPPOLETTI, J., TRAPNELL, B., LYMAR, S. V., ROWE, J. J., YOON, S. S., HILLIARD, G. M., PARVATIYAR, K., KAMANI, M. C. & WOZNIAK, D. J. (**2002).** Anaerobic metabolism and quorum sensing by Pseudomonas aeruginosa biofilms in chronically infected cystic fibrosis airways: rethinking antibiotic treatment strategies and drug targets. *Advanced drug delivery reviews,* 54**,** 1425-1443.

HENDRIKS, J., WARNE, A., GOHLKE, U., HALTIA, T., LUDOVICI, C., LÜBBEN, M. & SARASTE, M. (**1998).** The active site of the bacterial nitric oxide reductase is a dinuclear iron center. *Biochemistry,* 37**,** 13102-13109.

HENDRIKS, J., OUBRIE, A., CASTRESANA, J., URBANI, A., GEMEINHARDT, S. & SARASTE, M. (**2000).** Nitric oxide reductases in bacteria. *Biochimica et Biophysica Acta (BBA)-Bioenergetics,* 1459**,** 266-273.

HERRIDGE, D. F., PEOPLES, M. B. & BODDEY, R. M. (**2008).** Global inputs of biological nitrogen fixation in agricultural systems. *Plant and Soil,* 311**,** 1-18.

HEURLIER, K., DÉNERVAUD, V., HAENNI, M., GUY, L., KRISHNAPILLAI, V. & HAAS, D. (**2005)**. Quorum-sensing-negative (lasR) mutants of Pseudomonas aeruginosa avoid cell lysis and death. *Journal of Bacteriology,* 187**,** 4875-4883.

HEURLIER, K., DÉNERVAUD, V. & HAAS, D. (**2006).** Impact of quorum sensing on fitness of Pseudomonas aeruginosa. *International journal of medical microbiology,* 296**,** 93-102.

HORN, M.A., IHSSEN,J., MATTHIES,C., SCHRAMM,A., ACKER, G., & DRAKE, H.L. **(2005).** *Dechloromonas denitrificans* sp. nov., *Flavobacterium denitrificans* sp. nov., *Paenibacillus anaericanus* sp. nov. and *Paenibacillus terrae* strain MH72, N2O-producing bacteria isolated from the gut of the earthworm *Aporrectodea caliginosa*. International Journal of Systematic and Evolutionary Microbiology (2005), 55, 1255–1265. DOI 10.1099/ijs.0.63484-0

HØJBERG, O., BINNERUP, S. J. & SØRENSEN, J. (**1997).** Growth of silicone-immobilized bacteria on polycarbonate membrane filters, a technique to study microcolony formation under anaerobic conditions. *Applied and environmental microbiology,* 63**,** 2920-2924.

INSTRUCTION MANUAL for QX200. ***(01.12.2016)*** *13:16 pm*
Retrieved from
http://www.bio-rad.com/webroot/web/pdf/lsr/literature/10031906.pdf *p. 2*

IPCC. (2007). Climate change 2007. Synthesis report. Contribution of Working Groups I, II and III to the Fourth Assessment Report of the Intergovernmental Panel on Climate Change. Core Writing Team, Pachauri, R.K. and Reisinger, A. (Eds.). IPCC, Geneva, Switzerland. pp 104.

IPCC. (2014): Climate Change 2014: Synthesis Report. Contribution of Working Groups I, II and III to the Fifth Assessment Report of the Intergovernmental Panel on Climate Change. Core Writing Team, R.K. Pachauri and L.A. Meyer (eds.). IPCC, Geneva, Switzerland, 151 pp.
Retrieved from
http://www.ipcc.ch/pdf/assessment-report/ar5/syr/AR5_SYR_FINAL_SPM.pdf

ISHIDA, T., IKEDA, T., TAKIGUCHI, N., KURODA, A., OHTAKE, H. & KATO, J. (**2007).** Inhibition of quorum sensing in Pseudomonas aeruginosa by N-acyl cyclopentylamides. *Applied and environmental microbiology,* 73**,** 3183-3188.

JO, J., PRICE-WHELAN, A. & DIETRICH, L. E. (**2014)**. An aerobic exercise: defining the roles of Pseudomonas aeruginosa terminal oxidases. *Journal of bacteriology,* 196**,** 4203-4205.

JONES, C. M., STRES, B., ROSENQUIST, M. & HALLIN, S. (**2008)**. Phylogenetic analysis of nitrite, nitric oxide, and nitrous oxide respiratory enzymes reveal a complex evolutionary history for denitrification. *Molecular biology and evolution,* 25**,** 1955-1966.

JÜNGST, A. **& ZUMFT,** W. G. (**1992)**. Interdependence of respiratory NO reduction and nitrite reduction revealed by mutagenesis of nirQ, a novel gene in the denitrification gene cluster of Pseudomonas stutzeri. *FEBS letters,* 314**,** 308-314.

KERN, M. & SIMON, J. (2009). Electron transport chains and bioenergetics of respiratory nitrogen metabolism in Wolinella succinogenes and other Epsilonproteobacteria. *Biochimica et Biophysica Acta (BBA)-Bioenergetics,* 1787**,** 646-656.

KHOROSHILOVA, N., POPESCU, C., MÜNCK, E., BEINERT, H. & KILEY, P. J. (**1997).** Iron-sulfur cluster disassembly in the FNR protein of Escherichia coli by O2:[4Fe-4S] to [2Fe-2S] conversion with loss of biological activity. *Proceedings of the National Academy of Sciences,* 94**,** 6087-6092.

KHUU, P., SANDOR, M., DEYOUNG, J. & HO, P. S. (**2007).** Phylogenomic analysis of the emergence of GC-rich transcription elements. *Proceedings of the National Academy of Sciences,* 104**,** 16528-16533.

KIM, D.-J., CHUNG, S.-G., LEE, S.-H. & CHOI, J.-W. (**2012)**. Relation of microbial biomass to counting units for Pseudomonas aeruginosa. *African Journal of Microbiology Research,* 6**,** 4620-4622.

KLOCKGETHER, J., MUNDER, A., NEUGEBAUER, J., DAVENPORT, C. F., STANKE, F., LARBIG, K. D., HEEB, S., SCHÖCK, U., POHL, T. M. & WIEHLMANN, L. (**2010)**. Genome diversity of Pseudomonas aeruginosa PAO1 laboratory strains. *Journal of bacteriology,* 192**,** 1113-1121.

KÖHLER, T., CURTY, L. K., BARJA, F., VAN DELDEN, C. & PECHERE, J.-C. (**2000).** Swarming of Pseudomonas aeruginosa is dependent on cell-to-cell signaling and requires flagella and pili. *Journal of bacteriology,* 182**,** 5990-5996.

KNOBELOCH, L., SALNA, B., HOGAN, A., POSTLE, J. & ANDERSON, H. (**2000).** Blue babies and nitrate-contaminated well water. *Environmental Health Perspectives,* 108**,** 675.

KRAFT, B., STROUS, M. & TEGETMEYER, H. E. (**2011).** Microbial nitrate respiration–genes, enzymes and environmental distribution. *Journal of biotechnology,* 155**,** 104-117.

KUENEN, J. G. (**2008).** Anammox bacteria: from discovery to application. *Nature Reviews Microbiology,* 6**,** 320-326.

KUROKI, M., IGARASHI, Y., ISHII, M. & ARAI, H**. (2014)**. Fine-tuned regulation of the dissimilatory nitrite reductase gene by oxygen and nitric oxide in Pseudomonas aeruginosa. *Environmental microbiology reports,* 6**,** 792-801.

LABAUVE, A. E. & **WARGO,** M. J. (**2012**). Growth and laboratory maintenance of Pseudomonas aeruginosa. *Current protocols in microbiology***,** 6E. 1.1-6E. 1.8.

LAU, G. W., HASSETT, D. J., RAN, H. & KONG, F. **2004.** The role of pyocyanin in Pseudomonas aeruginosa infection. *Trends in molecular medicine,* 10**,** 599-606.

LESK, A.M**. (2012).** Introduction to Genomics: *Contents of the human genome*. 2 ED. Oxford New York. pp.397

LIU, B., MØRKVED, P. T., FROSTEGÅRD, Å. & BAKKEN, L. R. (**2010).** Denitrification gene pools, transcription and kinetics of NO, N2O and N2 production as affected by soil pH. *FEMS microbiology ecology,* 72**,** 407-417.

LIU, B., FROSTEGÅRD, Å. & BAKKEN, L. R. (**2014)**. Impaired reduction of N2O to N2 in acid soils is due to a posttranscriptional interference with the expression of nosZ. *MBio,* 5**,** e01383-14.

LØVÅS, G.G. (**2004).** Statistikk for universiteter og høgskoler. 2 ed. Univeristetsforlaget AS, 0105 Oslo. p.216

MACHIDA, T., NAKAZAWA, T., FUJII, Y., AOKI, S. & WATANABE, O. (**1995).** Increase in the atmospheric nitrous oxide concentration during the last 250 years. *Geophysical Research Letters,* 22**,** 2921-2924.

MADSEN, E.L. (**2008).** Envrionmental Microbiology. From Genomes to Biochemistry: a grand synthesis .pp. 479

MATHEE, K., NARASIMHAN, G., VALDES, C., QIU, X., MATEWISH, J. M., KOEHRSEN, M., ROKAS, A., YANDAVA, C. N., ENGELS, R. & ZENG, E. (**2008).** Dynamics of Pseudomonas aeruginosa genome evolution. *Proceedings of the National Academy of Sciences,* 105**,** 3100-3105.

MOLSTAD, L., DÖRSCH, P. & BAKKEN, L. R. (**2007).** Robotized incubation system for monitoring gases (O 2, NO, N 2 ON 2) in denitrifying cultures. *Journal of microbiological methods,* 71**,** 202-211.

MONTZKA, S. A., DLUGOKENCKY, E. J. & BUTLER, J. H. (**2011).** Non-CO2 greenhouse gases and climate change. *Nature,* 476**,** 43-50.

MORENO-VIVIÁN, C., CABELLO, P., MARTÍNEZ-LUQUE, M., BLASCO, R. & CASTILLO, F. (**1999).** Prokaryotic nitrate reduction: molecular properties and functional distinction among bacterial nitrate reductases. *Journal of bacteriology,* 181**,** 6573-6584.

MURPHY, L. M., DODD, F. E., YOUSAFZAI, F. K., EADY, R. R. & HASNAIN, S. S. (**2002).** Electron donation between copper containing nitrite reductases and cupredoxins: the nature of protein-protein interaction in complex formation. *Journal of molecular biology,* 315**,** 859-871.

NCBI. **(01.12.2016).** 19:53 pm. Genome Assembly and Annotation report [1739]. Retrieved from https://www.ncbi.nlm.nih.gov/genome/genomes/187

NUNN, J. (**1988).** Clinical relevance of the B12/N2O interaction A report of a seminar. *Anaesthesia,* 43**,** 587-589.

PASSADOR, L., COOK, J.M, GAMBELLO, M.J., RUST, L., & IGLEWSKI, B.H. **(1993).** Expression of *Pseudomonas aeruginosa* virulence genes requires cell-to-cell communication. Science, 260 (1993), pp. 1127–1130

PEARSON, J.P., GRAY,K.M., PASSADOR, L., TUCKER, K.D., EBERHARD, A., IGLEWSKI, B.H., & GREENBERG, E.B. **(1994)**. Structure of the autoinducer required for expression of *Pseudomonas aeruginosa* virulence genes. Proc. Natl. Acad. Sci. USA, 91(1994):197–201.

PENROSE, R. (**1910).** The nitrate deposits of Chile. The Journal of Geology, 18(1):1-32

PESSI, G. & **HAAS, D. (2000)**. Transcriptional Control of the Hydrogen Cyanide Biosynthetic Genes hcnABC by the Anaerobic Regulator ANR and the Quorum-Sensing Regulators LasR and RhlR inPseudomonas aeruginosa. *Journal of Bacteriology,* 182**,** 6940-6949.

PREMIERBIOSOFT. (25.11.2016). 10.31 am.
Retrieved from
http://www.premierbiosoft.com/tech_notes/PCR_Primer_Design.html

RAMASWAMY, V., BOUCHER, O., HAIGH, J., HAUGLUSTAINE, D., HAYWOOD, J., MYHRE, G., NAKAJIMA TAKAHITO., SHI GUANGYU., SOLOMON, S., BETTS, ROBERT E., CHARLSON, R., CHUANG, C. C., DANIEL, J.S., DEL GENIO, ANTHONY D., FEICHTER, J., FUGLESTVEDT, J., FORSTER, P. M., GHAN, STEVEN J., JONES, A., & KIEHL, J. T. **(2001).** SciTech Connect. Radiative Forcing of Climate Change. *Climate Change 2001: The Scientific Basis*. Houghton, J. T. et al; Cambridge University Press, New York, NY, United States(US). (see Table 6.2 of the TAR).

RAVISHANKARA, A., DANIEL, J. S. & PORTMANN, R. W. (**2009).** Nitrous oxide (N2O): the dominant ozone-depleting substance emitted in the 21st century. *science,* 326**,** 123-125.

REECE, J. B., URRY, L. A., CAIN, M. L., WASSERMAN, S. A., MINORSKY, P. V. & JACKSON, R. B. **(2011)**. *Campbell biology*, Pearson Boston. pp.1309

RICHARDSON, D., FELGATE, H., WATMOUGH, N., THOMSON, A. & BAGGS, E. (**2009).** Mitigating release of the potent greenhouse gas N2O from the nitrogen cycle – could enzymic regulation hold the key? *Trends in Biotechnology*, 27 (7): 388-397.

RINGEN, L. M. **& DRAKE**, C. H. (**1952).** A study of the incidence of Pseudomonas aeruginosa from various natural sources. *Journal of bacteriology,* 64**,** 841.

ROUM, J., BUHL, R., MCELVANEY, N., BOROK, Z. & CRYSTAL, R. (**1993).** Systemic deficiency of glutathione in cystic fibrosis. *Journal of Applied Physiology,* 75**,** 2419-2424.

RUPERT, M. G. (**2008)**. Decadal-scale changes of nitrate in ground water of the United States, 1988–2004. *Journal of Environmental Quality,* 37**,** S-240-S-248.

SALUNKHE, P., SMART, C. H., MORGAN, J. A. W., PANAGEA, S., WALSHAW, M. J., HART, C. A., GEFFERS, R., TÜMMLER, B. & WINSTANLEY, C. (**2005).** A cystic fibrosis epidemic strain of Pseudomonas aeruginosa displays enhanced virulence and antimicrobial resistance. *Journal of bacteriology,* 187**,** 4908-4920.

SAMAD, M. S., BAKKEN, L. R., NADEEM, S., CLOUGH, T. J., DE KLEIN, C. A., RICHARDS, K. G., LANIGAN, G. J. & MORALES, S. E. (**2016)**. High-Resolution Denitrification Kinetics in Pasture Soils Link N 2 O Emissions to pH, and Denitrification to C Mineralization. *PloS one,* 11**,** e0151713.

SCHAFER, F. Q. **& BUETTNER**, G. R. (**2001).** Redox environment of the cell as viewed through the redox state of the glutathione disulfide/glutathione couple. *Free Radical Biology and Medicine,* 30**,** 1191-1212.

SCHLESINGER, W. H. (**2009)**. On the fate of anthropogenic nitrogen. *Proceedings of the National Academy of Sciences,* 106**,** 203-208.

SCHREIBER, K., KRIEGER, R., BENKERT, B., ESCHBACH, M., ARAI, H., SCHOBERT, M. & JAHN, D. (**2007).** The anaerobic regulatory network required for Pseudomonas aeruginosa nitrate respiration. *Journal of bacteriology,* 189**,** 4310-4314.

SCHUSTER, M., LOSTROH, C. P., OGI, T. & GREENBERG, E. (**2003).** Identification, timing, and signal specificity of Pseudomonas aeruginosa quorum-controlled genes: a transcriptome analysis. *Journal of bacteriology,* 185**,** 2066-2079.

SCHUSTER, M**. & GREENBERG**, E. P. (**2006).** A network of networks: quorum-sensing gene regulation in Pseudomonas aeruginosa. *International journal of medical microbiology,* 296**,** 73-81.

SHARMA, V., NORIEGA, C. E. & ROWE, J. J. (**2006).** Involvement of NarK1 and NarK2 proteins in transport of nitrate and nitrite in the denitrifying bacterium *Pseudomonas aeruginosa* PAO1. *Applied and environmental microbiology,* 72**,** 695-701.

SILVESTRINI, M. C., GALEOTTI, C. L., GERVAIS, M., SCHININÀ, E., BARRA, D., BOSSA, F. & BRUNORI, M. (**1989)**. Nitrite reductase from Pseudomonas aeruginosa: sequence of the gene and the protein. *FEBS letters,* 254**,** 33-38.

ŠIMEK, M. & **COOPER**, J. (**2002)**. The influence of soil pH on denitrification: progress towards the understanding of this interaction over the last 50 years. *European Journal of Soil Science,* 53**,** 345-354.

SISTROM, W.R. (**1962)**, J. Gen. Microbiol. 28:607-616

SKINDERSOE, M. E., ZEUTHEN, L. H., BRIX, S., FINK, L. N., LAZENBY, J., WHITTALL, C., WILLIAMS, P., DIGGLE, S. P., FROEKIAER, H. & COOLEY, M. (**2009).** Pseudomonas aeruginosa quorum-sensing signal molecules interfere with dendritic cell-induced T-cell proliferation. *FEMS Immunology & Medical Microbiology,* 55**,** 335-345.

SMITH, K. & **CONEN**, F. (**2004)**. Impacts of land management on fluxes of trace greenhouse gases. *Soil Use and Management,* 20**,** 255-263.

SMITH, R. S. & **IGLEWSKI**, B. H**. (2003)**. *P. aeruginosa* quorum-sensing systems and virulence. *Current opinion in microbiology,* 6**,** 56-60.

SOOHOO, C. K. & **HOLLOCHER**, T. C. (**1990)**. Loss of nitrous oxide reductase in Pseudomonas aeruginosa cultured under N2O as determined by rocket immunoelectrophoresis. *Applied and environmental microbiology,* 56**,** 3591-3592.

SPIRO, STEPHEN. (**2012)**. Nitrous oxide production and consumption: regulation of gene expression by gas-sensitive transcription factors. A Review. Philosophical Transactions of the Royal Society B: Biological Sciences 367(1593): 1213-1225.

STOTZKY, G. (**1967)**. DIVISION OF ENVIRONMENTAL SCIENCES: CLAY MINERALS AND MICROBIAL ECOLOGY*,†. Transactions of the New York Academy of Sciences, 30**,** 11-21.

STOVER, C. K., PHAM, X. Q., ERWIN, A., MIZOGUCHI, S., WARRENER, P., HICKEY, M., BRINKMAN, F., HUFNAGLE, W., KOWALIK, D. & LAGROU, M. (**2000)**. Complete genome sequence of Pseudomonas aeruginosa PAO1, an opportunistic pathogen. *Nature,* 406**,** 959-964.

STROUS, M., PELLETIER, E., MANGENOT, S., RATTEI, T., LEHNER, A., TAYLOR, M. W., HORN, M., DAIMS, H., BARTOL-MAVEL, D. & WINCKER, P. (**2006).** Deciphering the evolution and metabolism of an anammox bacterium from a community genome. *Nature,* 440**,** 790-794.

SUHARTI, STRAMPRAAD, M. J., SCHRÖDER, I. & DE VRIES, S. (**2001).** A Novel Copper A Containing Menaquinol NO Reductase from Bacillus azotoforman s. *Biochemistry,* 40**,** 2632-2639.

TAVARES, P., PEREIRA, A., MOURA, J. & MOURA, I. **(2006)**. Metalloenzymes of the denitrification pathway. *Journal of inorganic biochemistry,* 100**,** 2087-2100.

THERMOFISCHER SCIENTIFIC. (26.11.2016).13.21pm. ThermoFischer Scientific, *260/280 and 260/230 Ratios*. T009-TECHNICAL BULLETIN. NanoDrop 1000 & 8000.
Retrieved from
http://www.nanodrop.com/Library/T009-NanoDrop%201000-&-NanoDrop%208000-Nucleic-Acid-Purity-Ratios.pdf

TORRES, M. J., ARGANDOÑA, M., VARGAS, C., BEDMAR, E. J., FISCHER, H.-M., MESA, S. & DELGADO, M. J. (**2014).** The global response regulator RegR controls expression of denitrification genes in Bradyrhizobium japonicum. *PloS one,* 9**,** e99011.

TORTORA, G.J., FUNKE, B.R., & CASE, C.L. (**2007).** Chapter 11: The Prokaryotes, Domains Bacteria and Archaea. Chapter 16: Interaction between Microbe and Host. Microbiology, an Introduction. 11th ed. 2007 Pearson Education, Inc. ISBN 10: 0-321-79854-6 pp.818

TOYOFUKU, M., NOMURA, N., FUJII, T., TAKAYA, N., MASEDA, H., SAWADA, I., NAKAJIMA, T. & UCHIYAMA, H. (**2007).** Quorum sensing regulates denitrification in Pseudomonas aeruginosa PAO1. *Journal of bacteriology,* 189**,** 4969-4972.

URBANSKY, E., BROWN, S., MAGNUSON, M. & KELTY, C. (**2001).** Perchlorate levels in samples of sodium nitrate fertilizer derived from Chilean caliche. *Environmental Pollution,* 112**,** 299-302.

USSIRI, D. & **LAL**, R. (**2013).** The role of nitrous oxide on climate change. *Soil Emission of Nitrous Oxide and its Mitigation.* Springer.

VAN ELSAS, J. D., TREVORS, J. T., JANSSON, J. K. & NANNIPIERI, P. (**2006).** *Modern soil microbiology*, CRc Press. pp. 646.

VAN SPANNING, R.J.M., RICHARDSON, D, & FERGUSON, S. (**2007)**. Introduction to the biochemistry and molecular biology of denitrification. In Biology of the nitrogen cycle, Introduction CH. 1 (eds H. Bothe, S.J., Ferguson & W.E. Newton), pp382-395. Amsterdam, the Netherlands: Esevier.

VASIL, M. L**.** & **CLARK**, V**. (2011)**. Regulation and function of versatile aerobic and anaerobic respiratory metabolism in Pseudomonas aeruginosa. *Pseudomonas Aeruginosa, Biology, Genetics, and Host-pathogen Interactions***,** 36.

WAGNER, V. E., BUSHNELL, D., PASSADOR, L., BROOKS, A. I. & IGLEWSKI, B. H. (**2003).** Microarray analysis of Pseudomonas aeruginosa quorum-sensing regulons: effects of growth phase and environment. *Journal of bacteriology,* 185**,** 2080-2095.

WANG, M., SCHAEFER, A. L., DANDEKAR, A. A. & GREENBERG, E. P. (**2015).** Quorum sensing and policing of Pseudomonas aeruginosa social cheaters. Proceedings of the National Academy of Sciences, 112, 2187-2191.

WATERS, C.M., & **BASSLER**, B.L. (**2005).** Quorum Sensing: Cell-to-Cell Communication in Bacteria. Annu. Rev. Cell Dev. Biol. 2005. 21:319–46

WESSEL, A. K., ARSHAD, T. A., FITZPATRICK, M., CONNELL, J. L., BONNECAZE, R. T., SHEAR, J. B. & WHITELEY, M. (**2014).** Oxygen limitation within a bacterial aggregate. MBio, 5, e00992-14.

WESTBROCK-WADMAN, S., SHERMAN, D. R., HICKEY, M. J., COULTER, S. N., ZHU, Y. Q., WARRENER, P., NGUYEN, L. Y., SHAWAR, R. M., FOLGER, K. R. & STOVER, C. K. (**1999).** Characterization of a Pseudomonas aeruginosa efflux pump contributing to aminoglycoside impermeability. *Antimicrobial agents and chemotherapy,* 43**,** 2975-2983.

WILLIAMS, D., ROWE, J., ROMERO, P. & EAGON, R. (**1978).** Denitrifying Pseudomonas aeruginosa: some parameters of growth and active transport. *Applied and environmental microbiology,* 36**,** 257-263.

WILKS, J. C**.** & **SLONCZEWSKI**, J. L. (**2007).** pH of the cytoplasm and periplasm of Escherichia coli: rapid measurement by green fluorescent protein fluorimetry. *Journal of bacteriology,* 189**,** 5601-5607.

WINTELER, H. V. & **HAAS**, D. (**1996)**. The homologous regulators ANR of Pseudomonas aeruginosa and FNR of Escherichia coli have overlapping but distinct specificities for anaerobically inducible promoters. *Microbiology,* 142**,** 685-693.

WOLFE, A. D. **& HAHN**, F. E. (**1965).** Mode of action of chloramphenicol IX. Effects of chloramphenicol upon a ribosomal amino acid polymerization system and its binding to bacterial ribosome. *Biochimica et Biophysica Acta (BBA)-Nucleic Acids and Protein Synthesis,* 95**,** 146-155.

WOOD, N. J., ALIZADEH, T., RICHARDSON, D. J., FERGUSON, S. J. & MOIR, J. W. (**2002).** Two domains of a dual-function NarK protein are required for nitrate uptake, the first step of denitrification in Paracoccus pantotrophus. *Molecular microbiology,* 44**,** 157-170.

YE, J., COULOURIS, G., ZARETSKAYA, I., CUTCUTACHE, I., ROZEN, S. & MADDEN, T. L. (**2012)**. Primer-BLAST: a tool to design target-specific primers for polymerase chain reaction. *BMC bioinformatics,* 13**,** 1.

ZHENG, J. & **DOSKEY**, P. V**. (2016)**. Simulated rainfall on agricultural soil reveals enzymatic regulation of short-term nitrous oxide profiles in soil gas and emissions from the surface. *Biogeochemistry***,** 1-12.

ZIERDT, C. & **SCHMIDT**, P. (**1964).** Dissociation in Pseudomonas aeruginosa. *Journal of bacteriology,* 87**,** 1003-1010.

ZUMFT, W.G. **(1997).** Cell Biology and Molecular Basis of Denitrification. *American Society for Microbiology*. Microbiology and Molecular Biology Reviews 61(4):533–616

ZUMFT, W. G. (**2005).** Nitric oxide reductases of prokaryotes with emphasis on the respiratory, heme–copper oxidase type. *Journal of inorganic biochemistry,* 99**,** 194-215.

ZUMFT, W. & **CARDENAS**, J. (**1979).** The inorganic biochemistry of nitrogen bioenergetic processes. *Naturwissenschaften,* 66**,** 81-88.

ZUMFT, W.G., & **KRONECK,** P.M.H**. (2007).** Respiratory Transformation of Nitrous Oxide (N2O) to Dinitrogen by Bacteria and Archaea. Elsevier Ltd. *Advances in Microbial Physiology* vol. 52 isbn 0-12-027752-2. DOI: 10.1016/S0065-2911(06)52003-X

APPENDIX

Medium preparation

Table I. *Stock medium: Sistrom´s medium with slight differences from the reference (Sistrom WR 1962, J. Gen. Microbiol. 28:607-616). A) Sistrom´s medium; B) Trace elements solution; C) Vitamins solution. Clean water, without any interfering elements perturbing the specific growth rate is a requirement when batch cultivating an organism, therefore sterile MilliQ-water was utilized for preparing the stock medium.*

A) *Sistrom´s* medium		**(Sistrom WR 1962, J. Gen. Microbiol. 28:607-616)**		
Component	**Grams**	**[] in 10x medium**		**Comment**
K_2HPO_4	34,80	200	mM	alkaline
NH_4Cl	1,95	36,4	mM	Obs: add after acids
Succinic acid/ravsyre	40,00	340	mM	acidic
L-Glutamic acid	1,00	6,7	mM	
L-Aspartic acid	0,40	2,5	mM	
NaCl	5,00	85	mM	
Nitrilacetic acid	2,00	10,5	mM	
$MgSO_4*7H_2O$	3,00	12	mM	
$CaCl_2*2H_2O$	0,15	1	mM	
$FeSO_4*7H_2O$	0,02	0,07	mM	
Trace elements solution	1,00		mL	
Vitamins solution (without vitamin B12)	1,00		mL	
TOTAL		1,00	L	
Store frozen (-20˚C), e.g. as 100 mL. When diluted 1x for growth of cells (i.e. 100 mL x 10), it should be brought to about pH 7.0 with KOH (E.g. 1 mL + 5 ½ pasteru pipette droplets).				

B) Trace elements solution (1000X for 10X medium)				
Component	(g/100mL)	Concentration		Comments
EDTA	1,765	0,05	M	
$ZnSO_4*7H_2O$	10,95	0,038	M	
$FeSO_4*7H_2O$	5	0,018	M	
$MnSO_4*H_2O$	1,54	0,01	M	
$CuSO_4*5H_2O$	0,392	1,50	mM	
$Co(NO_3)_2*6H_2O$	0,248	0,90	mM	Borsyre
H_3BO_3	0,114	1,80	mM	

TOTAL vol.	100	mL
$Co(NO_3)_2$*6H_2O replaced by $CoCl_2$ in "NO_3- free" trace elements solution.		
Store at 4˚C		
Add H_2SO_4 dropwise until solution clears		

C) Vitamins solution (1000X for 10X medium)		
Component	Amount (g/100mL)	
Nicotinic acid	1	
Thiamine HCl	0,5	
Biotin	0,01	
TOTAL vol.	100	mL
Store at 4˚C		

Media and cultivation conditions

In addition to protect sample from contamination, lab-worker is also protected from an opportunistic pathogen by sterile techniques performed. These involved autoclaving of filtertips, 70% ethanol washed surfaces of biosafety cabinets, Laminar air flow (LAF) benches, disposable gloves and lab-coat as standard procedure.

Plating of cultures on TSA medium (Tryptic soy agar: general medium), LB medium (Luria-Bertani: general medium) and *Sistrom´s* medium assured that strain specific growth curves were not contaminated. The plates confirmed that the cultures and stocks really contained *P. aeruginosa* spp. specifically and exclusively (fig. 1).

Method of plating: Streak bacteria (scarped directly from frozen stock) onto agar plate using sterile applicator sticks. Incubate at 37°C for 16–24 hours, and 22°C for 2 days. Large, opaque, and convex with a slightly rough edge and light tan in colour are seen as colonies on plates (LaBauve and Wargo). Early production of pyocyanin (2-aminoacetophenone (2AA) by *las* and *rhI* systems during *P. aeruginosa* growth makes it available for analysis after only 20 to 24 h of incubation (Cox and Parker, 1979; Lau et al., 2004).

Figure I. *Plating-example at late-stationary phase performed on Sistrom´s medium with P. aeruginosa PAO1 culture. Pigments of pyocyanin (2-aminoacetophenone (2AA)), are providing the turquoise colour. Its amount produced varies between strain, and smells like almonds (the type strain), or lotus flower (PAO1). Some rich media, like blood agar, or burn wounds have been reported to give a sweeter, grape-like odor (LaBauve and Wargo).*

Growth curve

Slope gives the specific growth rate (*μ) and* derives from the log linear relationship between optical densities (OD_{600}) and time, seen as a growth curve at 20˚C (fig.2 A, B).

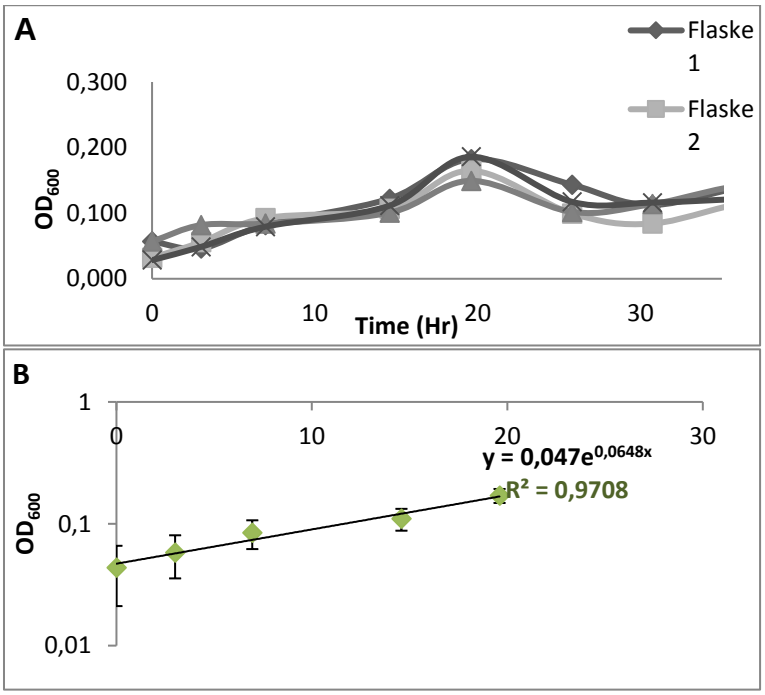

Figure II. *"OD to time" presented as (A) Growth curve and (B) Log linear growth curve, by P. aeruginosa PAO1 during anaerobic growth condition at 20˚C with continuous stirring (500 rpm) 7 mM KNO3 in Sistrom´s medium.*

Nitrite standard – NOA system

Table II. *The dilution series of KNO_2 in H2O (2000 µM; 200µM; 20 µM; and 2 µM KNO_2) was used as a nitrite standard, and its response factor from NOA system was used to find the response factor for assuring correct nitrite estimates per sample into the NOA-system.*

NO_2-standarder					
Conversion factors		*Vf or Mf*	*Vol. (L)/Molar*Mw=g*	*Vi or Mi*	*(Vi*Vf=Mi*Mf)*
KNO_2	**Mw (mol/g)**	**µM**		**Volume**	**UNITs**
	85,11	**2000**	0,17022	1	mL
		200		100	µL
		20		100	µL
		2		100	µL
Calculating sample concentration of nitrite **Response factor ~0.02**					
Response factor =		**Standard concentration injected (µM)** **peak area detected of standard**			
Concentration of sample (µM) = response factor *peak area detected of sample					
Converting µM NO_2^- to µmol NO_2^-					
µmol =		Concentration of sample (µM)*50 mL 1000 mL			

Table III. *Specially prepared solvents used during RNAextraction.*

Perform all steps 1-4. At room temperature (15-25°)C) without interruption	
1. TE buffer: **a. 1 mg/ml lysozyme** **b. 10 mM TrisCl** **c. 1 mM EDTA** **d. pH 8.0**	**1) In 40 samples I need 200 x 40 = 8000 uL = 8 mL ≈ 10 mL with 0.01 g lysoozym**
2. Add 10 uL β-mercaptoethanol per 1 mL Buffer RLT: **a. Mix.** **b. Stable for 1 month.**	**1) In 40 samples I need 700 x 40 = 28000 uL = 28 mL ≈ 30 mL RLT** **2) 10*30 = 300 uL β mercaptoethanol**

Table IV. *Experimental working solutions and their final concentrations.*

Reagent	Working solutions	Procedure	Comments	Final concentration
KNO3	1 M	MW: 101,1032 g/mol • 250 mL MRo H2O • 25,2758 g KNO3 • Autoclaved	Nitrate tolerates autoclavation, while nitrite does not, and usually an efficient protocol would promote the same routine for the both: no autoclavation of nitrate/nitrite, and addition to already autoclaved flasks.	2 mM (Optionally: send for the autoclave after addition to 50 mL Sistrom`s Medium, large magnetic bars.
KOH	10 M	MW: 56,11 g/mol • 50 mL MRo H2O • 28,055 g KOH	Strong base that quickly generates heat in water and must be slowly dissolved in a chemical fume hood. KOH solution could slowly dissolve glass, store it in a plastic container before using.	Add until Sistrom`s medium reaches pH 7.00
NaCl	15 mM	Filtersterilized	Isotonic salt solution for washing cells when finding dryweight; washing cells when counting DAPI stained cells	
Phosphate-buffered saline (PBS)		Salt: concentration, g/L • NaCl: 137, 8.0 • KCl: 2.7, 0.2 • Na_2HPO_4: 10, 0.24 • KH_2PO_4: 1.8, 0,24 • MQ H_2O: up to 700 mL • Adjust to pH=7.4with KOH and/or HCl • MQ H_2O: Add up to 1L • Filtersterilize	Filtersterilized	

Micro-GC

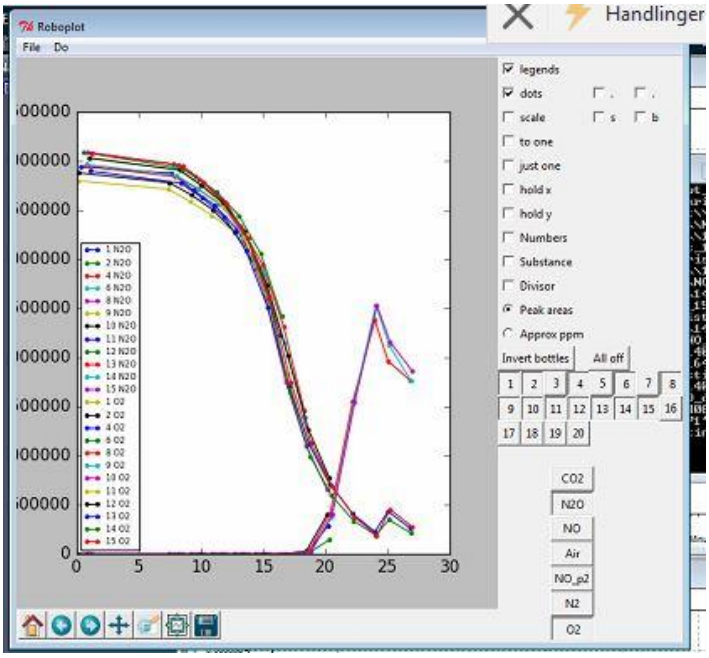

Figure III. *Time intervals for sampling from headspace (adjusted in Python) and measurements of gases (O_2 and N_2O) (illustrated by Roboplot) during transition from aerobic respiration to denitrification in P. aeruginosa PAO1 wild type.*

Initial experiments

Denitrification phenotype result from *P. aeruginosa* PAO1 (fig.3) and final cell density (fig.2) at 30˚C, and 2 mM KNO_3 are presented below to illustrate affect of temperature on denitrification phenotype, and effect of different initial oxygen concentrations on cell density.

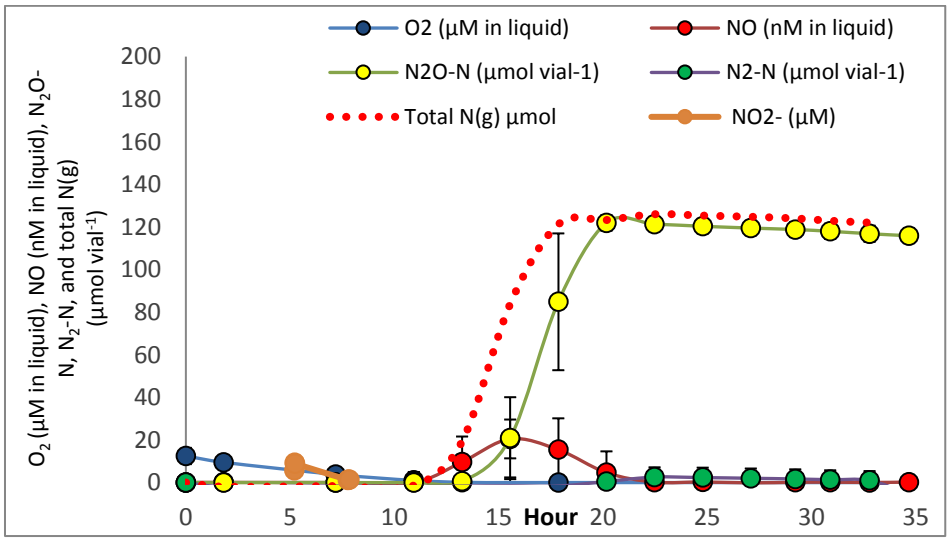

Figure IV. *Denitrification at 30˚C by P. aeruginosa PAO1 under 1 % initial O_2 concentrations with 2 mM KNO_3, Sistrom´s medium, continuously stirred (500 rpm) with (n=5).*

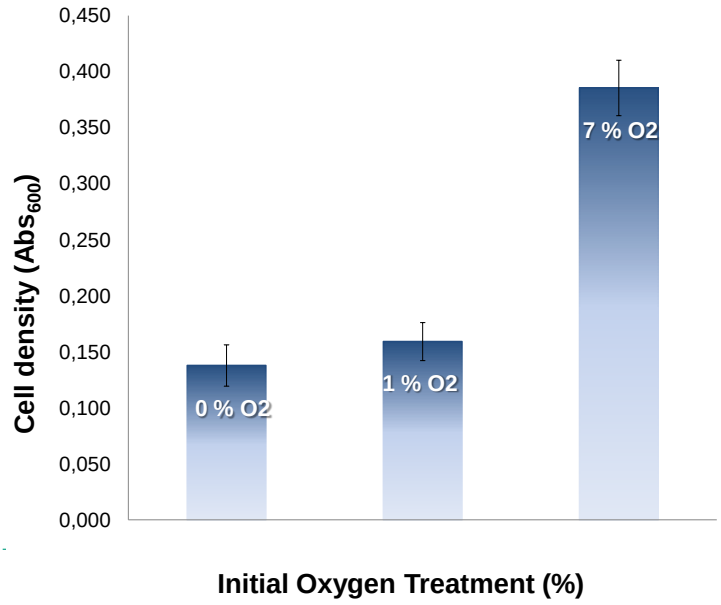

Figure V. *Final cell density of P. aeruginosa PAO1 culture after denitrifying through different initial oxygen concentrations (0, 1 and 7 %) at Standard conditions (2 mM KNO_3, 30˚C, 50 mL Sistrom´s medium, continuous stirring with large magnets (500 rpm).*

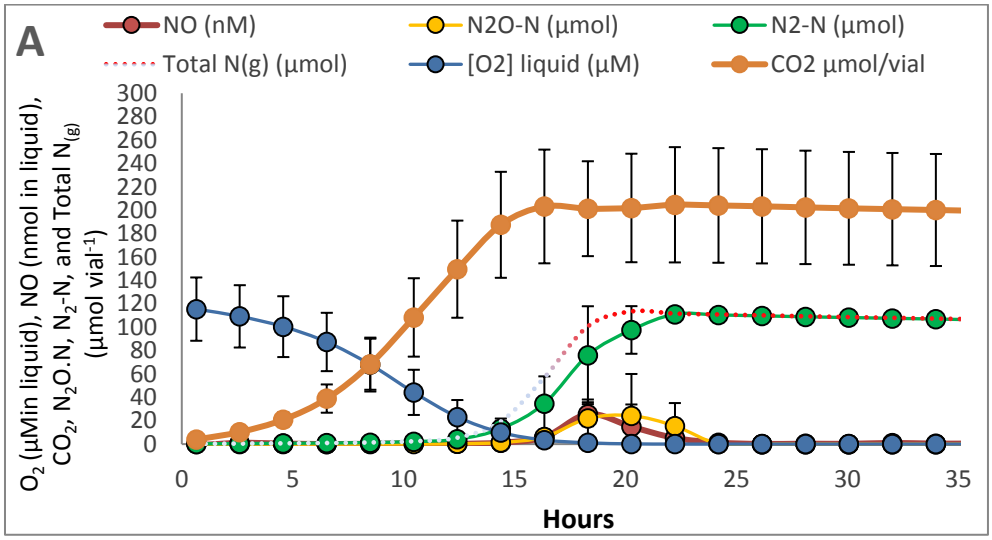

Figure VI. *CO_2 production by P. aeruginosa the type strain in transition from 7 % initial oxygen to denitrification of 2mM NO_3^- at standard conditions.*

Table V. *Meltpoints by real-time PCR (StepOnePlus) from desigend primer pairs on P. aeruginosa the type strain (TS) and PAO1.*

Tm1 (no Tm2 or Tm3)		(n=3)
TS and PAO1	AVG	SD
nosZ (standard)	89,6677678	0,08559836
napA:	91,1706696	0,20411125
narG:	90,4360199	0,12433706
nirS:	90,0387319	0,05515753
norB:	89,143748	0,06176962
nosZ:	89,5155411	0,1529847
Reporter		
SYBR		

Table VI. *An example of the number of accepted droplets (total of positive and negative) in one run during ddPCR (n=3).*

nirS	***AVG***	***SD***
INOKULUM	17554,00	366,28
INOKULUM		
1. Semi-aerobic	17963,00	772,38
2. Declining O_2	18002,00	1796,87
3. NO increase	17130,67	2421,47
4. N_2O increase (wild type)	17420,33	1338,58
5. N_2O max (wild type)	18020,00	166,44
6. End	17816,00	849,69
AVG	***17700,86***	
SD		***341,54***
CV%		

nirS	***AVG***	***SD***
INOKULUM	17875	2457,90
INOKULUM		
1. Semi-aerobic	18745,66	1159
2. Declining O_2	19288,66	1626,50
3. NO increase	16373,33	5087,64
4. N_2 increase	17527	1076,24
5. N_2 exponential	16494	461,94
6. End	15072	1795,65
AVG	***17532,17***	
SD		***1002,71***
CV%		

Norges miljø- og biovitenskapelig universitet
Noregs miljø- og biovitskapelege universitet
Norwegian University of Life Sciences

Postboks 5003
NO-1432 Ås
Norway